Master's thesis

NTNU
Norwegian University of Science and Technology
Faculty of Engineering
Department of Energy and Process Engineering

Kristoffer Wigdahl Lie

Model Development and Performance Analysis of an R290 Direct Expansion Solar Assisted Heat Pump System using PVT.

Master's thesis in Energy and the Environment
Supervisor: Vojislav Novakovic
Co-supervisor: Yanjun Dai
July 2022

NTNU
Norwegian University of
Science and Technology

Kristoffer Wigdahl Lie

Model Development and Performance Analysis of an R290 Direct Expansion Solar Assisted Heat Pump System using PVT.

Master's thesis in Energy and the Environment
Supervisor: Vojislav Novakovic
Co-supervisor: Yanjun Dai
July 2022

Norwegian University of Science and Technology
Faculty of Engineering
Department of Energy and Process Engineering

NTNU
Norwegian University of
Science and Technology

Norwegian University of Science and Technology

Faculty of Engineering
Department of Energy and Process Engineering

EPT-M-2022

MASTER THESIS WORK

for

student Kristoffer Wigdahl Lie

Spring 2022

Performance analysis and experiments on solar PVT heat pump system

Analyse av ytelser og forsøk med varmepumpesystem drevet av solbasert PVT

Background and objective

A Novel PVT module which may generate more than 10% electricity than that of the normal PV module and can also output thermal energy with about 40% of the received solar radiation is under development. The power from PVT module can be used for driving heat pump to further lift the temperature of heat from PVT module and thus meet the regiments for comfortable heating. This is one of the most efficient ways to harvest and use solar energy up to date.

The master thesis assignment is related to the ongoing research project between Norway and China with the title: "Key technologies and demonstration of combined cooling, heating and power generation for low-carbon neighbourhoods/buildings with clean energy – ChiNoZEN". The master thesis assignment is also a part of the Joint Research Centre in Sustainable Energy between NTNU and Shanghai Jiao Tong University (SJTU).

The aim of the master thesis assignment is to contribute to development of the mathematical model of the proposed system and to investigate the performance of such system under Shanghai and Trondheim climate conditions. A major part of the work should be performed as the Master thesis that is planned to be conducted at SJTU during the spring semester. If Covid situation does not allow it, tests will be performed in SJTU, and the acquired data will be used for supporting the master thesis work in Trondheim.

The following tasks are to be considered:

1. Simulation analysis of the performance of the proposed combined system (PVT+HP) using the developed mathematical model and simulation tool.
2. Validation of the simulation model with experimental results, which can be obtained from SJTU lab, and improve the mathematical model.
3. Investigation of the feasibility of the proposed combined system (PVT+HP) both in Trondheim and Shanghai, both in energy contribution and economic analysis.
4. Optimization of the system performance by controlling the operation and configuration parameters.
5. Make a draft proposal (6-8 pages) for a scientific paper based on the main results of the work performed in the master thesis.
6. Make proposal for further work on the same topic.

Address	Location	Tel.	+47 73 59 38 60
N-7034 Trondheim	K. Hejes vei 1b	Fax	+47 73 59 35 80
Norway		Org. no.	NO 974 767 880

Preface

This work is the final part of the two year MSc programme "Energy and the Environment" at Norwegian University of Science and Technology (NTNU), providing the evaluation basis for the last 30 out of a total of 120 ECTS. The work is mainly conducted in the spring semester of 2022, continuing a specialisation project from the autumn of 2021.

The master thesis assignment is related to the ongoing research project between Norway and China with the title: “Key technologies and demonstration of combined cooling, heating and power generation for low-carbon neighbourhoods/buildings with clean energy – ChiNoZEN”. The master assignment is also a part of the Joint Research Centre in Sustainable Energy between NTNU and Shanghai Jiao Tong University (SJTU).

The major part of the work was initially planned to be conducted at SJTU during the spring semester of 2022. Due to the ongoing COVID-19 pandemic, this was not possible as China faced strong restrictions and student visas were not granted. As a replacement, regularly digital meetings with relevant staff and students at SJTU were conducted.

I would like to thank my supervisor at NTNU, professor Vojislav Novakovic, for his guidance and sound advice through the project period, and co-supervisor professor Yanjun Dai at SJTU for providing feedback, suggestions, and technical knowledge of the investigated system. Also, thank you to Dr. Jian Yao at SJTU for his great feedback and help with the solar photovoltaic heat pump system, and for providing experimental data from ongoing research in Shanghai, China. His response and willingness to support my work has been really invaluable. Thank you to Mr. Wenjie Liu at SJTU for cooperation and discussions exchanging knowledge on the simulation model of the PVT-SAHP system. I hope that these sessions have been as interesting and constructive for your work as for my work.

To my fellow student Simon Bjerkan Steinvoll at NTNU; It is a shame that we could not travel to Shanghai as planned, but our meetings and discussions, both professional and off-topic, have been a decent replacement to keep our spirits strong. Thank you for this, and also for five great years as classmates.

Finally I would like to thank my family. All your support have really made it possible for me to go through five years of studies, for which I am forever grateful. Especially thank you to my siblings, Rannveig and Runar, for giving me moments to look forward to and inspiring me to become the best possible version of myself. I am grateful for having you all in my life, and I look forward to many good times to come.

Trondheim 10.07.2022

Abstract

As new governing strategies to stop the increase of global emission is developed and implemented, reduction of energy consumption in the building sector receives more focus, and providing green solutions becomes of importance.

A novel Photovoltaic-thermal (PVT) module which may generate more electricity than a normal PV module and can also output thermal energy from the received solar radiation is under development. The power from PVT module can be used for driving heat pump to further lift the temperature of heat from PVT module and thus meet the regiments for comfortable heating.

This master thesis investigates the modelling and simulation of a single-source Direct Expansion Photovoltaic Solar Assisted Heat Pump (DX PVT-SAHP) system with a propane (R290) vapor-compression cycle heating water from 7 °C to between 55 and 65 °C.

In the first part of the work the energy system was proposed, and a numerical simulation model developed in MATLAB. The model is a numerical transient thermodynamic simulation model with small time-steps of around one minute. The model can be used to simulate the behaviour of PVT-SAHP systems with both transient hourly and daily resolution, as well as overall yearly performance evaluations. It can also be utilised in the development of a compressor controller for the system. Part two of the work is a case study for the system operating in Trondheim, Norway. Feasibility with regards to both energy performance and economy were investigated, and also influence of system configurations on the performance.

The results show that the PVT-SAHP can achieve a COP of 2.8 in the winter and 5.8 in the summer, heating water from 7 °C to 55-65 °C in Trondheim, Norway. It also achieves better annual energy performance and leads to lower building net annual electricity demand than a traditional air-source heat pump (ASHP) (21 %) or electric heating (67 %) system in Trondheim. Consequently, annual energy costs are significantly reduced. The economic analysis shows that although with higher investment costs, the PVT-SAHP has a lifetime annual cost which is lower than for an ASHP and electric boiler.

System optimisation and parametric investigation results show that increasing the PVT area increases the COP and heating power of the PVT-SAHP slightly. Also, using a larger compressor to increase the heating power of the system significantly decreases the COP if PVT area is not increased accordingly.

As an additional task, a draft proposal for a scientific paper based on the main results are also included.

Sammendrag

Når nye politisk styrende strategier for å stoppe økningen av globale utslipp utvikles og implementeres, får energibruk i bygningssektoren større fokus. Å utvikle og bruke grønne energiløsninger blir derfor i enda større grad viktig.

En ny innovativ hybrid solcelle- og solfangermodul (PVT) er under utvikling. Denne har en høyere produksjon av elektrisitet enn et vanlig solcellepanel, og i tillegg omgjør den innstrålt solenergi til varmeenergi som videre kan utnyttes i en varmepumpe. Den produserte elektrisiteten kan brukes til å drive varmepumpa og løfte temperaturen på den absorberte varmen slik at den kan brukes til oppvarming i bygninger.

Denne masteroppgaven undersøker modellering og simulering av ei PVT-solassistert varmepumpe med arbeidsmediumet R290 (propan) til oppvarming av vann fra 7 °C til mellom 55 og 65 °C.

I den første delen av prosjektet ble energisystemet foreslått og en numerisk simuleringsmodell utviklet i MATLAB. Modellen er en numerisk transient termodynamisk simuleringsmodell med korte tidssteg på rundt ett minutt. Modellen kan brukes til å simulere hvordan den PVT-solassisterte varmepumpa opererer i et energiperspektiv med korte transiente oppløsninger som minutter, timer og dager. Den kan også brukes for lengre tidsperioder til evaluering og analyse av årlig energiytelse. Siden modellen simulerer den transiente ytelsen til systemet kan den også brukes til å designe en regulator og kontroll til kompressoren. Den andre delen av prosjektet er en mulighetsstudie der den solassisterte varmepumpa opererer i det kalde klimaet i Trondheim i Norge. Gjennomførbarhet med tanke på både energiytelse og økonomi ble undersøkt, og i tillegg ble påvirkningen fra forskjellige systemkonfigurasjoner evaluert.

Resultatene viser at den PVT solassisterte varmepumpa kan oppnå en COP på 2.8 på vinteren og 5.8 på sommeren når den varmer vann fra 7 °C til mellom 55 og 65 °C i Trondheim. Den presterer også bedre energimessig og fører til lavere netto levert elektrisitet enn tradisjonell luft-til-luft varmepumpe (21 %) eller elektrisk oppvarming (67 %). En konsekvens av dette er at energikostnaden gjennom året blir redusert. Selv om det krever en større investering for PVT solassistert varmepumpe sammenlignet med luft-til-luft varmepumpe eller elektrisk oppvarming, er den totale årlige kostnaden gjennom levetiden lavere.

For optimalisering og parametrisk analyse viser resultene at ved å øke PVT-arealet, øker både COP og varmekapasiteten til den PVT solassisterte varmepumpa litt. Ved bruk av en større kompressor for å øke varmekapasiteten til systemet blir COP betydelig redusert hvis ikke PVT-arealet også økes.

Som en ekstra oppgave er det også laget forslag til et utkast for en vitenskapelig artikkel basert på hovedresultatene i arbeidet.

Content

List of symbols

Symbol	Definition	Unit
h	Specific enthalpy	kJ/kg
η	Efficiency	-
τ	Transmittance factor	-
α	absorption ratio	
β_{pv}	Temperature coefficient	1/K
β_p	Packing factor	-
ε	Emissivity	-
σ	Stefan-Boltzmann constant	W m^{-2} K^{-4}
$\varkappa$	Thermal conductivity	W/(m*°C)
ρ	Density	kg/m^3
δ	Material thickness	m
Π	Pressure ratio	-
λ_c	Volumetric efficiency	-

List of therms

Term	Definition
PVT	Photovoltaic thermal
PV	Photovoltaic
TES	Thermal energy storage
DHW	Domestic hot water
SH	Space heating
RE	Renewable energy
HP	Heat pump
LMTD	Logarithmic mean temperature difference
COP	Coefficient of performance
MAE	Mean absolute error
NMAE	Normalised mean absolute error
GWP	Global warming potential
CW	Cold city water
HX	Heat exchanger
EEV	Electronic expansion valve
PVT-SAHP	Photovoltaic thermal solar assisted heat pump

List of Figures

List of Tables

1 Introduction

The pertaining issue which is often referred to as global warming has become a well-known topic for most people. Increased global emissions to the atmosphere since the industrial revolution are continuing to rise, although many countries are currently in the process of addressing the problem. To limit the global warming and temperature rise in the atmosphere, and secure a sustainable planet for future generations, this trend must be reversed.

One of the most influential sectors to these emissions is the building sector, contributing with large amounts of energy consumption, in addition to embedded emissions from both construction and demolition. The high-tempo development of urban areas results in even larger activity, and special focus in the planning of future energy systems must be given to achieve low-emission and low energy solutions.

This thesis investigates the feasibility and performance of a solar energy system for utilisation in buildings, with special focus on heating.

A novel Photovoltaic-thermal (PVT) module which may generate more than 10 % electricity than that of the normal PV module and can also output thermal energy with about 40 % of the received solar radiation is under development [1–3]. The power from PVT module can be used for driving heat pump to further lift the temperature of heat from PVT module and thus meet the regiments for comfortable heating [4].

1.1 Purpose and problem to be addressed

The system which will be analysed is a solar Photovoltaic-thermal (PVT) heat pump energy system, delivering both heat and electricity. By developing a mathematical- and simulation model to represents the physical behavior of the system, the performance can be evaluated in different surroundings and operating conditions. The ability to investigate the performance of the system using simulations will be of great use in the design stage of energy systems for low-carbon neighbourhoods and buildings.

The proposed system is a solar assisted heat pump system using a novel roll-bond PVT module. It includes a roll-bond PVT direct expansion evaporator, compressor, condenser, and an expansion valve.

The aim of this master thesis is to contribute to development of the mathematical model of the proposed system and to investigate the performance under Trondheim and Shanghai climate conditions.

The following research questions are set out to be investigated in this report:

1. What mathematical model, simulation tools and methods are used in the literature for performance analysis of combined PVT and heat pump system.
2. Is using a PVT + heat pump system feasible in the Nordic climate of Trondheim, Norway?
3. How do the PVT + heat pump system behave under transient and dynamic operation?
4. Which system configuration parameters mainly affect the energy performance, and what is the best configuration for the proposed system?
5. Which operation strategies and control could be used in the system?
6. Which main considerations should be done when designing a PVT + heat pump system for residential building utilisation?

1.2 Outline

This thesis is divided into seven main chapters. **Chapter 2** gives an introduction to the terminology and technical aspects of the PVT, heat pump, system control and integrated energy system through a literature review ; **Chapter 3** explains the method used to develop and validate the proposed energy production system and simulation model. It also contains a description of the case study, proposal of key performance indicators, and method for error analysis and economic analysis ; in **Chapter 4**, the simulation model is described in detail. First, an overview of the modelled system is provided, followed by the model development story, giving insight into the process and the different versions of the model. Next, an in-detail description of the model components and their solution methods is included, leading to the final model and algorithm for solving it. As a last part of the chapter, the model is validated using comparisons with experimental data.

Chapter 5 presents and discusses the results from the case study in Trondheim, Norway, including a feasibility analysis for both energy performance and economics, followed by optimisation in regards to system specifications and control strategy.; Finally **Chapter 6** provides the conclusions of the thesis. In addition, further work on the topic are proposed in Chapter 7.

2 Theory and Literature Review

This chapter provides the necessary background theory needed to understand and evaluate the PVT+HP system and answer the research questions. It contains short introductions, literature review, description of the composition and working principle for both solar PVT and heat pumps at the start. Next, the combination of the two are reviewed. Lastly, system control, integrated energy system and simulation tools for modelling and performance analysis are presented.

2.1 Solar PVT

The photovoltaic thermal (PVT) panel was first introduced by Wolf [5] in 1976. Since then, large amounts of research have been done to develop the system, and an overview of recent scientific review papers can be seen in Table 2.1. The PVT harvest the solar energy by converting it into both useful electric and thermal energy. Compared to the more common photovoltaic (PV) panel, the PVT can therefore achieve a higher overall energy efficiency.

There are many ways of composing a PVT module in regards to both components, structure and layout. The main components of the PVT are the PV panels and the thermal absorber. Other components include glass cover, electrical insulation, and thermal insulation. An example of the composition of a PVT module is depicted in Figure 2.1.

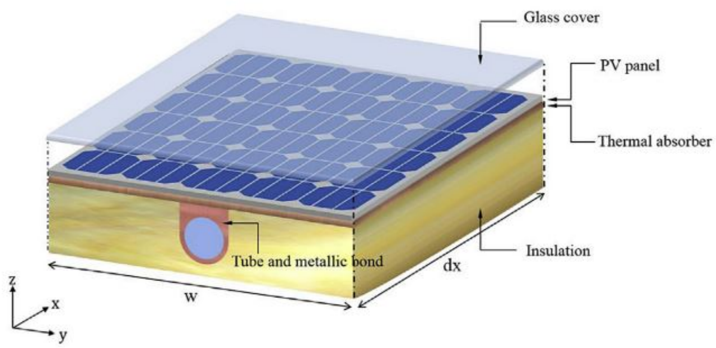

Figure 2.1: *Graphical view of the composition of a PVT [6].*

The thermal absorber of the PVT module can be amongst other:

- Copper tubes
- Microchannels
- Roll-bond panel

Most PVT modules are fairly similar in that PV panels are covered with a glass cover to minimize the heat loss to the ambient [7]. Glazed PVT collectors have lower heat loss, but also lower electric efficiency due to reduced solar radiation absorption [7]. Although, the higher heat gain of the glazed PVT (10-30 %) is relatively larger than the decrease in electric efficiency (1-10 %) compared to the unglazed PVT [8]. A covered PVT will therefore be more efficient when evaluating the energy efficiency of the system.

Chandrasekar and Senthilkumar [9] investigated the development in PVT technology in the last 50 years, by structuring and categorizing a various published review articles. This was done to make an easy reference guide for researchers and professionals working with the topic. The review articles were grouped into 11 major themes, with regards to the goals and scopes of the articles.

Table 2.1: *Review articles on PVT.*

Authors	Year	Topic
Chandrasekar and Senthilkumar [9]	2021	Review of PVT Review articles
Mohanraj et al. [10]	2018	Solar assisted HP modelling and modifications
Mohanraj et al. [11]	2018	Solar assisted HP applications
Good et al. [12]	2015	Hybrid PVT systems in buildings
James et al. [13]	2021	Thermal analysis of PVT + HP systems
Good et al. [12]	2015	Hybrid PVT systems in buildings
Good, Andresen, and Hestnes [14]	2015	Solar energy in nZEB buildings

2.1.1 Working principle

The PVT harvest the solar energy by converting it into both useful electric and thermal energy. PV panel on the top produce electricity using the energy in the incoming solar radiation, and some of the energy are absorbed as heat in the thermal absorber.

The global solar radiation at a horizontal surface (G_h) is described using the direct horizontal radiation (B_h) and the diffuse horizontal radiation (D_h) (Equation 2.1).

$$G_h = B_h + D_h \tag{2.1}$$

The effective solar radiation (G_{eff}) hitting the PV panel surface:

$$G_{eff} = \alpha_p * I * A_{pv} \tag{2.2}$$

The PV panels electrical efficiency (η_e) can be calculated using the panel electrical efficiency at reference conditions (η_{rc}) and the temperature coefficient (β_{pv}) (Equation 2.3). These values are obtained by the producer of the panels through real life experimental tests. The reference efficiency is the electrical efficiency at a certain reference panel temperature, most commonly 25 °C. By testing the panel at other temperatures, an efficiency "map" is obtained, and the temperature coefficient can be calculated. This value, with the unit of [1/ K] describes the sensitivity of the electrical efficiency to operating temperature change in the panel.

$$\eta_e = \eta_{rc} \left[1 - \beta_{pv}(T_p - T_{rc})\right] \tag{2.3}$$

The total power output from the PV panel then becomes [4]:

$$P_{pv} = A_{pv} I \tau_{g,pv} \alpha_p \beta_p \eta_{pv} \tag{2.4}$$

A_{pv} is the PV area [m^2], I is the solar radiation intensity (insolation) [W/m^2] at the panel surface, $\tau_{g,pv}$ is the PV glazing cover transmittance factor [-], α_p and β_p are respectively the absorption ratio and packing factor of the PV cells.

Heat absorbed by the PVT panel can then be described as in Equation 2.5 [4]:

$$Q_{abs} = (1 - \eta_e) \cdot A_{pv} \cdot I \cdot \tau_{g,pv} \cdot [\alpha_p \cdot \beta_p + \alpha_b \cdot (1 - \beta_p)] \tag{2.5}$$

,where α_b is absorption ratio (-) of the baseboard.

2.1.2 Thermal model

The thermal model of the PVT can be describes using the three forms of heat transfer; Radiation, Conduction, and Convection.

Heat transfer due to **radiation** can be calculated using the radiative heat transfer coefficient and temperature difference. The radiative heat transfer coefficient (h_{rd}) due to radiation between two objects *a* and *b*, considering emissivity (ε), the Stefan-Boltzmann constant (σ=5.6703*10^{-8} $Wm^{-2}K^{-4}$) and temperature (T) [15]:

$$h_{rd} = \epsilon * \sigma * (T_a + T_b) * (T_a^2 + T_b^2) \tag{2.6}$$

The **conductive** heat transfer coefficient is described as:

$$h_{cd} = \frac{1}{R} = \frac{1}{\delta/\kappa} \tag{2.7}$$

Convective heat transfer is an intricate subject, and can not be determined in detail with one simple equation. Although, many empirical equations have been proposed which can be used to determine the heat transfer. Table 2.2 presents some empirical relations to represent the convective heat transfer coefficient (h_{cv}) as a function of wind speed (v_{air}).

Hu et al. [16] investigated how wind speed, tilt angle, and dust deposition influences the convective heat transfer coefficient.

Table 2.2: *Convection heat transfer coefficient empirical relations.*

Equation	Reference	Comment
$h_{cv} = 2.8 + 3 * v_{air}$	[17]	0< v_{air} < 7 m/s
$h_{cv} = 5 + 4.5 * v_{air} - 0.14 * v_{air}^2$	[15]	windward, v_{air} <10 m/s
$h_{cv} = 5 + 4.5 * v_{air}$	[15]	leeward, v_{air} <8 m/s
$h_{cv} = 18 * \sqrt{\frac{v_{air}}{L}}$	[15]	L=Length of surface
$h_{cv} = 25 + 1.2 * v_{air}$	[18]	
$h_{cv} = 6.9 + 3.87 * v_{air}$	[19]	v_{air} < 1.12 m/s
$h_{cv} = (13.07 + 2.18 * 0) + (3.65 - 0.26 * 0) * v_{air}$	[16]	0< v_{air} < 7 m/s, tilt angle = 0°
$h_{cv} = (13.07 + 2.18 * \frac{\pi}{6}) + (3.65 - 0.26 * \frac{\pi}{6}) * v_{air}$	[16]	0< v_{air} < 7 m/s, tilt angle = 30°

Heat loss (Q_{loss}) to the surroundings is described using the heat loss coefficient (U_{loss}):

$$Q_{loss} = A_{pv} * U_{loss} * (T_a - T_{pv}) \tag{2.8}$$

Important parameters to evaluate the thermal efficiency of a PVT is the heat removal factor (F_R) and efficiency factor (F') [20]. The efficiency factor is an indicator of the thermal efficiency of the PVT module using the local fluid temperature of the refrigerant. Heat removal factor is the same but utilising the inlet fluid temperature instead. In simpler therms, the heat removal factor describes how much of the total absorbed heat (Q_{abs}) can be transferred to the fluid. The remaining portion of the absorbed heat is either lost to the ambient or used to increase the temperature of the PV cells. Efficiency factors (F') for PVT and solar evaporator can be found in Yao et al. [20].

By implementing the heat removal factor, the heat gain of the fluid in the PVT (Q_u') can be described using the heat loss coefficient (U_{loss}), inlet fluid temperature (T_f) and ambient temperature (T_a) [20]:

$$Q_u{}' = A_{pv} * F_R * [(\tau_{g,pv}\alpha_p) * I * (1 - \eta_{pv}) - U_{loss} * (T_f - T_a)] \tag{2.9}$$

The **thermal capacity** of the PVT module affect the sensitivity of the PV temperature, and the possible amount of stored heat energy in the module. Armstrong and Hurley [21] proposed a thermal capacity model of a PV module, to be able to investigate the dynamic temperature behaviour and thermal response time of the PV. It describes the thermal capacitance ($C_{material}$) of a material as:

$$C_{material} = \rho c_p A \delta \tag{2.10}$$

,where ρ, c_p, A, and δ are respectively the density, specific heat capacity, surface area, and thickness. Each layer of the PV module is evaluated separately to determine the total thermal capacitance of the PV module:

$$C_{pv} = A_{pv} * \Sigma(\rho c_p \delta) \tag{2.11}$$

2.2 Heat Pump

2.2.1 Working principle

The most simple heat pump cycle, which is used to describe the working principle of the HP, includes the evaporator, compressor, condenser and expansion valve (Figure 2.2). Heat is transferred from the heat source to the working fluid in the evaporator (Q_e), evaporating the fluid from liquid/gas-state to gas-state. The gas is then compressed to a higher pressure and higher temperature in the compressor using electricity (W_c), before heat is dissipated to the heat sink through condensation of the working fluid (Q_c).

The thermodynamic properties of the working fluid in the simple heat pump cycle can be expressed using the four state points 1,2,3, and 4. These represent the evaporator outlet, compressor outlet, condenser outlet and valve outlet/evaporator inlet respectively. The performance of the heat pump cycle is defined either by the heating- or cooling COP:

$$COP_{heat} = Q_c / W_c \tag{2.12}$$

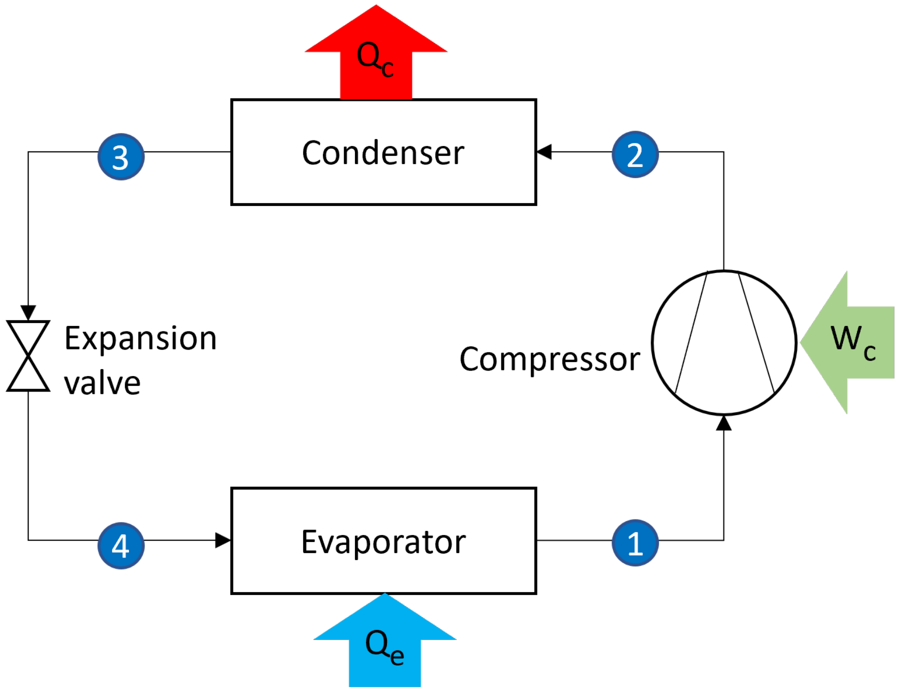

Figure 2.2: *Schematic view of a simple vapor compression heat pump cycle.*

$$COP_{cool} = Q_e/W_c \tag{2.13}$$

2.2.2 Components

Evaporator

The heat rate (Q_{evap}) transferred from the heat source to the refrigerant in the evaporator can be expressed as

$$Q_e = \dot{m}_R * (h_1 - h_4) \tag{2.14}$$

,where $\dot{m}_R$ is the refrigerant mass flow rate [kg/s], h_1 and h_4 is specific enthalpy (kJ/kg) at evaporator outlet and inlet respectively.

Compressor

The work by the compressor with isentropic compression ($w_{c,is}$, [kJ/kg]) (no losses) is described using the enthalpy at compressor outlet ($h_{2,is}$), and enthalpy at compressor inlet (h_1):

$$w_{comp,is} = (h_{2,is} - h_1) \tag{2.15}$$

Due to internal operation losses in the compressor, the actual compressor work can be described using the isentropic compressor efficiency (η_{is});

$$w_{comp} = \frac{h_{2,is} - h_1}{\eta_{is}} = \frac{w_{comp,is}}{\eta_{is}} \tag{2.16}$$

Some of the compressor work is not transferred to the refrigerant due to heat loss to the surroundings (q_{hl}). The heat loss is often given as a fraction of the compressor work, making the actual outlet enthalpy:

$$h_2 = h_1 + w_{comp} * (1 - q_{hl}) \tag{2.17}$$

The volumetric efficiency of the compressor can be expressed using Equation 2.18 [22]. $\dot{V}_{displ}$ is the displacement volume [m^3/s] and ρ is the density of the refrigerant on the suction side.

$$\lambda = \frac{\dot{m_R}}{\dot{V}_{displ} \cdot \rho(T_{suction}, p_{suction})} \tag{2.18}$$

The mass flow of the refrigerant can be decided using either compressor equations (2.19) or (2.20):

$$\dot{m}_R = \frac{\lambda_c V_{disp}}{\nu} \tag{2.19}$$

$$\dot{m}_R = \frac{N}{60} * \rho_{comp,in} V_{th} \lambda_c \tag{2.20}$$

λ is volumetric efficiency, N is the rotational speed of the compressor (rpm), V_{th} is theoretical suction volume [m^3/round].

Using Equation 2.16 and Equation 2.20, the power consumption of the compressor (W_{comp} [kW]) becomes

$$W_{comp} = \dot{m}_R * w_{comp} \tag{2.21}$$

Condenser

Delivered heat rate in the condenser is described by:

$$Q_c = \dot{m}_R * (h_2 - h_3) \tag{2.22}$$

Heat transferred through the condenser is calculated using the condenser overall U-value (U_c), heat exchanging area (A_c), and the logarithmic mean temperature difference (LMTD).

$$Q_{cond} = U_c * A_c * LMTD_c \tag{2.23}$$

LMTD is:

$$LMTD = \frac{\Delta T_1 - \Delta T_2}{ln \frac{\Delta T_1}{\Delta T_2}} \tag{2.24}$$

where ΔT_1 and ΔT_2 is the temperature difference (thermal length) between the two fluids at each side of the condenser.

The absorbed heat (Q_{sink}) by the secondary fluid (heat sink) in the condenser can be calculated using Equation 2.25.

It is a product of the temperature difference of the fluid at inlet and outlet (T_{in} and T_{out}), isobaric specific heat (C_p) and mass flow rate ($\dot{m}$) of the secondary fluid.

$$Q_{sink} = \dot{m}_{sink} * c_p * (T_{out} - T_{in}) \tag{2.25}$$

The refrigerant pressure is relieved in the **expansion valve**, and temperature also decreases as a consequence. Because of only minor losses in this process, it can be described as isenthalpic:

$$h_4 = h_1 \tag{2.26}$$

2.2.3 Working fluids

In 2016, the Kigali Amendment to the Montreal Protocol was signed, in which a commitment to phase out HFCs (Hydrofluorocarbons) due to high GWP was made [23]. The need for using environmentally friendly refrigerants in heat pump system are therefore receiving increasingly more attention [24]. Natural fluids such as ammonia (R717), propane (R290) and carbon dioxide (R744) can provide refrigerant solutions with low Global Warming Potential (GWP) and Ozon Depletion Potential (ODP), but also maintaining the energy efficiency required to provide sustainable heating [25, 26]. Due to R744 having a GWP of 1, being non-flammable and non-toxic, it has emerged as one of the most prominent working fluids for usage in heat pump and refrigeration systems [27]. R290, R1270, R290, R152a, R744 and HC/HFC mixtures are found to provide the best low-GWP alternatives for heat pump applications in the future [28]. Table 2.3 presents properties of some common relevant working fluids used as refrigerants.

Table 2.3: *Working fluids for heat pump applications. [29]*

ASHRAE number	Type	GWP	T_{crit} [°C]	P_{crit} [bar]
R134a	HFC	1300	101.1	40.6
R152a	HFC	138	113.3	45.2
R290	HC	3.3	96.7	42.5
R600a	HC	4	134.7	36.3
R717	Inorganic	0	132.3	113.3
R744	Inorganic	1	31.0	73.8
R1234yf	HFO	<1	94.7	33.8

Sánchez et al. [30] investigated the energy performance of low-GWP refrigerants R1234yf, R1234ze(E), R600a, R290 and R152a compared to using the more usual high-GWP R134a. The refrigerants were replaced with R134a in a refrigeration system using a compressor designed for R134a. The authors concluded that R290 gave the best cooling capacity and COP, with an increase of 41-67 % and 3-22 % respectively. Although, a larger compressor work was needed to achieve this, meaning the compressor displacement can be decreased to achieve the same cooling capacity as the R134a system. Use of R152a was found to increase the COP slightly (1-5 %), while using R1234yf, R1234ze(E) and R600a reduces both cooling capacity and COP. Sánchez et al. [29] later optimised the refrigerant mass charge by changing compressor according to the thermophysical properties and operation performance of the refrigerant. They concluded that using R290, R152a, R744 and R600a could reduce the energy consumption, with the former achieving the highest reduction of 28 %.

Longo et al. [31] conducted an energy assessment of the refrigerants R600a, R1234ze(Z) and R1233zd(E) for use in low-pressure heat pump applications, concluding that they can be valuable long-term replacements to traditional low-pressure HFC refrigerants. Ozsipahi et al. [32] experimentally investigated the effect of R290 on the performance of a variable speed compressor. They concluded that the energy performance using R290 instead of R600a is increased, with COP being 10-20 % higher.

Using micro-channel heat exchangers to reduce the refrigerant charge, thus reducing flammability concerns, has become more popular lately [33]. The use of a micro-channel evaporator will therefore be favourable if flammable refrigerants such as R290 are utilised in a heat pump.

2.3 PVT solar assisted heat pump

Since the electrical efficiency of the PV panels in the PVT decrease due to increasing temperature (Equation 2.3 and Equation 2.4), it is advantageous to keep temperature as low as possible to achieve the highest possible electric power output. To achieve this, some kind of cooling need to be assorted to the PV panels, which in done by the structure of the PVT, removing heat through the fluid channels. By combining the PVT and a heat pump to utilise the PVT heat, synergies can be achieved; The performance of the HP cycle could be improved due to better conditions in the evaporator, and the HP can enhance the energy quality of the collected solar heat energy by lifting the temperature level. This system combination is referred to as a Photovoltaic-thermal solar assisted heat pump (PVT-SAHP) or simply PVT+HP.

A PVT-SAHP can be categorised into two main types, and several sub types [34], depicted in Figure 2.3. The two main types, Direct expansion (DX) and Indirect (IDX) expansion system, refers to how the PVT is utilised in the heat pump system. In the former, PVTs replace the evaporator of the HP cycle and refrigerant are flowing directly through the PV, gaining heat through an evaporation process. In the latter, the PVT is instead placed in a secondary loop, utilising it as more of a traditional solar collector, and the working fluid (most often water) flows to the secondary side of the evaporator as the heat source of the HP system.

The sub types of the PVT-SAHP system are categorised according to the heat source. Either a single-source, using only the heat from the PVT, or a dual-source, which includes an additional heat source (e.g. air or ground) is utilised. A dual-source system can be more appropriate if the solar heat is not enough to fulfill the requirements of for the system, which is especially relevant during cold or cloudy times.

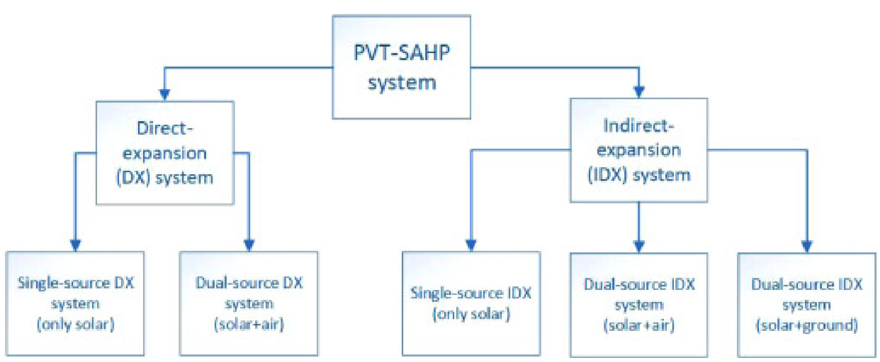

Figure 2.3: *Categorisation of PVT-SAHP systems. From Alessandro et al. [34].*

Table 2.4: *Articles on PVT and heat pump combined.*

Authors	Year	Topic	PVT Type
Braun et al. [35]	2020	Trigeneration with PVT for ZEB office buildings	
Zhou et al. [36]	2019	Roll-bond PVT + HP system	Roll-bond DX
Gunasekar and Mohanraj [37]	2016	PVT + HP evaporator (circular or triangle)	DX PVT
Yao et al. [3]	2021	Roll-bond PVT + HP	DX PVT

James et al. [13] reviewed the thermal analyses performed in literature of PVT+HP systems. Both the modelling of the collectors in regards to temperature prediction, electric performance and heat transfer coefficients with ambient influencing factors, and the modelling of the heat pump system were evaluated. Limitations and further research needs are also presented, in which amongst others the need for investigation of environmentally friendly refrigerants in the system. The authors grouped the PVT+HP into six sections:

- photovoltaic-thermal air collectors
- photovoltaic-thermal liquid collectors
- direct expansion photovoltaic-thermal collectors
- photovoltaic-thermal collectors as condensers
- control of heat pumps using renewable energy
- future environmentally friendly refrigerant options

Yao et al. [20] theoretically investigated the efficiency factor of the two-phase flow channel pattern of the direct expansion photovoltaic-thermal collector (PVT evaporator). The results and conclusions was further used to investigate the two-phase flow channel pattern of the PVT evaporator experimentally [3]. The authors optimized the fluid pattern, and proposed a hexagon-grid coupled fluid channel unit with one-way arrangement. The system had significant improvement in temperature uniformity, thermal and electrical efficiencies, and hydraulic behaviour. The authors concluded that the solution could reduce the working temperature of the PV module significantly. The investigated system is schematically depicted in Figure 2.4.

Yao et al. [4] proposed a dual source DX parallel PVT/air-source HP system combined with a build-in PCM storage and heating for buildings. The algorithm used for deciding the COP of the system by numerical simulation were based on hourly steady state conditions.

Chen, Riffat, and Fu [38] experimentally studied the energy performance of PVT+HP system using a glass vacuum tube type PV panel using R134a in Nottingham, England. They found that the COP increased with increasing radiation with COP ranging from 2.9 to 4.6 with a condenser water supply temperature of 35 °C and radiation from 200-800 W/m^2.

Yao et al. [39] proposed a district heating system consisting of a deep borehole heat exchanger (DBHE) and dual source DX PVT SAHP (Figure 2.5) connected in series. The DBHE will provide heat at temperatures up to 30-40 °C, and the HP will further lift the temperature to reach the system requirements.

The simulation of a PVT+HP system can be solved in many different ways. According to the complexity of the system and the desired detail level of the model, it can either be mass-transfer models, or thermodynamic models, steady state considerations or transient processes etc. Steady state can be utilised to simulate a system with short

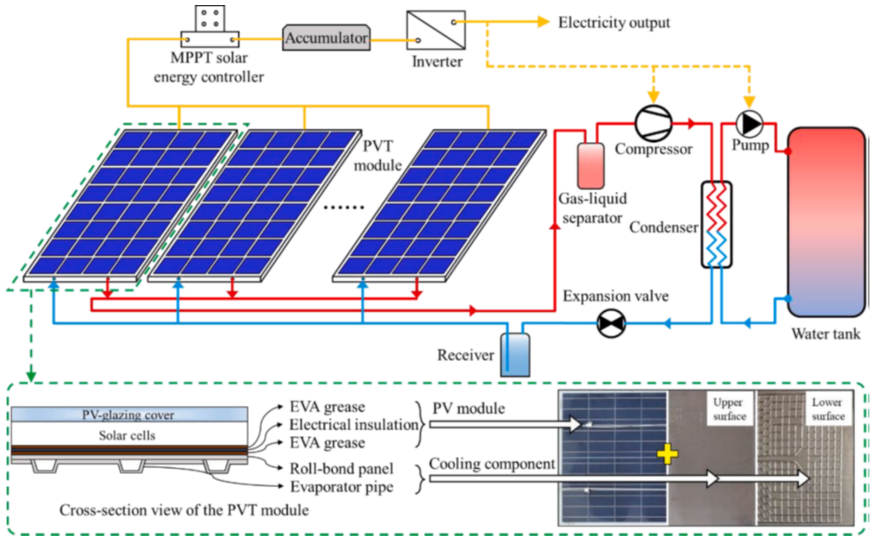

Figure 2.4: *The DX SAPVT-HP system proposed by Yao et al. [3] in 2021.*

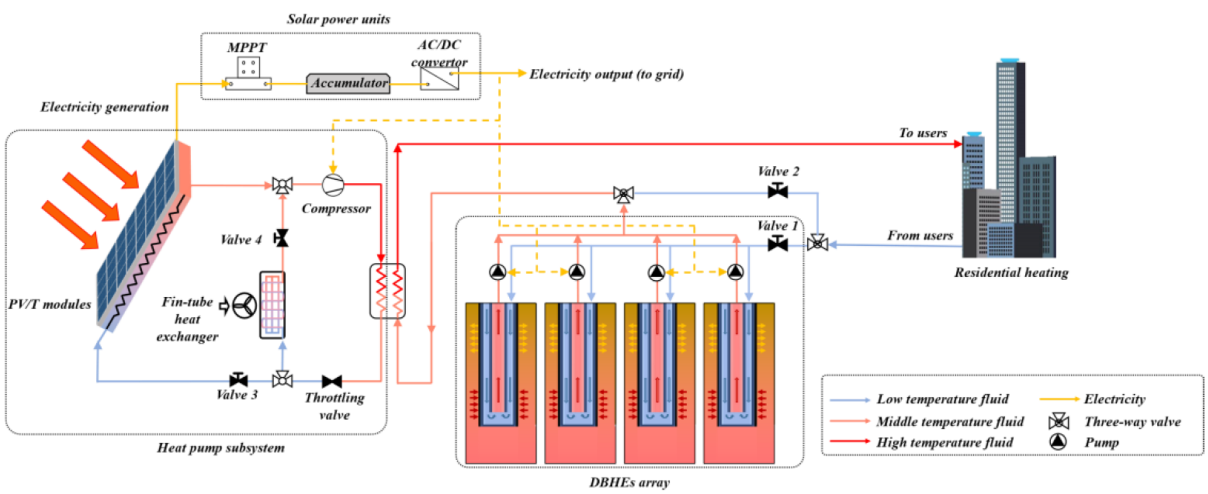

Figure 2.5: *The proposed district heating system by Yao et al. [39].*

response time (time-constant) compared to the time step in the simulation, e.g hourly/daily/weekly simulations, when the dynamic behaviour of the system is not under investigation, but rather the behaviour with given boundary conditions. These models are often simplified to a certain extent, and are useful for quick analyses of the system characteristics. If the transient behaviour is going to be considered more complex models needs to be developed, taken into account the time specific parameters of the system and their influence on each other.

The type and subtype of the PVT-SAHP also influences the intricacy of the system. In a direct expansion system the two-phase flow of refrigerant in the PVT-evaporator will need to be considered, while in a indirect expansion system only the liquid phase could be considered. Also, using a double source system complicates the modelling.

There are some examples of modelling and simulation of PVT-SAHP systems in the literature. For example, Zhou et al. [17] developed and verified a numerical simulation model of a DX PVT HP system using microchannel PVT evaporator. Cai et al. [40] proposed an air/PVT dual source HP using copper tube PVT evaporator, and made a numerical simulation model of the system. They evaluated the performance and behaviour of the system from influence of parameters as ambient temperature, solar irradiation and packing factor. Faria et al. [41] developed a dynamic simulation model of a solar evaporator CO_2 HP.

2.4 System control

Because of variable operating conditions (outdoor temperature, wind speed, solar radiation etc.) for the PVT, the load on the PVT-evaporator in a DX SAHP will fluctuate accordingly. If a constant capacity compressor is used, there will be a mismatch between the compressor and PVT-evaporator when the operating conditions deviate significantly from the design values [42]. The varying heat source temperature has to be taken into consideration in any heat pump system, but due to having an extra influencing factor (solar insolation), the operation of a solar evaporator will be somewhat different.

Chaturvedi, Chen, and Kheireddine [42] investigated the use of a a VSD/VFD (Variable speed drive / Variable frequency drive) in a DX SAHP system utilising a solar collector as the evaporator. The authors conclude that such a system significantly improve the thermal performance, compared to using a constant capacity compressor. Especially with reduced speed in the summer, when the solar insolation and ambient temperature is high, but heating load is relatively low.

This mismatch between the load on the evaporator and the compressor operation is also of interest when using a PVT as the evaporator. Although having similar thermal characteristics as the solar collector, the electric efficiency should in addition be taken into consideration. Because the temperature in the PVT has an opposite effect on the thermal COP and the electrical efficiency of the system, the operation should be modulated/optimised to provide the best overall efficiency.

There are several ways that the overall system performance can be evaluated, and controlling it according to them can lead to different optimal operation methods. It can be separated into two main categories, i.e. exergy analysis and energy analysis. Using an exergy analysis will take into consideration the higher energy quality of the electrical power compared to the thermal power.

In addition to evaluate the control strategy in regards to energy performance, safety and practical operation considerations must also be taken. Du, Wu, and Wang [43] proposed a new control method of an R290 air-source HP for low temperature conditions, improving the reliability and dynamic control strategy for the R290 HP.

2.5 Integrated energy system

A pertaining issue with renewable energy production is the mismatch in time between production and energy load. Utilising renewable sources such as solar, energy can only be produced when the solar radiation is sufficient. The time at which this happens can be unreliable and sometimes there is no production at all for an amount of time. With solar radiation being at its highest during specific times of the day, a mismatch between the power produced and the load of a system occurs, as can be seen in Figure 2.6.

The energy produced from the renewable source which exceeds the load demand is regarded as oversupply. By including an energy storage system, this surplus energy can be stored and used at times when the renewable production is low, thereby increasing the self-sufficiency of the energy system. The self-sufficiency ratio (SSR) of the system can be described as:

$$SSR = \frac{E_{prod,renewable} + E_{storage-load}}{E_{load}} \tag{2.27}$$

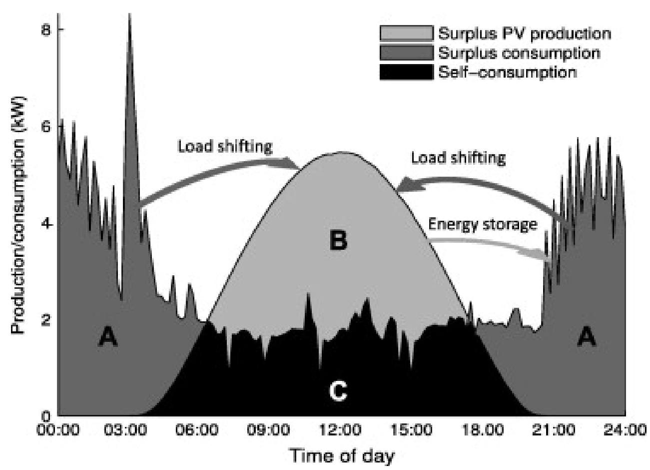

Figure 2.6: *Mismatch between produced PV power and load side power demand [44].*

The system performance of an integrated energy system with PV, HP, battery, and TES can be evaluated by considering the ability to use the produced energy locally. Two KPIs which can be used are Self Sufficient Ratio (SSR) and Self consumption Ratio (SCR):

$$SSR = \frac{E_{pv-load} + E_{bat-load} + E_{TES-load}}{E_{load}} = \frac{E_{load} - E_{grid-load}}{E_{load}} = 1 - \frac{E_{grid-load}}{E_{load}} \tag{2.28}$$

$$SCR = \frac{E_{pv-load} + E_{pv-bat} + E_{pv-TES}}{E_{pv}} = \frac{E_{pv} - E_{pv-grid}}{E_{pv}} \tag{2.29}$$

An oversupply index or Supply-Demand ratio (SDR) is described as [45]:

$$SDR = \frac{\Sigma\left(P_{RE-load} + P_{ESS-load} + P_{losses} + P_{dump}\right)}{\Sigma P_l - \Sigma P_{NS}} \tag{2.30}$$

Describing the SSR and SCR in simple terms:

Self-sufficiency is the fraction of the provided energy to meet the load that comes from the RES (PV+Storage). i.e. what portion of the load is not provided by grid energy.

Self-consumption is what fraction of PV production is either used directly for the load or stored locally. For example, with an infinitely large energy storage, the SCR would be 1 for any renewable production.

3 Method

To provide insight into the process of obtaining the results and answering the research questions, this chapter describes the methods used in this work. First, the work process is shortly presented with an overview of the tasks to be conducted, followed by a short presentation of the utilised software. Next, the method for the model development is swiftly explained, as a preview of the more in-depth description in Chapter 4. Key performance indicators for the work and system in then presented, and the method for model validation continues afterwards. As the last parts of the chapter, the case study in Trondheim, Norway is described, and method used for economic analysis finishes the chapter.

3.1 Work process

The work starts by creating a research plan for the project period, containing phases, specific tasks, and a timeline. This is done to be able to maintain a systematic overview and track the progress of the project.

The first task to be conducted is a literature review of the current status of PVT, HP, and PVT+HP systems, evaluating the recent progress and state of the art solutions in the field. Since the author possesses no specific knowledge of PVT modules and systems, a lot of time is used in the start to build a sufficient knowledge base.

An analysis of mathematical models used to describe PVT+HP systems is then done, followed by an analysis of simulation tools used for investigating the performance of the system.

The next task, to propose a suitable mathematical model and simulation method/tool for investigating the system, is done starting with a simple mathematical model and developing a working simulation. Since no model for the PVT system or the heat pump system is provided before or supplemented during the project period, the simulation model is to be made from scratch.

It will first be made an attempt of creating the simulation model in TRNSYS. Other simulation tools are also considered in the first stage of the project period according to appropriateness.

3.1.1 Simulation tools

The most popular building performance simulation (BPS) softwares are IDA ICE, TRNSYS and EnergyPlus [46]. TRNSYS is a graphically based software mainly developed and used for transient simulation of energy systems. It could be used in the simulation of PVT systems [9, 35, 47–51], and also HP systems [52, 53]. MATLAB could be used to code a dynamic model and simulate the system, but demands more in-depth knowledge, mathematical knowledge and modelling skills than TRNSYS. Others possible simulation tools which could be used are IDA ICE, a software developed for dynamic simulations of buildings performance, EnergyPlus, Excel, Fortran and Python.

The available PVT models in the standard TRNSYS component library are:

- Concentrating Collectors
  - Constant losses (Type 50g and Type50e)
  - Top Loss f(Wind, Temp) (Type50h and Type 50f)
- Flat Plate Collectors
  - Angular dependence of Transmitance (type 50c)

- Constant Losses (Type50a)
- Losses=f(T,WS,G and t=f(angle) (Type50d)
- Loss=f(Temp,wind,geometry) (Type50b)

The first attempt of creating the simulation model is in TRNSYS, using generic components to build a working system. Since the standard library does not have thermophysical properties of the relevant working fluids or model of a a direct expansion HP, it is not a plug-and-play modelling.

The second attempt of modelling is to use TYPE155 to connect TRNSYS to a MATLAB script containing the heat pump model. This do not work because compatibility problems arises when importing the CoolProp database into MATLAB.

Type62 is then attempted used to be able to connect to an Excel file containing the properties, but compatibility issues when running the simulation gives no results. This is due to the CoolProp database missing out from the Excel file when connecting it to TRNSYS.

Due to the complications with simulating the system in TRNSYS, a decision is made to develop the model from scratch in MATLAB. The model development will later in this chapter and the next chapter be described in detail.

3.1.2 Software

Fluid properties databases contains tabulated thermophysical properties, which can be extracted to find wanted properties at certain states. Examples of these are REFPROP and CoolProp.

REFPROP (REFerence fluid PROPerties), developed by National Institute of Standards and Technology (NIST), calculates thermodynamic and transport properties of fluids and mixtures of them using the most accurate models available [54]. Three models for thermodynamic properties of pure fluids are used:

1. Equations of state explicit in Helmoltz energy
2. The modified Benedict-Webb-Rubin equation of state
3. Extended corresponding states (ECS) model

3.2 Model development

Development of the numerical simulation model is done in an iterative process containing many steps.

The first step of the modelling is drawing an overview figurative schematic containing all components of the system and their interconnections. Next, functionality descriptions and mathematical representation of each component's separate physical behaviour is provided.

3.3 Key Performance Indicators

To be able to evaluate the energy system, some key performance indicators are proposed. These will be used when analysing the system with different specifications and operation control. The main KPI for the system is the heating COP, which is abbreviated and referred to as only "COP" for the rest of the thesis. The overall COP for the system, also containing the electrical power production from the PVs, is also included to be able to integrate the increased

PV production/efficiency from the PVT Equation 3.1 [13].

$$COP_{sys} = \frac{Q_{cond} + (\frac{P_{pv}}{0.38})}{W_{comp}} \tag{3.1}$$

To evaluate the self-sufficiency of the PVT+HP, battery, and TES system, the SSR as described in Equation 2.28 is used. Because of the duality of the PVT+HP system comprising both thermal and electrical production, two separate SSRs, thermal (SSR_{th}) and electric (SSR_{el}) are proposed:

$$SSR_{th} = \frac{Q_{TES-HeatLoad} + Q_{cond-HeatLoad}(\frac{P_{pv-comp}+P_{bat-comp}}{W_{comp}})}{Q_{HeatLoad}} \tag{3.2}$$

$$SSR_{el} = \frac{P_{pv-comp} + P_{bat-comp} + P_{bat-el.heat}}{P_{el.heat} + W_{comp}} \tag{3.3}$$

The parameters used for the SSRs can be seen in Table 3.1, and all of the proposed KPIs for the whole system can be seen in Table 3.2.

Table 3.1: *Parameters used to evaluated the renewable energy system (RES).*

Parameter	Label	E nergy type
PV electrical production	P_{pv}	electricity
PVT thermal production	Q_{evap}	heat
Power from PV to compressor	$P_{pv\text{-}comp}$	electricity
Power from PV to battery	$P_{pv\text{-}bat}$	electricity
Power from PV to grid	$P_{pv\text{-}grid}$	electricity
Power from grid to compressor	$P_{grid\text{-}comp}$	electricity
Power used by top heater	$P_{el.heat}$	electricity
Heat from TES to DHW	$Q_{TES\text{-}DHW}$	heat

Table 3.2: *KPIs for the proposed system.*

Parameter	Label	Unit
Coefficient of performance	COP	-
Average coefficient of performance	COP_{avg}	-
System COP	COP_{sys}	-
Condenser heat rate	Q_{cond}	W
Compressor consumption	W_{comp}	W
PVT thermal efficiency	$\eta_{pvt,th}$	-
Self consumption rate	SCR	-
PV efficiency	$\eta_{pv,el}$	-
PV production improvement	$E_{pv,el,imp}$	-
Net present value	NPV	EUR
Annual cost		EUR/year
GHG emissions		$kgCO_2$-eq/kWh

3.4 Model validation

To validate the simulation model, experimental data from a test rig are used. The data are gathered in February 2022 in Shanghai, China. The test rig is located at the top of an educational building at the Shanghai Jiao Tong University (SJTU). It consists of 24 PVT modules, a heat pump host, water tank, cooling tower, water pump, piping, necessary electrical equipment for the PVs, and piping.

Because of restrictions due to the covid-19 pandemic, resulting in long periods of lockdown at the SJTU, the planned experiments could not take place. The lockdowns also lead to difficulties retrieving data from earlier experiments, and consequences of this are restricted amount of data.

The performance of the system from the experimental test rig are evaluated by measuring certain parameters at specific places in the system. The measurements are done read in intervals of one minute for the solar radiation and one second for the rest of the parameters. An overview of the main measurement components are presented in Table 3.3.

Table 3.3: *Measurement components for test-rig in Shanghai, China.*

Parameter	Component type	Label
Ambient temp.	Temperature sensor (Air)	T_a
Solar radiation	Sensor	I
Condenser secondary side water flow	Flow meter	m_w
Condenser secondary side temperature - Inlet	Temperature sensor (Water)	$T_{w,in}$
Condenser secondary side temperature - Outlet	Temperature sensor (Water)	$T_{w,out}$
System power (Compressor+water pump)	Digital power meter	P_{sys}

A snippet from the acquired data are depicted in Figure 3.1. Wind speed is not measured in the test-rig and is set to 2 m/s for the validation simulation. Compressor power (W_c) is calculated by subtracting the pump power from the system power (P_{sys}), in which the pump power is assumed constant at 1080 Watts. Condenser power (Q_{cond}) and COP are calculated using Equation 2.25 and Equation 2.12 respectively:

$$Q_{cond} = \dot{m}_w * c_p * (T_{w,out} - T_{w,in})$$
$$COP = \frac{Q_{cond}}{W_c}$$

To be able to evaluate the accuracy and reliability of the simulation model and results, quantification of the error compared to the experimental data is needed. Parameters that could be used are the Mean Bias Error (MBE) or Mean absolute error (MAE) , where n is the sample size (number of data point or time-steps), $x_{mod,i}$ and $x_{exp,i}$ are the value of model results and experimental results [55]:

$$MBE = \frac{1}{n}\sum_{i=1}^{n}(x_{mod,i} - x_{exp,i}) \tag{3.4}$$

$$MAE = \frac{1}{n}\sum_{i=1}^{n}|x_{mod,i} - x_{exp,i}| \tag{3.5}$$

	T_w,in	T_w,out	T_a	m_w	P_sys	W_c	Q_cond	COP
	°C	°C	°C	m3/h	W	W	W	-
28.02.2022 12:10	23.2	30	18.2	6.7	5997	4917	53153.333	10.81011
28.02.2022 12:10	23.2	30	18.2	6.7	5997	4917	53153.333	10.81011
28.02.2022 12:10	23.2	30.1	18.2	6.7	5997	4917	53935	10.96909
28.02.2022 12:10	23.2	30.1	18.2	6.7	5975	4895	53935	11.01839
28.02.2022 12:10	23.2	30.1	18.2	6.7	5975	4895	53935	11.01839
28.02.2022 12:10	23.2	30.1	18.2	6.7	5975	4895	53935	11.01839
28.02.2022 12:10	23.2	30.1	18.2	6.7	5975	4895	53935	11.01839
28.02.2022 12:10	23.2	30.1	18.2	6.7	5975	4895	53935	11.01839
28.02.2022 12:10	23.2	30.1	18.2	6.7	5960	4880	53935	11.05225
28.02.2022 12:10	23.2	30.1	18.2	6.7	5960	4880	53935	11.05225

Figure 3.1: *Snippet of acquired data from PVT+HP test rig in Shanghai.*

Although providing a magnitude of the error, MBE and MAE does not shows the error relative to the value of the parameter. To evaluate this, i.e. the importance of the error, a Normalized mean absolute error (NMAE, [%]) is introduced [55]:

$$NMAE = \frac{\sum_{i=1}^{n} |x_{mod,i} - x_{exp,i}|}{\sum_{i=1}^{n} x_{exp,i}} \tag{3.6}$$

The threshold for marking the simulation model as reliable is set to a maximum NMAE (Equation 3.6) of 20 % for all key parameters. Keeping all the simulated parameters within this tolerance can be considered good enough for simulating the performance and system behaviour at this stage in the research of the PVT-SAHP system.

3.5 Case study

The building modelled in the case study is a 150 m^2 residential family house with two floors located in Trondheim, Norway. It is assumed built in the 1990s, and the energy requirements in the Norwegian building regulation from 1987 (TEK87) is used as a foundation for input values. Relevant TEK87 and TEK 17 building energy requirements, as well as a comparison to an nZEB proposal, are provided in Table D.1, and specifications for the case study building is provided in Table 3.4.

The heating demand for the building is simulated in the simulation software SIMIEN [56]. An electric heating system with unlimited capacity is used to calculate the heating power for each hour during the year, with a set point for the room temperature of 22 °C. The building is modelled as one energy zone, and the internal loads (Figure 3.2) are gathered from the Norwegian standard SN-NSPEK 3031 [57]. Ventilation rates are set according to the minimum requirements in TEK17 [58].

To investigate the yearly energy- and economic performance of the system, several configurations of the PVT-SAHP system is evaluated and compared against all-electric heating and an ASHP system. The different system configurations can be seen in Table 3.5. The ASHP is set to cover 90 % of the space heating demand for the year, and an SCOP of 3.0 is used in the simulations. The electric efficiency for the electric boiler is set to 0.9.

Table 3.4: *Specifications for the building used in the case study.*

Parameter	Input	Comment
Heated floor area	150 m^2	
Floors	2	
Area per floor	75 m^2	
Floor height	3 m	
Facade lengths	$\sqrt{75}$ m	
Window area	15 % of BRA	
Windows	8	One at each facade at each floor
Window area	2.8 m^2	Included frame area
Heat from equipment	60 %	Fraction of equipment load
Heat from lights	100 %	Fraction of lights load
Heat from occupants	1.5 W/m^2	
Heating set point	22 °C	Room temperature set point

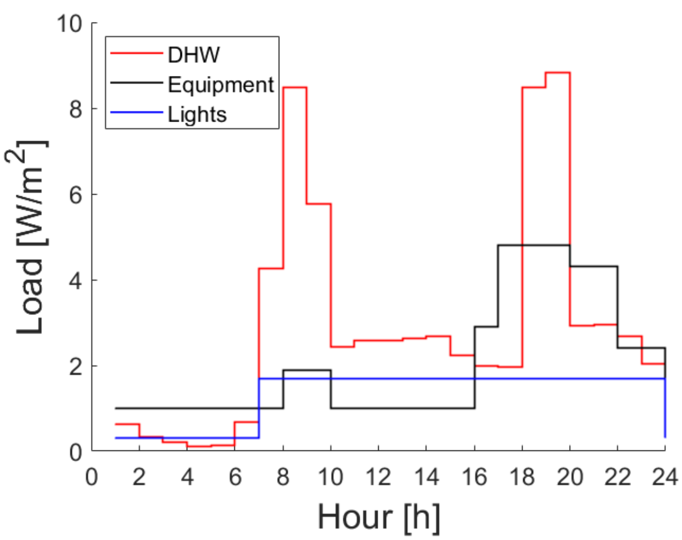

Figure 3.2: *Internal loads through the day for a Norwegian residential family house. [57].*

Table 3.5: *Evaluated case study system configurations.*

Label	Abbreviation	Configuration	PVTs	PVs
Base	El.only	Electric boiler	0	0
1A	ASHP	Base + ASHP	0	0
1B	ASHP+3PVs	Base + ASHP and PV	0	3
1C	ASHP+6PVs	Base + ASHP and PV	0	6
1D	ASHP+12PVs	Base + ASHP and PV	0	12
2A	3PVT-SAHP	Base + PVT-SAHP	3	0
2B	6PVT-SAHP	Base + PVT-SAHP	6	0
2C	12PVT-SAHP	Base + PVT-SAHP	12	0

3.6 Economic analysis

The economic feasibility of the PVT-SAHP system is evaluated using the annual cost method. This is done to be able to compare it to the other energy system configurations with different component lifetimes. The discount rate is set to 4 %, and the electricity price to 1 NOK/kWh.

The parameters used in the economic analysis can be seen viewed in Table 3.6. The investment cost per PV module is calculated based on the cost per rated power (0.47 $/W), to have the same rated power as the PVT module. This parameter is multiplied with the rated power of the PVT, which is 360 W. The investment cost of one PV module then becomes 1658 NOK/module, using a currency rate of 10 NOK/$.

Table 3.6: *Parameters used in the economic analysis.*

Parameter	Value	Unit	Note
Electricity cost	1	NOK/kWh	
PVT module cost	2935	NOK/module	
PVT module rated power	360	W/module	
Compressor cost	4116	NOK/(10^{-5}m^3	
PV investment cost	0.47	$/W	
ASHP investment cost	4286	NOK/kW	
PVT additional component cost	15 000	NOK	
Discount rate	0.04	-	

4 Simulation Model

To further explain the simulation model and the method used to solve the PVT-SAHP system, this chapter includes an in detail explanation of the proposed system, components and the numerical system solving approach. Although most of the chapter is to be seen as description of the method for achieving the results in Chapter 5, the numerical simulation model, solving approach and algorithm can be viewed as results themselves, which could be further developed or used in other simulation work for the proposed system.

4.1 Model overview and working principle

The system modelled in this work is a single-source DX PVT-SAHP system using R290 (Propane) as the refrigerant. It is modelled and simulated in MATLAB. The thermophysical properties of the refrigerant and water are extracted from the REFPROP database using a plug-in dll. A simplified schematic of the investigated PVT-SAHP can be seen in Figure 4.1.

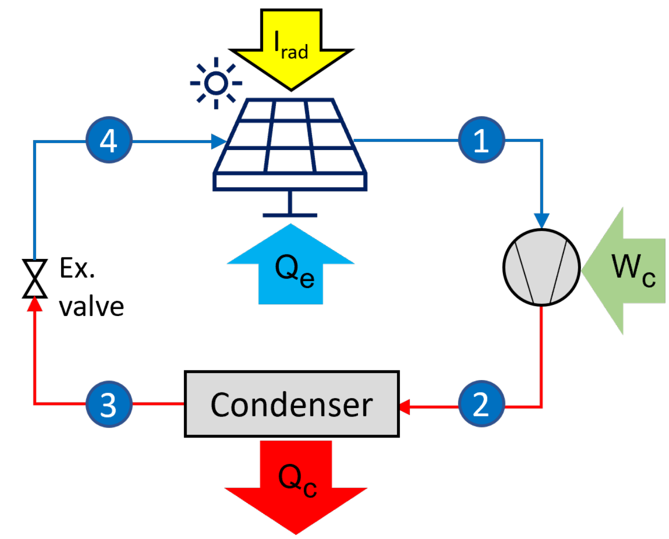

Figure 4.1: *Components, energy flows, and thermodynamic state points for the PVT-SAHP system.*

In addition to the renewable energy (RE) production system (PVT-SAHP), the building energy system consist of two other subsystems: thermal energy storage (TES), and load side system (building model). The main components in the RE production is PVT, compressor, condenser, expansion valve, and pump. The energy storage is a water tank, and the building model consist of a HX to the production subsystem, electric boiler (boiler), space heating heat exchanger (HX), DHW tap, pump and several valves to control the water flow. A principal system schematic are visualised in Figure 4.2.

The energy flows in the system is solar radiation (I_{rad}), PVT evaporator heat transfer (Q_e), compressor work (W_c), condenser heat transfer (Q_c), electricity to boiler (P_{boil}), heat to space heating (Q_{SH}), and DHW tap heat (DHW or Q_{DHW}).

The **working principle** and main **operation strategy** of the energy system is hierarchy-based, and it provides both heating and electricity to the building. The PVT-SAHP subsystem produces electricity from solar radiation in the

PVT module, in addition to transferring heat to the refrigerant in the in the cycle through an evaporation process. The heat is transferred to either the TES, DHW or space heating (SH) through heating of water in the secondary loop. If the RE heat production (Q_c) is larger than the demand (Q_{DHW}+Q_{SH}), the surplus heat is stored in the TES. On the other hand, if the demand is larger than the RE heat production, there are two options. Either provide the remaining power from the TES or the boiler. Using the energy storage is the preferred solution, and then the boiler is operated when necessary. Listing the strategy in a ranked order it becomes:

1. If RE heat production > Heat load => Store surplus heat
2. If RE heat production < Heat load => Use RE+TES to provide deficit heat to load
3. If RE heat production < Heat load and the TES can not provide sufficient power => Use boiler to provide deficit heat to load

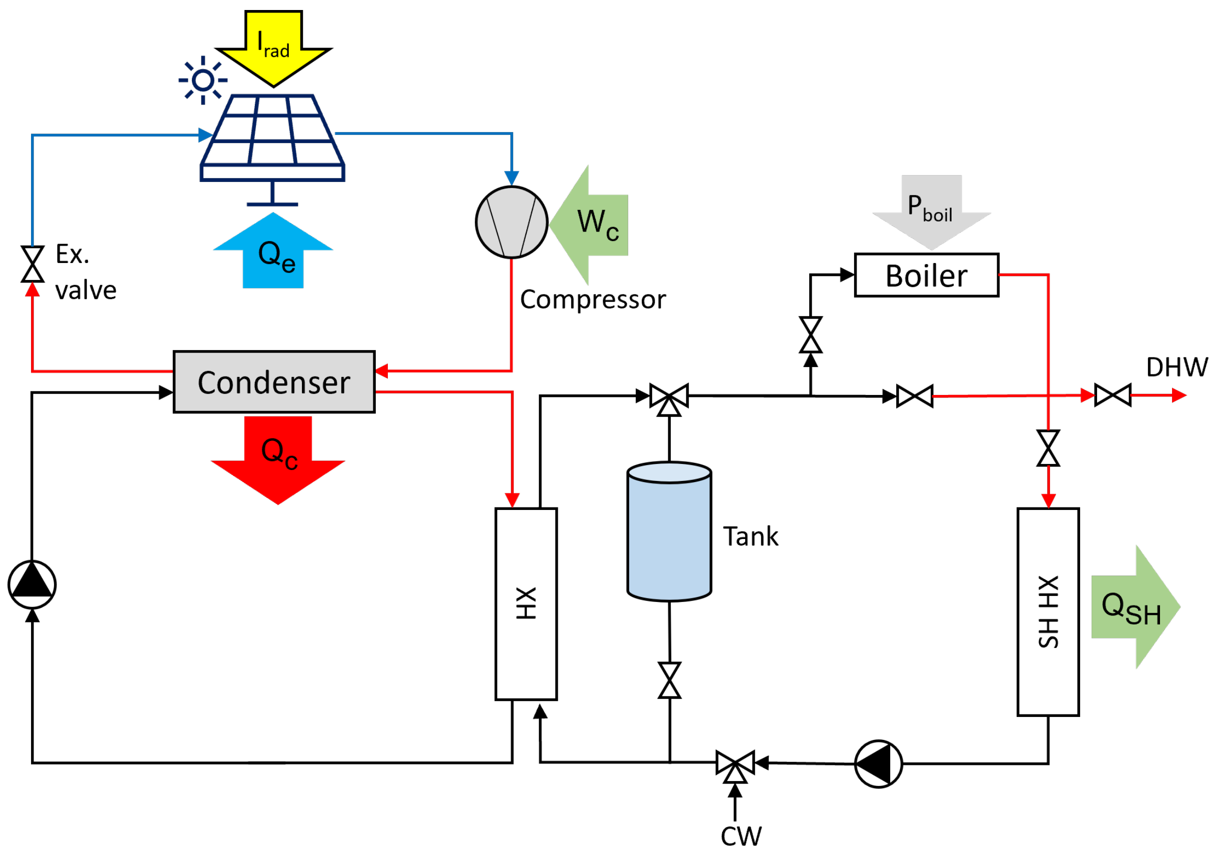

Figure 4.2: *Schematic diagram for the whole energy system. Including both energy production (PVT+HP and boiler), energy storage (tank), and load side model. Ex.valve = expansion valve; HX = Heat exchanger; CW = Cold city water; DHW=Domestic hot water; I_{rad}=Solar radiation; Q_e=Evaporation heat transfer; Q_c=Condenser heat transfer; W_c=Compressor work; P_{boil}=Boiler power; Q_{SH}=Heat transfer to space heating.*

4.2 Model description

Describing the PVT-SAHP system simulation model is done by going through each component in an iterative manner in this section. The mathematical models are represented with references to the theory in section 2, inputs and outputs of each component model is presented, in addition to the solution strategy.

4.2.1 PVT evaporator model

The PVT evaporator model is based on transient energy balance in the component, in which the evaporator heat rate (Q_{evap}) is equal to the useful heat transfer rate (Q_u) and energy conservation of the control volume which is the PVT component.

Assumptions for the PVT evaporator model:

- Uniform temperature distribution across the PV surface.
- No pressure loss for the refrigerant flow
- Uniform heat transfer coefficient between the roll-bond and the refrigerant (not taking into account the change from liquid/2-phase/gas)
- Ground temperature is the same as the ambient temperature

The transient balance equation (energy conservation) can be described as:

$$C_{pv}\frac{\delta T_{pv}}{\delta t} = G_{eff} - P_{el,pv} - Q_{loss} - Q_{evap} \tag{4.1}$$

m_{pv} is the mass [kg] of the PV module, c_{pv} is specific heat of PV [J/(kgK)], δT_{pv} and δt is change in PV temperature and time respectively, G_{eff} is effective solar irradiation (Equation 2.2), $P_{el,pv}$ is the electrical power production (Equation 2.4), Q_{loss} is heat loss from the PV, and Q_{evap} is heat transfer to the refrigerant in the evaporator.

Heat transfer rate (Q_{th}) from the PV cells to the refrigerant (Equation 4.2):

$$Q_{th} = Q_u = Q_{abs} - Q_{loss} \tag{4.2}$$

,where Q_u is the total useful solar heat received by the PVT and Q_{loss} is the overall heat loss in the PVT.

The heat loss (Q_{loss}) is calculated using overall heat loss coefficient (U_{loss}), PVT collector area (A_{pvt}) and temperature of PV cells (T_p) and ambient air (T_a):

$$Q_{loss} = U_{loss} \cdot A_{pv} \cdot (T_{pv} - T_a) \tag{4.3}$$

U_{loss} is calculated as [20]:

$$U_{loss} = \left[\frac{1}{h_{cd,p-c} + h_{rd,p-c}} + \frac{1}{h_{cv,c-a} + h_{rd,c-a}}\right]^{-1} \tag{4.4}$$

,where cd is conduction, rd is radiation, cv is convection, "p" is pv panel, "c" is glazing cover, and "a" is ambient.

The radiative and conductive heat transfer coefficients are found using Equation 2.6 and Equation 2.7, while convective heat transfer coefficients is calculated with the correlation from Hu et al. [16] :

$$h_{rd,p-c} = \epsilon_p * \sigma * (T_p + T_c) * (T_p^2 + T_c^2) \tag{4.5}$$

$$h_{rd,c-a} = \epsilon_p * \sigma * (T_c + T_a) * (T_c^2 + T_a^2) \tag{4.6}$$

$$h_{cv,c-a} = (13.07 + 2.18 * 0) + (3.65 - 0.26 * 0) * v_{air} \tag{4.7}$$

$$h_{cd,p-c} = \frac{1}{\delta_c / \kappa_C} \tag{4.8}$$

The useful energy gain which can be transferred to the refrigerant can be described as [20]:

$$Q'_u = 12 * \frac{1}{2} * \frac{W}{\sqrt{3}} * \frac{T_{pv} - T_R}{\frac{1}{D} * (\frac{\delta_{eva}}{\kappa_{eva}} + \frac{\delta_{ei}}{\kappa_{ei}} + \frac{\delta_{rb}}{\kappa_{rb}}) + \frac{1}{h_{eq} * \pi * D}} \tag{4.9}$$

W is the roll-bond fluid-channel pattern width, D is roll-bond fluid channel width, δ is the layer thickness of eva grease (eva), electric insulation (ei) and roll-bond panel (rb), while h_{eq} is equivalent heat transfer coefficient between roll-bond panel and refrigerant. For further description of the PVT module with roll-bond layout and parameters, see Yao et al. [20].

Because the evaporating process is isothermal in a DX evaporator, the refrigerant temperature (T_R) is the same as the evaporation temperature (T_{evap}) through the whole component, and the heat removal factor (F_R) is then equal to the efficiency factor (F') [20], and:

$$F_R = F' \tag{4.10}$$

Using Equation 2.9, Equation 4.9, Equation 4.10, the efficiency factor is calculated as:

$$F' = 12 * \frac{1}{2} * \frac{W}{\sqrt{3}} * X2 * \frac{1}{A_{pv}} * \frac{1}{X1} \tag{4.11}$$

where "X1" is

$$X1 = (\tau_{g,pv} \alpha_p) * I * (1 - \eta_{pv}) - U_{loss} * (T_{evap} - T_a)$$

and "X2" is:

$$X2 = \frac{T_{pv} - T_{evap}}{\frac{1}{D} * (\frac{\delta_{eva}}{\kappa eva} + \frac{\delta_{ei}}{\kappa_{ei}} + \frac{\delta_{rb}}{\kappa_{rb}}) + \frac{1}{h_{eq} * \pi * D}}$$

The calculated efficiency factor (F')(Equation 4.11) is then used to obtain the useful heat gain (Q_u') through Equation 2.9:

$$Q_u{}' = A_{pv} * F' * [(\tau_{g,pv} \alpha_p) * I * (1 - \eta_{pv}) - U_{loss} * (T_{evap} - T_a)]$$

The heat transfer from the PV to the roll-bond evaporator is assumed to be ideal, with no pressure losses. The evaporation heat transfer is then described as:

$$Q_{evap} = Q'_u \tag{4.12}$$

Equation 4.12, Equation 2.9 and Equation 2.14 is used to check if the energy balance in the PVT evaporator is reached for a given time step, I.e check if the HP thermodynamic cycle and PVT component has the same Q_{evap}. If the difference between the two sides of the equation is larger than a set tolerance criteria, the evaporation temperature is adjusted. The new evaporation temperature is calculated using Equation 2.9:

$$T_{evap} = \frac{(\tau_{g,pv}\alpha_p) * I * (1 - \eta_{pv}) - \frac{Q_{evap}}{A_{pv} * F'} + U_{loss} * T_a}{U_{loss}}$$

Table 4.1: *Inputs, outputs, and parameters for the PVT evaporator model.*

Parameter	Label	Value	Unit	Inp/Outp	Type
PVT area	A_{pv}	1.68	m^2/module	Input	Constant
Solar irradiation	I	Variable	W/m^2	Input	Disturbance
Ambient temp.	T_a	Variable	K	Input	Disturbance
PV efficiency at ref. temp.	η_{rc}	0.19	-	Parameter	Constant
Temperature coefficient	β_{pv}	0.0039	1/K	Parameter	Constant
Reference temperature	T_{rc}	298.15	K	Parameter	Constant
Glazing cover transmittance	$\tau_{g,pv}$	0.9	-	Parameter	Constant
PV absorption ratio	α_p	0.85	-	Parameter	Constant
PV baseboard absorption ratio	α_b	0.8	-	Parameter	Constant
PV packing factor	β_p	1	-	Parameter	Constant
PVT heat loss rate	U_{loss}	Variable	$W/(m^2K)$	Parameter	Variable
PV temperature	T_{pv}	Variable	K	Output	Variable
PV efficiency	η_{pv}	Variable	-	Output	Variable
PV power	P_{pv}	Variable	W	Output	Variable
Useful heat gain	Q_u'	Variable	W	Output	Variable

The thermal capacitance of the PV module is calculated using Equation 2.11 and the module layer properties in Table C.1. All PVT model inputs, outputs, parameters and technical specifications are shown in Table 4.1.

The change in the PV-temperature is calculated using Equation 4.1:

$$\frac{\delta T_{pv}}{\delta t} = \frac{G_{eff} - P_{el,pv} - Q_{loss} - Q_{evap}}{C_{pv}}$$

The new PV temperature for the next time (t) then becomes:

$$T_{pv}(t) = T_{pv}(t-1) + \frac{\delta T_{pv}}{\delta t} * dt$$

4.2.2 Thermodynamic heat pump cycle model

Some assumptions are made for the heat pump cycle:

- No vapor at compressor inlet (X=1)
- Constant superheating after outlet of evaporator
- No pressure losses in condenser and PVT evaporator (isobaric)
- No pressure losses in the pipes (isobaric)
- Isenthalpic expansion valve

The inputs, outputs and parameters which are used in the simulation model are described in Table 4.2, and a principal ph-chart of the system thermodynamic refrigerant cycle with state points can be seen in Figure 4.3.

The thermodynamic state point calculation in the cycle is: $p_1 = p(T{=}T_{evap})$, then $T_1 = T(p{=}p_1,x{=}1)+\Delta T_{sh}$ and $h_2{=}h(T{=}T_1,p{=}p_1)$. To find state point two, first the isentropic compression is used to find 2': $h_{2,is}{=}h(p{=}p_{cond},s{=}s_1)$. Then, Equation 2.16 and Equation 2.17 is used to find h_2. h_3 is calculated at the saturation line as $h_3{=}h(p{=}p_{cond},x{=}0)$. finally $h_4{=}h_3$, and $T_4{=}T(p{=}p_1,h{=}h_4)$.

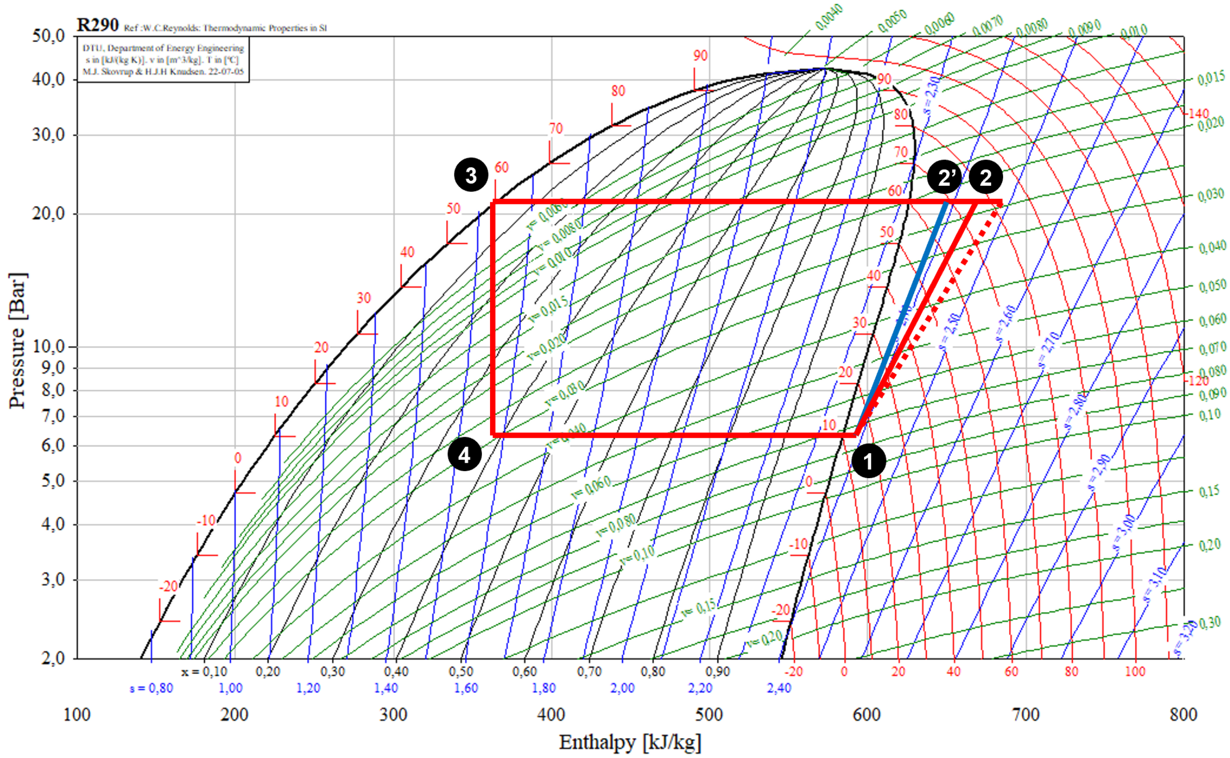

Figure 4.3: *Principal ph-chart for the PVT+HP system using R290. Blue line (2') is the state point if the compression was isentropic, dotted red line is if the compression was adiabatic, and red line (2) is real compression.*

The **compressor model** calculates the refrigerant temperature out of the compressor/into the condenser (T_2), enthalpy at compressor outlet (h_2), mass flow rate of the refrigerant ($\dot{m}_R$), and compressor work (W_c). Equations used are Equation 2.16, Equation 2.18, Equation 2.16. The inputs to the compressor model is refrigerant pressure (P_{evap}), density (ρ_1), enthalpy (h_1) and entropy (s_1) at the evaporator outlet; pressure (P_{cond}) in the condenser; and compressor speed (N). The isentropic and volumetric efficiencies are calculated using the compressor pressure ratio (Π). Since it is assumed no pressure losses in the heat exchangers or pipes, they become [4]:

$$\Pi = \frac{P_{cond}}{P_{evap}} \tag{4.13}$$

$$\eta_{is} = -0.17938 + 0.87501 * \Pi - 0.30014 * \Pi^2 + 0.04135 * \Pi^3 - 0.00206 * \Pi^4 \tag{4.14}$$

$$\lambda_c = 0.0011 * \Pi^2 - 0.0487 * \Pi + 0.9979 \tag{4.15}$$

Table 4.2: *Inputs, outputs, and parameters for the heat pump model.*

Condition	Label	Value	Unit	Input/output
Outdoor temperature	T_a	Variable	°C	Input
Condenser heat rate	Q_{cond}	Variable	W	Input
Condenser pressure	P_{cond}	Variable	bar	Input
PV temperature	T_{pv}	Variable	K	Input
Solar irradiation	I	Variable	W/m^2	Input
Compressor Isentropic efficiency	η_{is}	Variable	-	Input
Compressor volumetric efficiency	λ	Variable	-	Input
Temperature water into condenser	$T_{w,in}$	7	°C	Input
Temperature water out of condenser	$T_{w,out}$	55-65	°C	Input
Superheating out of evaporator	ΔT_{sh}	5	K	Input
Compressor heat loss	-	10	%	Input
Evaporating temperature	T_{evap}	Variable	K	Output
Evaporator heat rate	Q_{evap}	Variable	W	Output
Suction side pressure	P_{evap}	Variable	bar	Output
Refrigerant mass flow rate	$\dot{m}_R$	Variable	kg/s	Output
Water mass flow rate	$\dot{m}_w$	Variable	kg/s	Output

The **condenser model** is based on the LMTD and heat exchanger heat balance equations. Since the condensing temperature is "guessed" before the compressor model is solved, a loop is made to determine the actual temperature. The outlet water temperature is calculated using Equation 2.25 giving:

$$T_{w,out} = T_{w,in} + Q_{cond}/(C_{p,w} * m_w); \tag{4.16}$$

To calculate the new condensing temperature, Equation 2.24 and Equation 4.16 is combined [59]:

$$T_{cond} = \frac{T_{w,in} - T_{w,out} * e^{\left(\frac{T_{w,out} - T_{w,in}}{LMTD}\right)}}{1 - e^{\left(\frac{T_{w,out} - T_{w,in}}{LMTD}\right)}}$$

The available **evaporator** heat rate (Q_{evap}) for the given cycle is calculated using Equation 2.14.

4.3 Model development - First version

Through the continuous process of modelling the system and developing the numerical simulation model, many version have been used to simulate the system and the improving the model in an iterative manner. This section swiftly describes the modelling, solution method and algorithm of one of the first model versions.

The numerical simulation model used in the first version of the model is a steady-state approach where the condenser power (Q_{cond}) is exactly meeting a set heating demand for the load side. The simulation uses a successive-substitution approach solving for the PV temperature (Equation 4.17).

The temperature in the PV panels (T_{pv}) can be expressed using eqs. (2.4), (2.5), (4.2) and (4.3), which gives Equation 4.17. The variables in the simulation will then be T_{pv}, Q_{evap}, T_a and I.

$$T_{pv} = \frac{Q_{evap} - A_{pv}U_{loss}T_a - A_{pv}I\tau_{g,pv}\left[\alpha_p\beta_p + \alpha_b(1-\beta_p)\right]\cdot\left[1-\eta_{rc}-\beta_{pv}T_{rc}\eta_{rc}\right]}{A_{pv}\cdot\left(\eta_{rc}\beta_{pv}I\tau_{g,pv}\left[\alpha_p\beta_p + \alpha_b(1-\beta_p)\right] - U_{loss}\right)} \tag{4.17}$$

The residual is the amount which is left after a comparison of two values. It is in this case used to decide when steady state conditions in the PVT heat balance is reached, and defined as:

$$Residual = \left|\frac{T_{pv}(t) - T_{pv}(t-1)}{T_{pv}(t)}\right| \tag{4.18}$$

The algorithm used to solve the system and find the performance parameters is described below:

1. Input system boundary conditions and model parameters (PVT specs, refrigerant etc.).
2. Initialise t as time-step.
3. Input ambient temperature (T_a), solar irradiation (I) and heating load/condenser heat rate (Q_{cond}).
4. Guess the PV temperature (First guess is $T_{pv} = T_a$).
5. Calculate the evaporating temperature.
6. Calculate the state points of the heat pump cycle
7. Calculate mass flow rate (m_R)
8. Calculate compressor work (W_{comp}), condenser heat rate (Q_{cond}) and PVT evaporator heat rate (Q_{evap}).
9. Input PVT evaporator heat rate into the energy balance of PVT model to find PV temperature (T_{pv}).
10. Check residual.
    - If less than stopping criteria (<0.01 K), go to next step.
    - If more than stopping criteria, go to step 4 and repeat loop. New guess is new T_{pvt}.
11. Calculate COP and efficiencies.
12. Next time step, start at step 3 in this algorithm.

This steady state simulation model of the PVT+HP system is in a principal way working to simulate the energy performance of the system. Although, the accuracy is not nearly the same as the final model, and also the complexity and flexibility is not even close. This simple model can be utilised to evaluate the isolated performance of the PVT+HP as presented in Figure 4.1, but do not take into account the dynamic load of a building model.

4.4 Final model algorithm

The algorithm for the final model of the system:

1. Start.
2. Input simulation parameters, system specifications and component specifications.
3. Set initial conditions.
4. Input weather conditions from weather file.
5. Calculate heat pump refrigerant state point properties (pressure, enthalpy, temperature, entropy, density)
6. Run compressor model (Solve compressor equations).

7. Run condenser model.
8. Check difference between new and old condensation temperature.
    - If larger than convergence criteria, adjust condensation temperature and go back to step 5.
    - If convergence criteria reached, go to next step.
9. Run valve model.
10. Run PVT model.
11. Check energy balance, difference between useful heat and evaporation heat transfer.
    - If larger than convergence criteria, correct/adjust evaporation temperature and go back to step 5.
    - If convergence criteria is reached, go to next step.
12. Check if the outlet water temperature from the condenser (load side) is in the desired range ($T_{w,out,low} < T_{w,out}(t) < T_{w,out,high}$).
    - If outside of range, adjust water mass flow (m_w).
    - If OK, go to next step.
13. Output results for time-step t.
14. Solve PVT differential equation.
15. Check if t is the last time-step.
    - If YES, output simulation results.
    - If NO, go to next time-step (t=t+1).
16. Calculate new PV temperature for next time-step, and go back to step 4.

The compressor control is added as an own block. The controller reads the results, and based on that, provides the compressor speed as output. The compressor speed is then input at the start of each time-step. The flow diagram for the numerical simulation model for the PVT+HP system are presented in Figure 4.4.

Due to sensitivity in the temperature of the PV, a time-step of one minute is used for iterations of the system. For example, when simulating using a time-step of around 10 minutes, the PV temperature would increase significantly due to not taking changed heat transfer coefficients with each change in temperature into account. Hourly time-step is used for the weather data.

The convergence criteria for the condenser model (T_{cond}) is set to 0.01 and for the evaporator model (Q_u and Q_{evap}) to 0.05. See subsection 4.2 for further explanation of the convergence criteria.

The full MATLAB code for the numerical simulation model can be viewed in detail in Appendix B.

4.5 Model validation

To evaluate the model accuracy, experimental data from a middle scale solar PVT HP rig were compared to model results.

The PV temperature of the experimental rig were controlled to around 10 °C during the operation. It can be seen in Figure 4.5 that the simulated PV temperature drops to approximately this temperature after about 15-20 minutes of operation. Although the solar radiation is slightly fluctuating (440-510 W/m^2), the PV temperature is kept almost steady during the last 15 minutes of simulated operation. The accuracy of the PV temperature is the main parameter to validate the PVT-evaporator thermal model, and from the comparison, it seems that the model performs close to

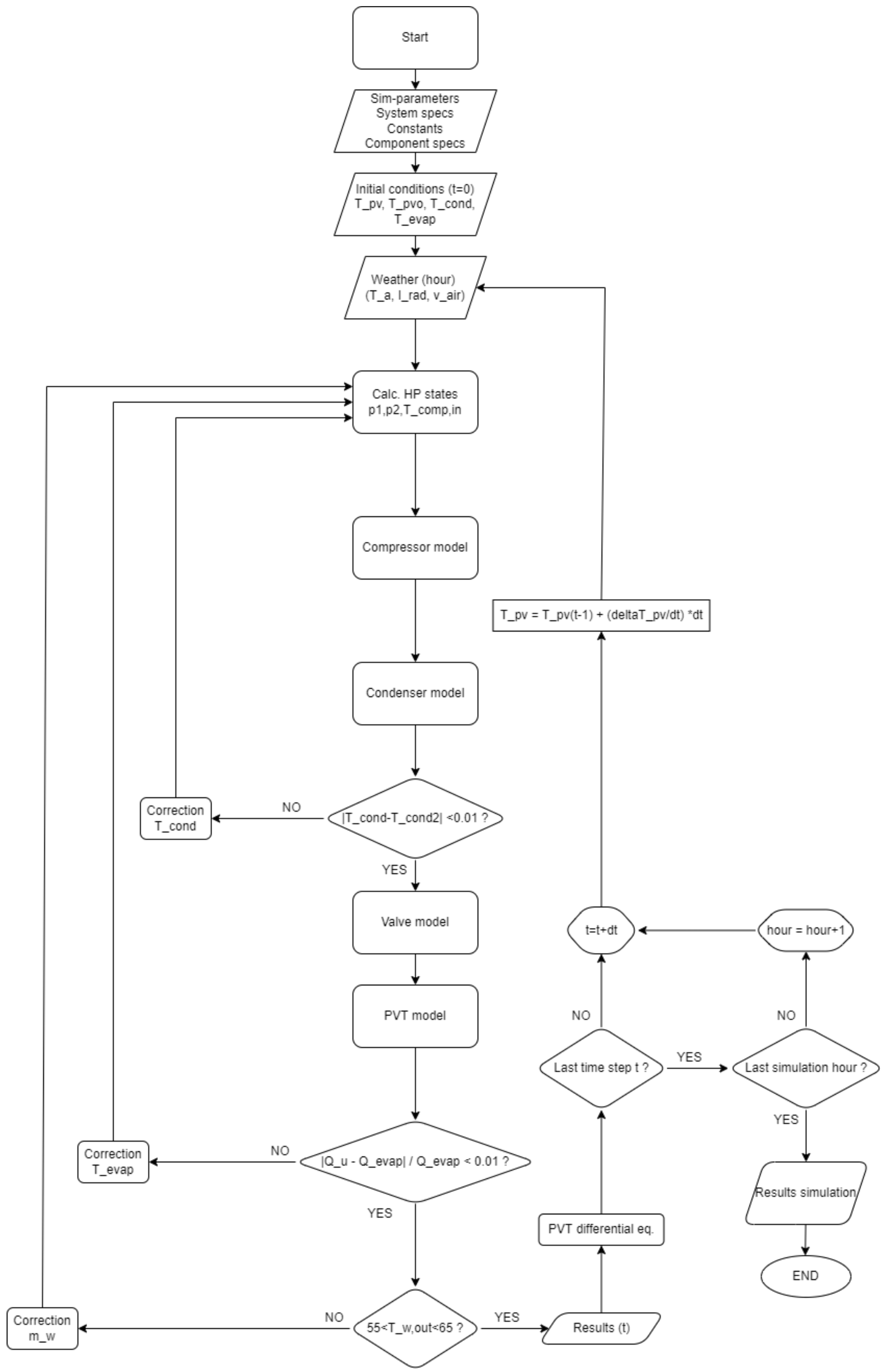

Figure 4.4: *Algorithm for numerical simulation model of the PVT-SAHP. Not including compressor control or load side model.*

reality.

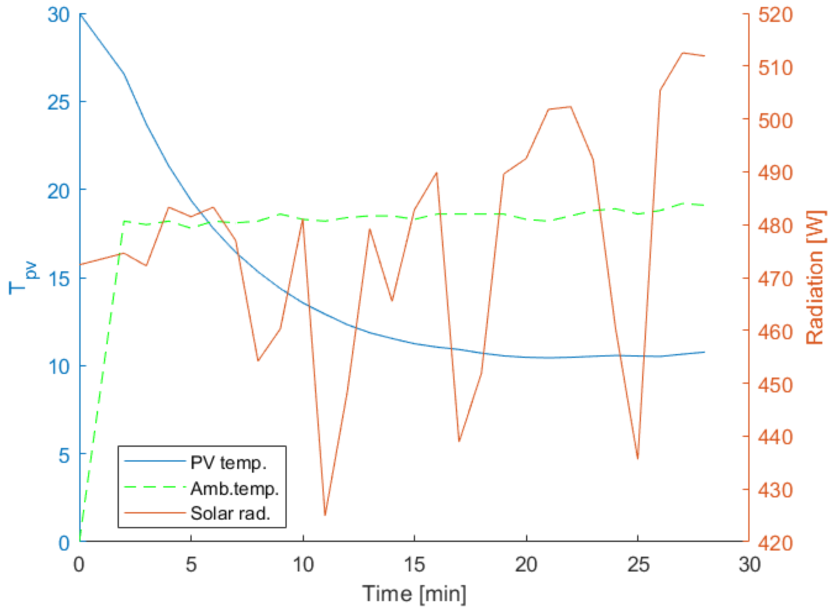

Figure 4.5: *Validation simulation results PV temperature. PV temperature (T_{pv}), ambient temperature (T_a), and solar radiation (I).*

The COP of the simulation model is lower than the COP of the experimental results (Figure 4.6a). The MAE is 1.5 and NMAE is 19 % for the simulation. The simulated COP has a smooth decline, due to smooth reduction of the PV temperature, but the experimental COP has more fluctuations. The experimental COP increases from 5-7, 11-13, 18-19, and 22-24 minutes with 0.8, 0.8, 0.1 and 0.7 respectively. The reason for the increase in COP is the increase of heat transfer in the condenser (Figure 4.6b) at the same time (3.9 kW, 4.7 kW, 0.8 kW, and 4.1 kW).

Simulated condenser heat transfer rate compared to experimental has the same tendencies as the COP. Simulated results are smooth and not fluctuating during the operation, while the experimental transfer rate had some significant increases. The reason for these sudden increases in condenser power is not clearly distinguishable. To provide such an increase in the condenser power, the compressor power has to be increased, which it is not. Another explanation could be a change in evaporation temperature, but this is also not the case, due to the fact that neither the ambient temperature or the solar radiation changes too much. In addition, Figure 4.6c shows that the compressor power does not change significantly during the specified periods. The MAE of the condenser heat transfer rate is 8.4 kW, and NMAE is 20 %. MAE of compressor power is 162 W, with NMAE of 1 %.

The deviation of the simulated results from the experimental results could be mainly explained by measurement errors. Errors in the temperature sensors at the secondary side (water/load side) of the condenser is significant when calculating the heat transfer rate, as well as the flow meter. Also, the sensors measuring solar radiation and ambient temperature could have certain deviations. There is also the effect of wind speed in which a change will impact the heat transfer of the PVT-evaporator.

The determination of the heat loss coefficient (U_{loss}) is a significant step in calculating the energy balance of the

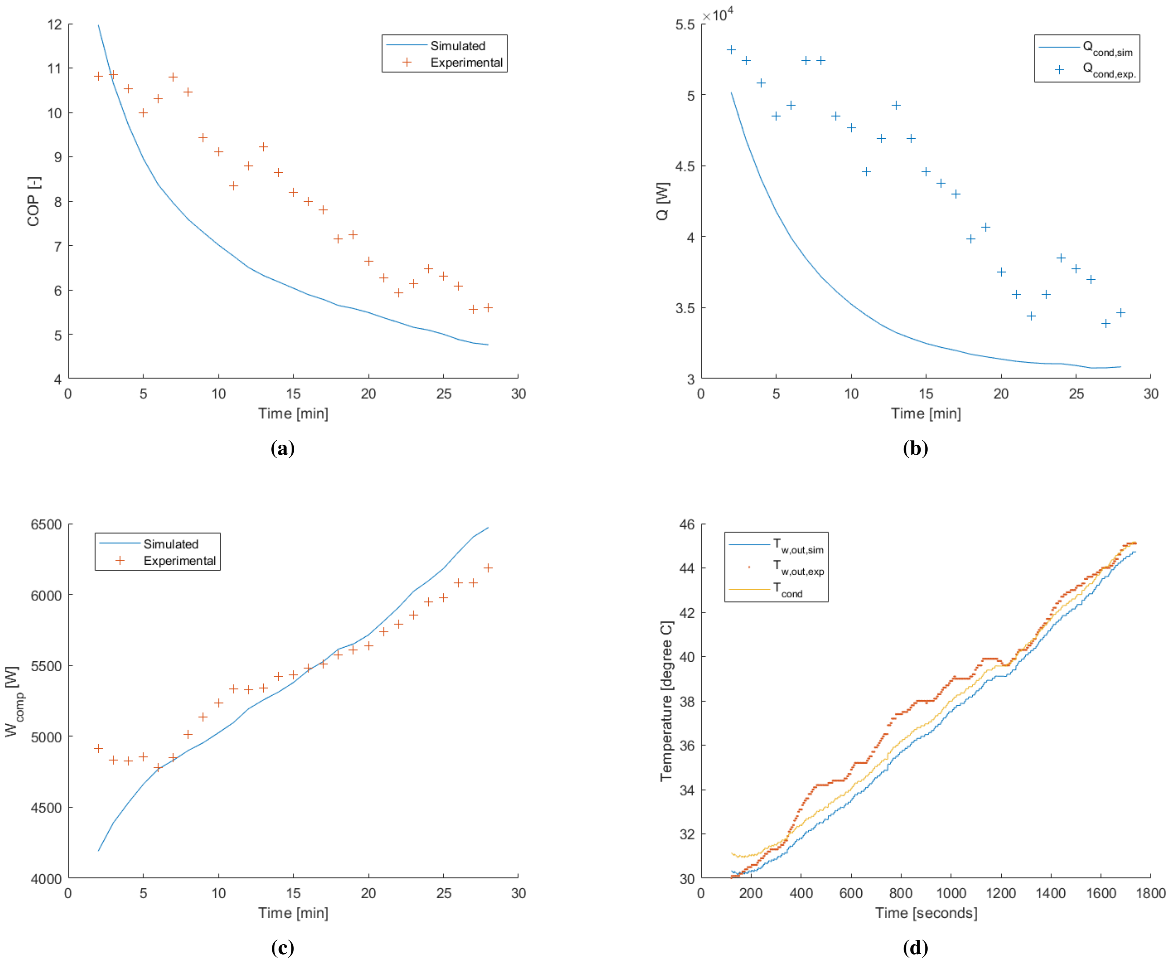

Figure 4.6: *Simulation results vs experimental results. (a), COP; (b), Condenser heat transfer (Q_{cond}); (c), Compressor power (W_{comp}); (d); Temperature levels in the condenser.*

PVT-evaporator during the operation. Chaturvedi et al. [60] used a heat loss coefficient of 6 W/m^2K for their single glazed solar collector/evaporator. Ghabuzyan et al. [61] used CFD simulations to find that the overall heat loss coefficient ranged from approximately 20 W/m^2K to 60 W/m^2K at wind speeds from 1 m/s to 10 m/s at high solar irradiance (700 to 1100 W/m^2). This is in good compliance with the validation simulation results, in which the heat loss coefficient is 36 W/m^2K with the specified assumptions.

Although there is some deviations from the simulated results to the experimental results, the model can be seen as a good representation of the proposed system. The model shows the same tendencies of the compared parameters as the real life system, which is the most important aspect when simulations will be run with different boundary conditions, climate, and system specifications. All the compared parameters can be predicted/simulated within the tolerated range of error (max. 20 % NMAE, see subsection 3.4). The numerical model is therefore proposed as a reliable model to simulate the transient/dynamic operation of the PVT+HP system, and used in the following chapters to analyse different aspect of the system.

4.6 Weakness of model

The numerical simulation model has some weakness, and the most problematic or obvious ones are:

- Computational time
- Inlet Water temp to condenser
- Storage tank simplification
- Convergence issues

The computational time for simulating one day (24 hours) in the summer is 1.7 minutes, while it is 5.1 minutes for the Autumn. Due to limited knowledge of modelling, algorithms, and programming when starting the work, the simulation model has some flaws which could have been better. Convergence issues arises for some instances when the water mass flow rate can not be adjusted with enough accuracy, or the cooling capacity becomes very high resulting in very low PV temperatures.

Also, flexibility and hierarchy is something that can be improved for the model to make it better. Being able to modify certain parts of the code individually without interfering with the rest would be beneficial.

Inlet water temperature is set to be constant at 7 °, while in a real-life application it will fluctuate between the seasons. Also, if a secondary loop is used between the condenser and heat exchanger for the load side, a perfect match of the heat rates to achieve 7 °C is difficult in practice.

The storage tank is modelled with no heat loss or distribution loss, which will influence the duration in which the heat can be stored significantly.

5 Case Study - Results and Discussion

In this chapter, results from the case study in Trondheim, Norway are presented and discussed. The description of the case study method, building model and PVT-ASHP simulation model can be found in Chapter 3. First, weather conditions for Trondheim is provided, followed by design evaluations for the PVT-SAHP system. Then, the feasibility and energy performance of the proposed system is analysed for different seasons, ending with an annual analysis with regards to both energy contribution and economics. System optimisation results investigating the PVT area, compressor size, compressor control, and temperature levels are also presented as the closing part of the chapter.

5.1 Weather conditions and heating load

The weather conditions for Trondheim, Norway through the year are presented in Figure 5.1. The solar radiation is low in the winter, not surpassing 100 W/m^2 for almost 1000 hours. In the summer, radiation intensity is much higher, reaching a maximum of around 800 W/m^2 and daily averages (Figure 5.1c) of up to 300 W/m^2. The duration curve (Figure 5.1) for the solar radiation intensity provides information that for 4500 hours of the year there is zero radiation intensity. This is just over half of the year with no solar radiation.

Figure 5.1b shows the ambient air temperature for a each hour in a year. The winter in Trondheim is cold with temperatures as low as -15 °C, and the duration of the heating season is also long. This means that both the necessary heating power and seasonal heating energy could be high. As seen in Figure 5.1d, the temperature is below 5 °C for 4000 hours of the year, but below -5 °C for only 500 hours. Ambient temperatures can reach 25-30 °C in the spring and summer, with the temperature at night dropping towards zero at some hours during the spring/early summer.

The long heating season, highly fluctuating ambient temperature, and relatively low solar radiation in the winter results in large yearly heating demand with significantly variations in heating power. Figure 5.2 shows the resulting heating load and el.specific load through the year for the building used in the case study. The space heating peak load is 7 kW and total net heating peak load is 8.5 kW. Only for a short duration of the year the space heating load is above 4 kW (800 hours).

5.2 Design evaluation

To be able to design the system components sizing, a performance analysis at different operation point are conducted. The PVT-SAHP can be dimensioned according to either of the following parameters:

- Desired condenser heating power
- Desired PV area or PV power

When the PVT is utilised as the evaporator, additional considerations to the HP cycle have to be done such as evaluating PVT-area, electrical performance of PVs and different system control. The intricacy and synergies in the energy system makes designing it a no straight forward process. Figure 5.3 depicts an example of condenser power for different compressor sizes (displacement volumes). It must be noted that the condenser heat rate are daily averages for days with ambient temperature of 2.5 °C and solar radiation of 187 W/m^2 for the spring, and ambient temperature of 18 °C and 350 W/m^2 for the summer.

The choice of refrigerant for the system can be difficult due to their different thermophysical properties and thereby

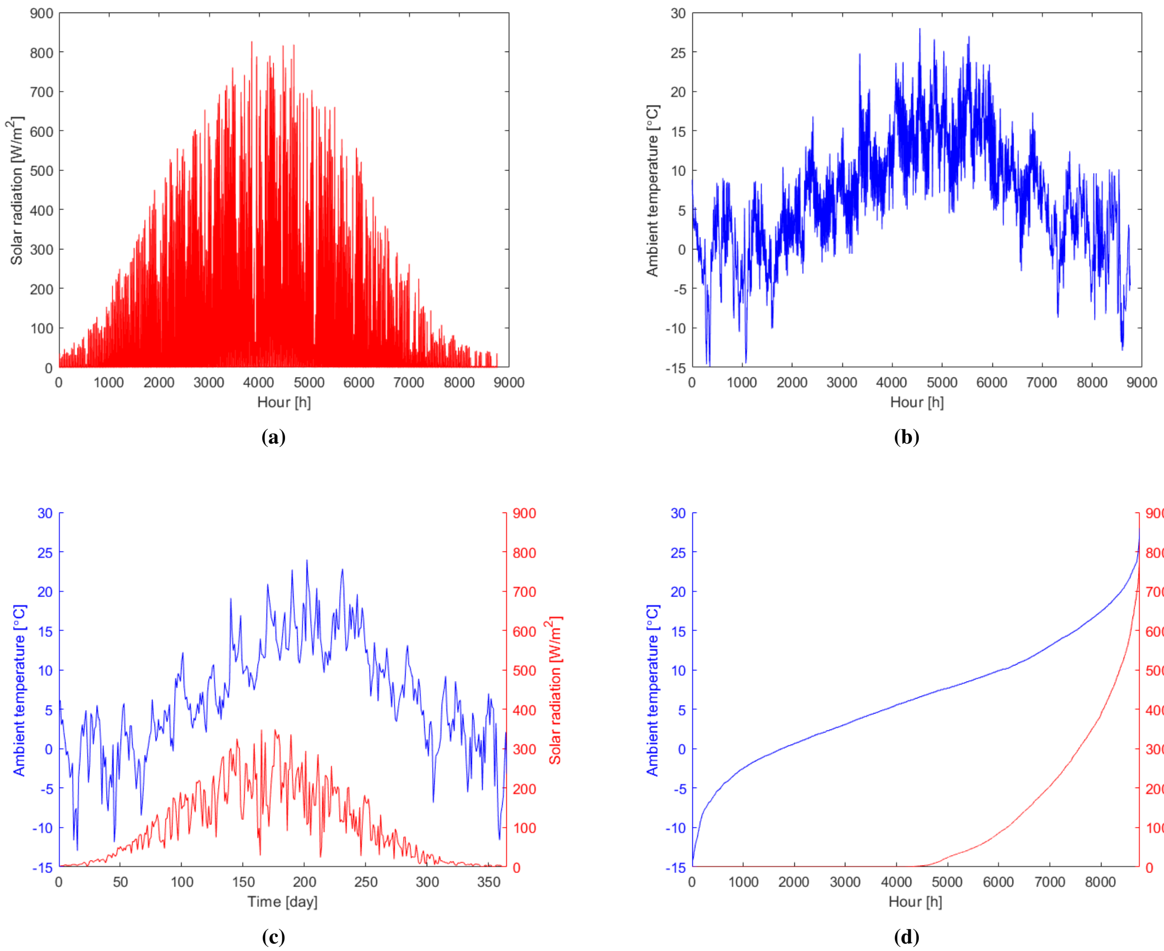

Figure 5.1: *Weather conditions in Trondheim, Norway. (a), Hourly solar radiation ; (b), Hourly ambient temperature. ; (c), Daily averages for ambient temperature and solar radiation. ; (d), Duration curves for ambient temperature and solar radiation.*

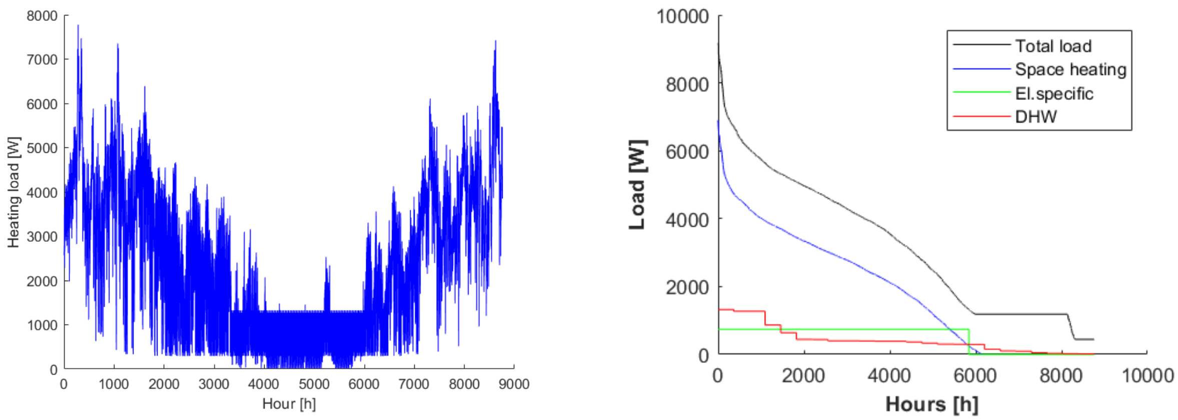

(a) **(b)**

Figure 5.2: *Heating load for the building model. (a), Heating load (space heat + DHW) through the year; (b), Load duration curves.*

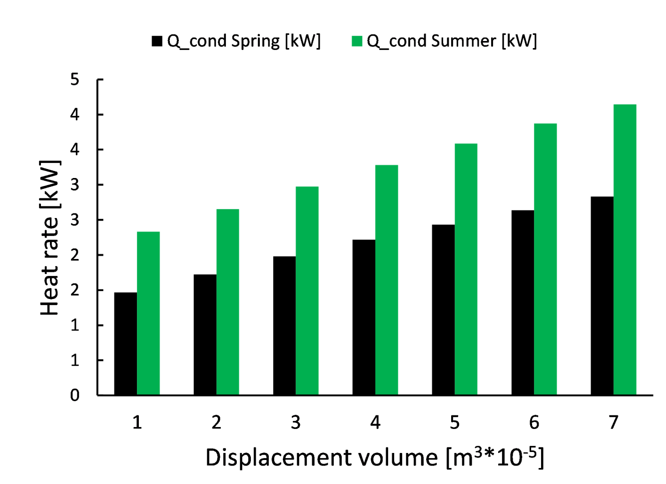

Figure 5.3: *Principal condenser power for different compressor displacements for a day in both the spring and the summer.*

the performance of the system. Many factors have to be included to find the optimal choice for a HP cycle: GWP and ODP of the refrigerant; system COP and SFP; component sizes, especially compressor size; components costs; security equipment and measures needed. To be able to evaluate the refrigerants influence on the performance of the proposed system, simulations are done to compare a selection of relevant refrigerants. The chosen refrigerants are R134a, R290 (propane), R600a (isobutane), R717 (ammonia), and R1234ze(E) based on the literature review in section 2.2.3. R134a is included to be able to compare the natural refrigerants and the HFO to it.

The results are from the first version of the simulation model (steady state) with PV temperature set to 5°below ambient temperature, 2 PVT modules (2x1.68m^2), solar radiation of 500 W/m^2, and condensation temperature of 60 °C.

From Figure 5.4a it can be seen that the highest COP is achieved using ammonia at ambient temperatures above 4 °C and propane below 4 °C. At reference PV temperature conditions (25 °C), the COP using ammonia (5.4) is 0.4 higher than using R134a (5.0), 0.2 higher than isobutane (5.2), and 0.7 higher than with propane (4.7). Although showing promising COP, an ammonia system will have a discharge gas temperature which is way to high (327 °C and 127 °C at T_a of -10 °C and 25 °C respectively). Ammonia is therefore evaluated to not being applicable for this system due to high temperature lift.

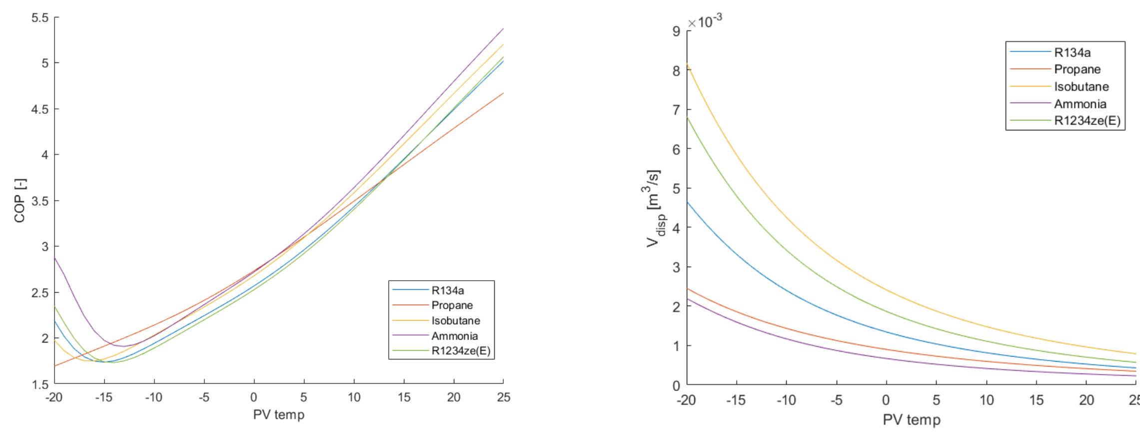

(a) (b)

Figure 5.4: *Evaluation of different refrigerants at PV temperatures from -20 °C to 25 °C. (a), COP; (b), necessary compressor size.*

Using propane achieves a higher COP at low temperatures (<4 °C), but lower COP at high temperatures (>4 °C) compared to isobutane. The difference is 0.5 at reference PV conditions (T_a=25 °C), and 0.1 at traditional design conditions for Trondheim, Norway (T_a=7 °C). The propane cycle has a COP of 0.1 higher than isobutane at T_a= -5 °C. Although isobutane is showing slightly better energy performance than propane for higher temperatures, it is evident that the necessary compressor size using the former is significantly larger than using the latter(5.4b). To reach the design heating condenser power at -15 °C using isobutane, a compressor of 0.006 m_3/s must be used. Using propane, a compressor displacement of 0.002 m_3/s is sufficient. I.e. an isobutane compressor must be three times the size of a propane compressor in this case.

Accordingly, the literature review in subsubsection 2.2.3 shows that using R290 (propane) in a traditional heat pump/refrigeration cycle results in better energy performance, i.e. COP, and lower possible compressor displacement, than using the other low-GWP refrigerants.

Due to the results presented in this section, it is decided to mainly evaluate the PVT-SAHP system using R290, but including comparisons with R600a where it is convenient.

5.3 Feasibility

The feasibility of the PVT-SAHP system in Trondheim is examined by simulating the system operation in different seasons of the year. Energy performance and transient system behaviour are analysed using the proposed KPIs in Chapter 3.

5.3.1 Summer conditions

The simulation for summer conditions (Figure 5.5) were done using 6 PVT modules and a compressor with V_{th}=1.2*10^{-5} m^3 at June 25th. The simulated day is a hot and sunny day with a maximum ambient temperature of 28 °C, and maximum solar radiation of 790 W/m^2. The COP is 5.1 at the highest, providing 3.3 kW of condenser power. The average COP through the day is 4.5 with an average ambient temperature of 17.8 °C and average solar radiation of 349 W/m^2. The maximum temperature of the PV panels in the PVT is 31 °C, compared to 41 °C for the PVs only. The cooling from the PVT-SAHP system is reducing the PV temperature with about 10 °C at 4 pm. The reduced temperature of the PVs results in an electricity production increase of 3.3 % (0.37 kWh). The daily SSR and SCR of the system is 0.63 and 0.74 respectively.

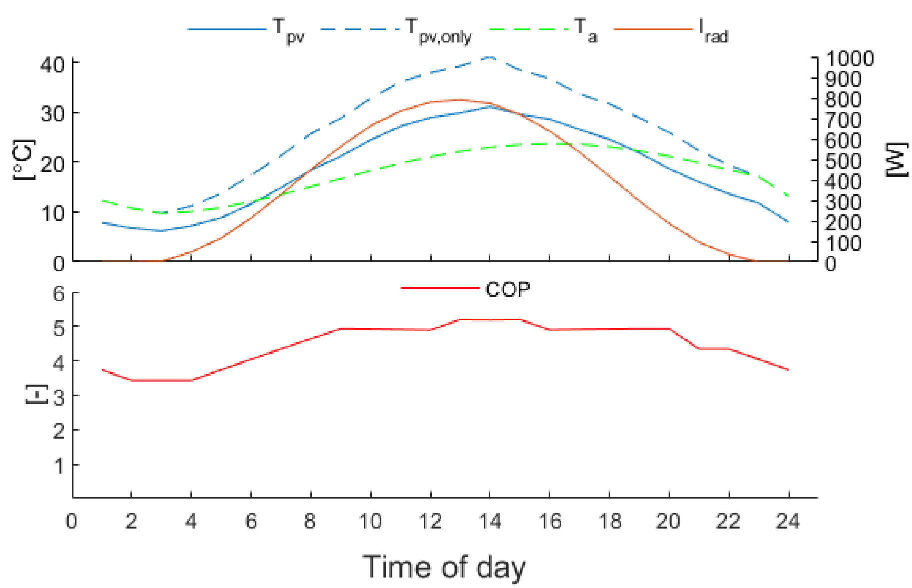

Figure 5.5: *PV temperature (T_{pv}), ambient temperature (T_a), solar radiation (I_{rad}), and COP for June 25th.*

The PV temperature and COP reaches the daily maximum at 13-15, right after the peak solar radiation occurs at 13 and the ambient temperature is almost at the highest. As the solar radiation drops after 13, the PV temperature also does so accordingly. The condenser heat rate peaks when the PV temperature is highest. From Figure 5.6a it can be seen that there is an overproduction from the heat pump compared to the heating load. The ambient temperature is high through the day, therefore no space heating is needed, and the DHW demand is not that large. There are several ways in which this problem could be solved. Controlling the compressor speed to meet the heating load is the most effective way to do it at a regular basis, as the solution is dynamic in regards to changing boundary conditions. Another option is to store the excess heat in the water tank (TES), providing the opportunity to use it later. Although, as depicted in Figure 5.6b, when the maximum capacity of the TES is reached there is no further way to store the excess heat. The compressor must then either be shut off or the speed reduced to meet the load. In this particular case, if the compressor is shut-off when the energy storage is maximised, this would happen at 6'o clock. The PVT-SAHP will then not operate when the solar radiation is increasing and it is most efficient, but operated at the less efficient times up to 6.

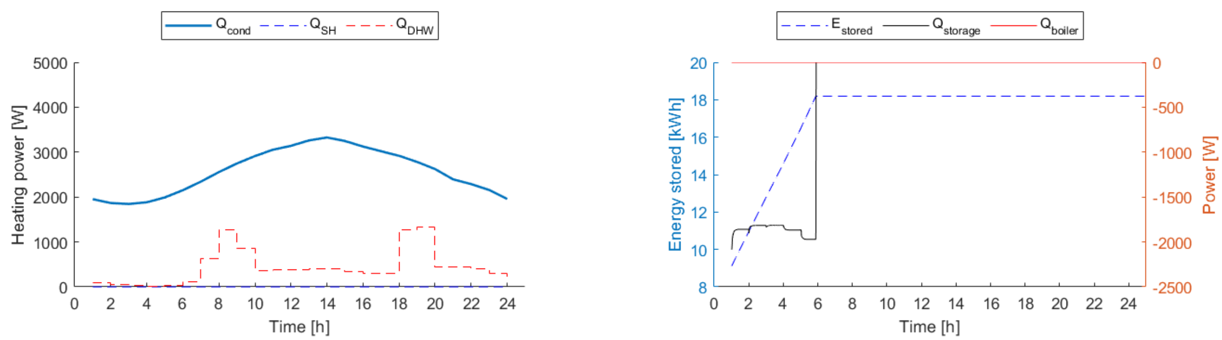

(a) **(b)**

Figure 5.6: *Simulation results for June 25th. (a), PVT-SAHP condenser power (Q_{cond}), and heating load for space heating and DHW (Q_{SH},Q_{DHW}).; (b), Energy stored ($E_{storage}$), storage heat rate ($Q_{storage}$) and boiler heat rate (Q_{boiler}).*

Another way to deal with the overproduction in the summer, will be to reduce the compressor size or PVT area in the design of the system. This will although result in reduced heating capacity for the PVT-ASHP and it might not produce enough heat in colder periods.

5.3.2 Winter conditions

At winter conditions (February 14th), with 6 PVT modules and a compressor with V_{th}=1.2*10^{-5} m^3, the COP is 2.8 at the highest, providing 1.5 kW of condenser power (Figure 5.7). The average COP through the day is 2.1 with an average ambient temperature of -10.8 °C and average solar radiation of 30 W/m^2. The simulated day is a cold day with a maximum ambient temperature of -0.1 °C, and maximum solar radiation of 207 W/m^2. The temperature of the PV panels in the PVT is -11.2 °C at peak solar radiation (14.00), compared to -8.8 °C for the PVs only. The reduced temperature of the PVs results in an electricity production increase of 0.7 % (0.37 kWh). The average thermal efficiency (η_{th}) is 62 %. The daily SSR and SCR of the system is 0.09 and 1.0 respectively.

The condensing power of the PVT-ASHP system is only delivering about 1 kW of heating power through the day, while the space heating load (4-6 kW) is much higher (Figure 5.8). Therefore, much of the heat energy to meet the load is provided by the electric boiler. Although not meeting the space heating demand of the 150 m^2 building, the DHW demand is fully covered by the PVT-ASHP system. The heat pump system delivers a total of 27.0 kWh heat

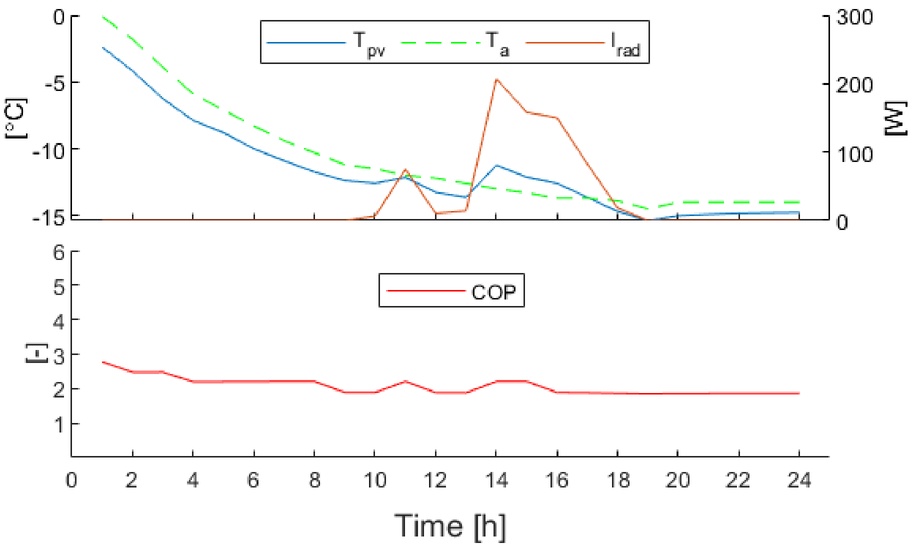

Figure 5.7: *PV temperature (T_{pv}), ambient temperature (T_a) and solar radiation(I_{rad}), and COP for February 14th.*

energy through the day, while the DHW demand is only 10.3 kWh. Only in three hours of the day (8-9, and 18-20), the DHW demand slightly exceed the condenser power. This specific system design is therefore sufficient to meet the DHW demand through the year, but covering only a small portion of the space heating power demand when the ambient temperature is low. An increase of the refrigerant displacement, utilising a larger compressor, would result in a better power coverage for the PVT-ASHP. Although, this would also enhance the overproduction discussed in the previous section, resulting in a larger mismatch between heating load and available heat production in times with higher ambient temperature.

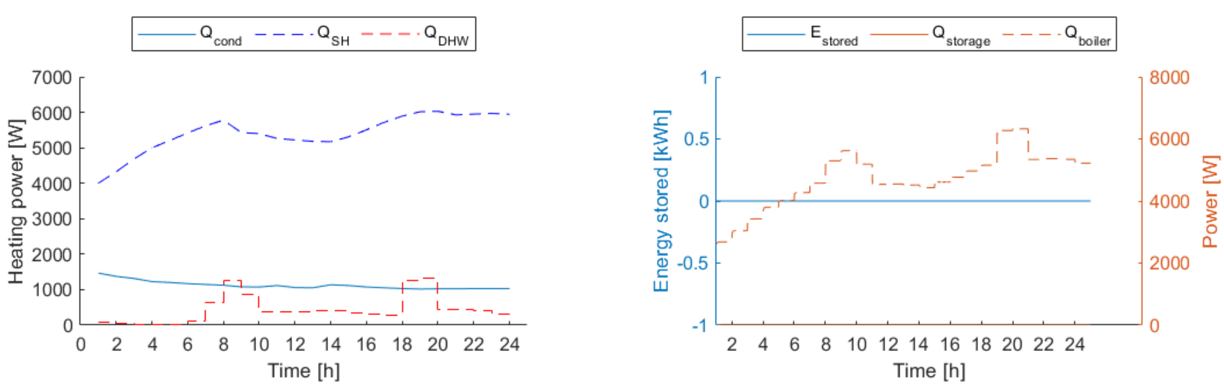

(a) **(b)**

Figure 5.8: *February 14th. (a), Heating load for space heating and DHW (Q_{SH},Q_{DHW}), and PVT+HP condensation power (Q_{cond}).; (b), Energy stored ($E_{storage}$), storage heat rate ($Q_{storage}$) and boiler heat rate (Q_{boiler}).*

5.3.3 Spring conditions

To test the system in spring conditions, a simulation for the first week of March is done. The resulting PV temperature and COP are presented in Figure 5.9.

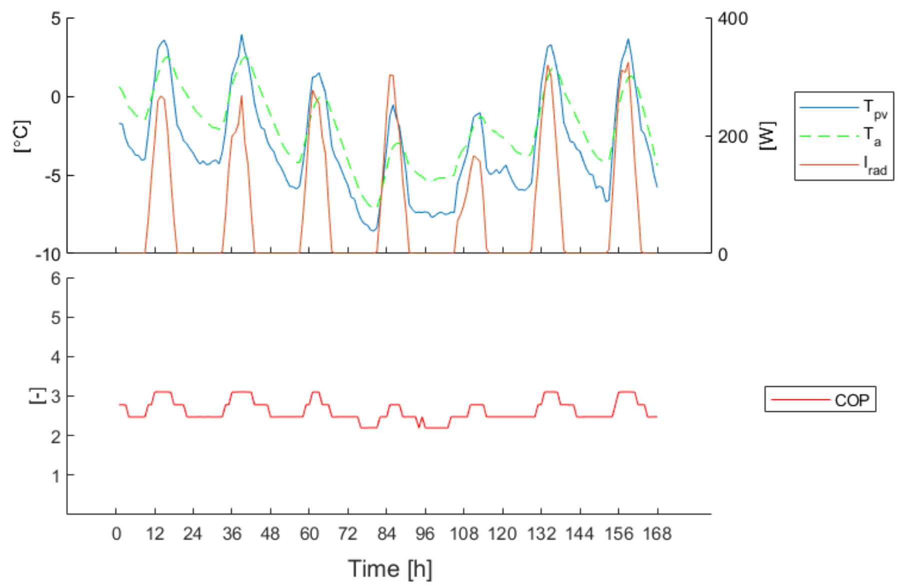

Figure 5.9: *PV temperature and COP for the first week of March.*

The simulated period is a cold week with a maximum ambient temperature of -3.9 °C, minimum of -8.5 °C, and maximum solar radiation of 324 W/m^2. The COP is 3.1 at the highest, providing 1.7 kW of condenser power. The average COP through the week is 2.6 with an average ambient temperature of -2.0 °C and average solar radiation of 67 W/m^2. The maximum temperature of the PV panels in the PVT is 3.9 °C, compared to 7.9 °C for the PVs only. The reduced temperature of the PVs results in an electricity production increase of 1.2 % (0.2 kWh).

The weekly SSR and SCR of the system is 0.19 and 1.0 respectively.

5.3.4 Autumn conditions

To test the system in autumn conditions, a simulation for the first week of October is done. The resulting PV temperature and COP are presented in Figure 5.10.

The simulated period is a week with temperature fluctuating between night and day. The maximum ambient temperature is 10.8 °C, minimum is -2.8 °C, and maximum solar radiation of 353 W/m^2. The COP is 4.0 at the highest, providing 2.2 kW of condenser power. The average COP through the week is 3.2 with an average ambient temperature of 5.7 °C and average solar radiation of 61 W/m^2. The maximum temperature of the PV panels in the PVT is 11.8 °C, compared to 17.6 °C for the PVs only. The reduced temperature of the PVs results in an electricity production increase of 1.4 % (0.2 kWh).

The weekly SSR_{el}, SSR_{th} and SCR of the system is 0.17, 0.67, and 1.0 respectively. η_{th} is 103 %.

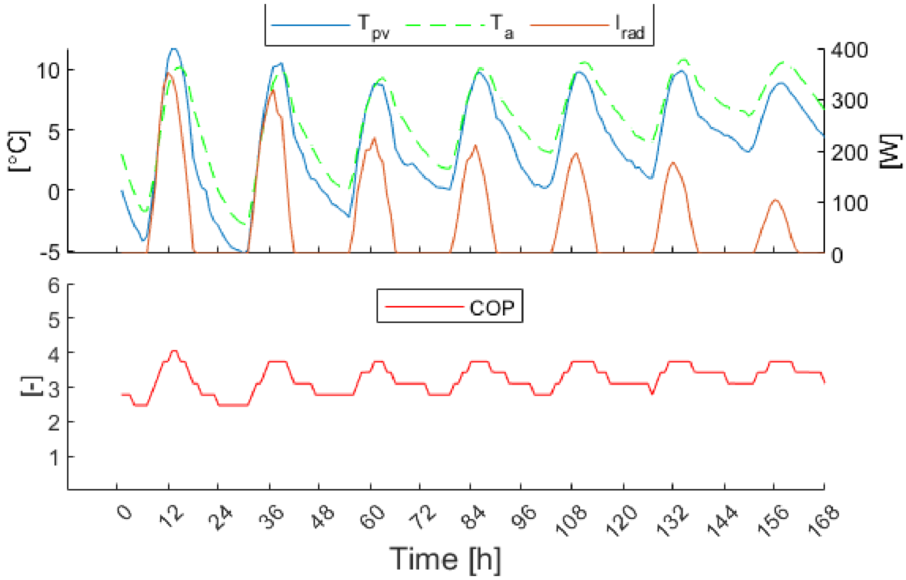

Figure 5.10: *PV temperature and COP for the first week of October.*

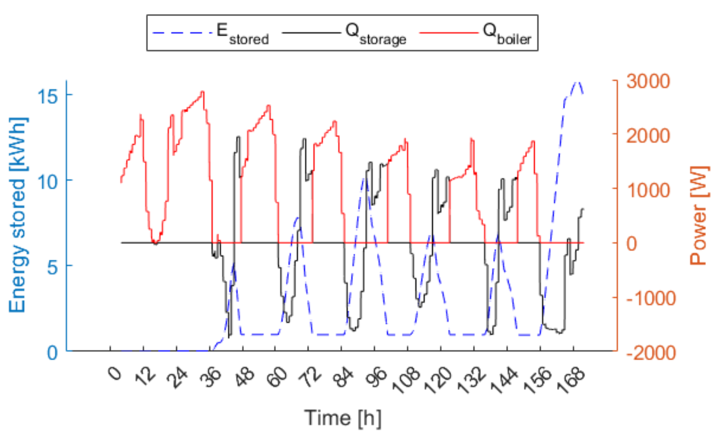

Figure 5.11: *Energy stored ($E_{storage}$), storage heat rate ($Q_{storage}$) and boiler heat rate (Q_{boiler}) through the first week of October.*

5.3.5 Seasonal overview

A seasonal overview of the PVT-ASHP performance are presented in Figure 5.12, using five representative days through the year based on the simulation in the previous sections. 6 PVT modules and a compressor with V_{th}=1.0*10^{-5} m^3 are used in the simulations. The PVT-SAHP system achieve a significantly higher COP is the summer than in the winter. Although, a COP of 2-3 in the winter is reasonably high when heating water from 7 °C to 55-65 °C at ambient temperatures of around -10 °C.

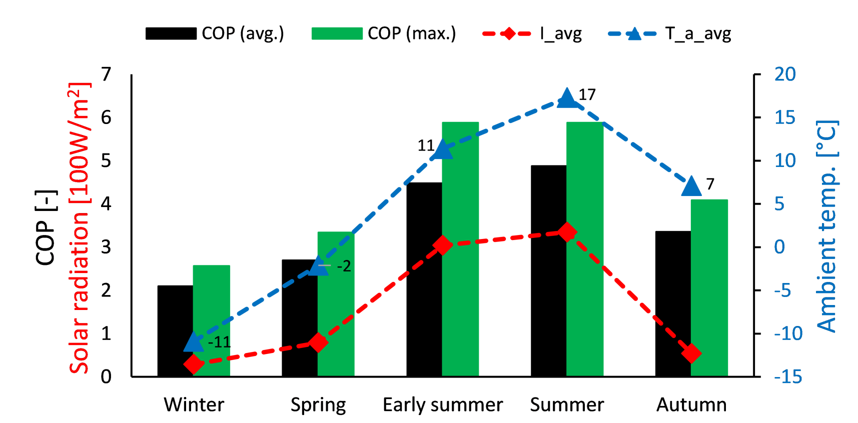

Figure 5.12: *Seasonal overview for the performance of the DX PVT-SAHP system in Trondheim.*

The results from simulating three months (January 1st to March 31st) during the heating season can be viewed in Figure 5.13. The COP fluctuates between 1.8 at the lowest when there is no solar radiation and ambient temperature is -16 °C, and 4.1 when solar radiation is high and ambient temperature is 10.4 °C. The average COP of the PVT-SAHP is 2.8 for the simulated period, total SSR is 0.12 and thermal SSR (SSR_{th}, see subsection 3.3) is 0.41. This means the heat pump can cover 40 % of the total heating demand, both space heating and DHW, through the period. The rest is covered by the electric boiler. Because the utilised compressor is relatively small, and designed for covering the DHW demand, this is a significant energy coverage factor. If the compressor size is increased, an even higher coverage can be reached for the year.

The annual delivered energy, electricity usage, PV electricity production, and net electricity for the building model with the different system configurations are presented in Figure 5.14. The delivered heating power from the electric boiler (Q_{el}) is 100 % for the baseline configuration since it is the only heating component. If an ASHP with an SCOP of 3.0 is utilised for space heating, the electricity usage for the building is significantly reduced. Comparing the PVT-SAHP system against the electric boiler, the net electricity demand for heating purpose is reduced with 52 %, 75 %, and 93 % using the 3, 6, and 12 PVT systems respectively. The PV production through the year for these PVT-SAHP configurations are 1294 kWh, 2589 kWh and 5178 kWh respectively.

Compared to the ASHP, the first PVT-ASHP configuration (3PVT-ASHP) does not reduce the net electricity demand or the heating electricity demand. This configuration is designed to cover the DHW load, which results in the electric boiler supplying most of the energy for space heating.

The second PVT-SAHP configuration (6PVT-SAHP) has double the amount of PVT modules and a compressor with two times the displacement volume as in the first configuration. This results in the system having higher heating

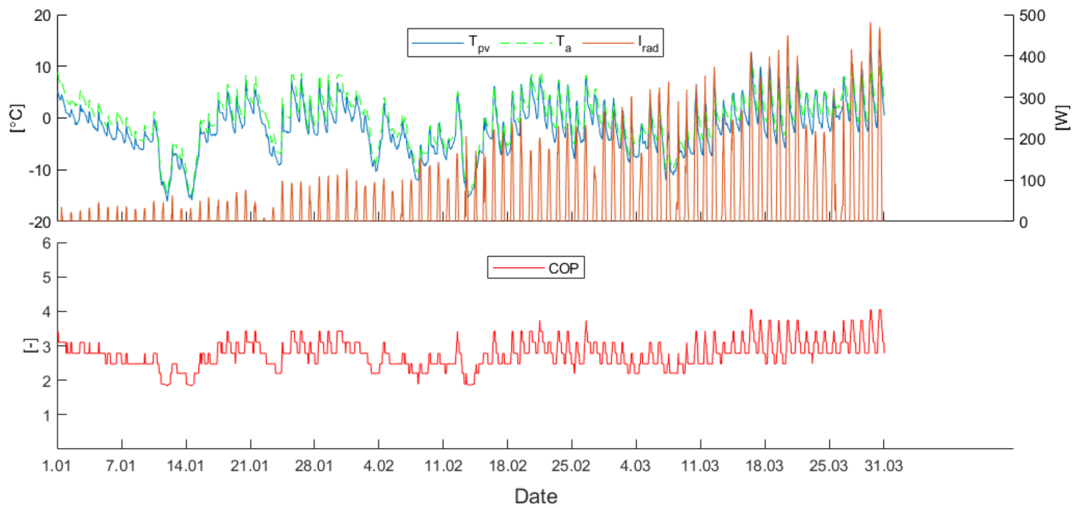

Figure 5.13: *PV temperature and COP from January 1st to March 31st.*

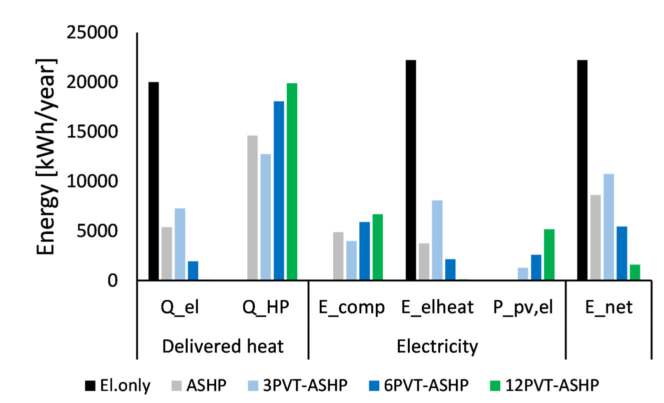

Figure 5.14: *Delivered heat energy, electricity usage and production, and net electricity for a year. Q_{el} and Q_{HP} is delivered heat from el.boiler and heat pump; E_{comp}=compressor electricity usage; E_{elheat}= Boiler electricity usage; $P_{pv,el}$=PV electricity production; and E_{net}=Net electricity usage.*

condenser power and can cover the building heating load for more hours of the year. As a result, the electric boiler only need to operate as a peak load unit, and is delivering only 10 % of the heating energy demand for the year. The PVT-SAHP produces 18 000 kWh through the year, resulting in a heating energy coverage of 90 %. Compared to the ASHP system, using this configuration also results in a higher net electricity demand reduction (14 %-points compared to El.only). The PVT-ASHP uses 7 % less gross electricity (without PV prod.), and 37 % less net electricity (with PV prod.) than the ASHP system.

Using 12 PVT modules and a compressor with a displacement volume of $6*10^{-5}m^3$ (12PVT-ASHP), results in a 99 % heating energy coverage. The el.boiler only need to deliver 96 kWh through the year because of the significant heating power of the condenser, also during cold periods. The net electricity demand is 19 % of the ASHP configuration, due to high PV power production (5178 kWh) and low el.boiler usage.

From an energy performance point of view, using the PVT-SAHP in Trondheim, Norway is very feasible, especially if both DHW and space heating can be produced. Also, for DHW-only purposes, the system reduces the net electricity significantly, although overproduction and load-production mismatches are an obstacle.

5.3.6 Economic analysis

Figure 5.15 presents the results from the economic analysis. Annual energy costs are significantly reduced by investing in a PVT-SAHP. Compared to the ASHP system with no PVs, the energy cost is reduced with 81 % by using the 12PVT-ASHP configuration. The reduction is 54 % if the same PV area as the PVT area is included in the ASHP system (ASHP+12PVs). Utilising the 3PVT-SAHP reduces the annual energy cost with 52 % from the El.-only system, but increases it from the ASHP systems.

The total annual cost of the investigated energy systems shows that the PVT-SAHP is an economically feasible energy system for residential houses in Trondheim. The lowest total annual cost are achieved with the largest system (12PVT-SAHP). It is reduced with 38 % and 5 % compared to the ASHP system without PVs and with 12 PVs respectively. The reduction is 93 % when evaluating it against the El.-only system.

5.4 System optimisation

5.4.1 PVT area

By increasing the number of PVT modules from 6 to 12, the PVT area is doubled from 10.1 to 20.2 m^2. In the winter (Figure 5.16), this has small consequences due to short days (10-18) with low solar radiation. It results in an increase of SSR from 0.09 to 0.17, but a minimal increase in average COP (<0.1) condenser heat transfer (0.7 kWh), and PV temperature. It also results in a decrease of η_{th} and SCR from 62 to 29 % and 1.0 to 0.95 respectively. The decrease in thermal efficiency is due to the PV temperature being higher, both when it is above (11 and 14-17) and below the ambient temperature. Increment in COP is more distinct when 3 and 12 PVT modules are compared, with a difference of 0.3 during most of the day (1-16).

In the summer (Figure 5.17), the effect is more noticeable due to higher solar radiation. The average and max. COP is increased from 4.5 to 4.8 and 5.1 to 5.8 respectively. The reason is higher PV temperature, which is increased from 31 to 34 °C because of a higher heat exchanging area of the PVT modules. The thermal efficiency drops from 52 to 19 %.

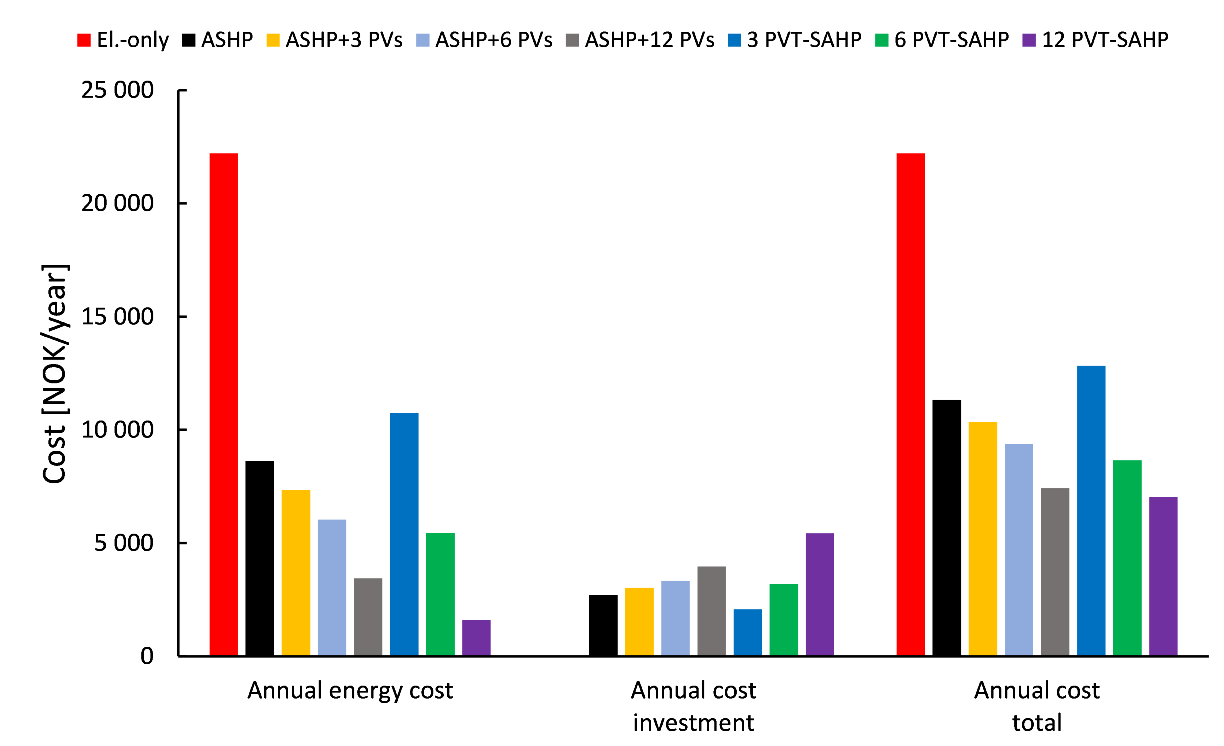

Figure 5.15: *Annual investment cost, energy cost and total cost for the different energy system configurations.*

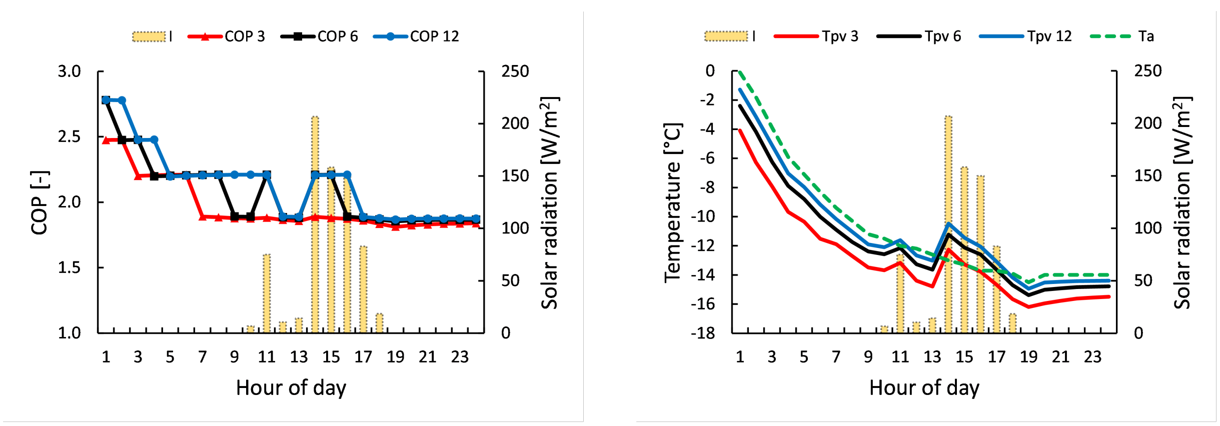

(a) **(b)**

Figure 5.16: *PV temperature (T_{pv}), ambient temperature (T_a), solar radiation(I), and COP for February 14th using 3, 6 and 12 PVT modules. (a), COP; (b), PV and ambient temperature.*

Reducing the number of PVT modules to 3, the average COP decrease to 4.1 and max. COP to 4.9 (Figure 5.18c). The PV temperature becomes lower with a max. of 26 °C. PV efficiency improvement is increased to 5.2 %, and thermal efficiency to 78 %. SSR is 0.44.

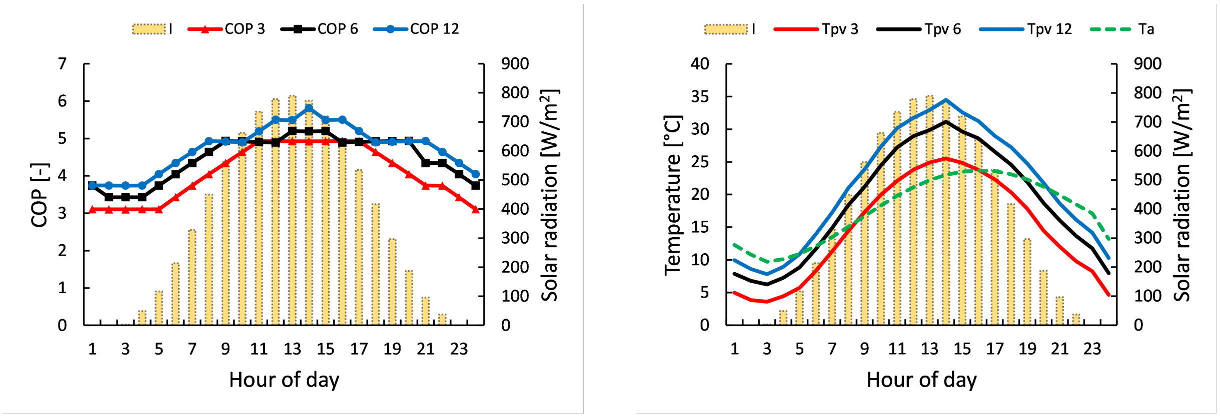

(a) (b)

Figure 5.17: *PV temperature (T_{pv}), ambient temperature (T_a), solar radiation(I), and COP for June 25th using 3, 6 and 12 PVT modules. (a), COP; (b), PV and ambient temperature.*

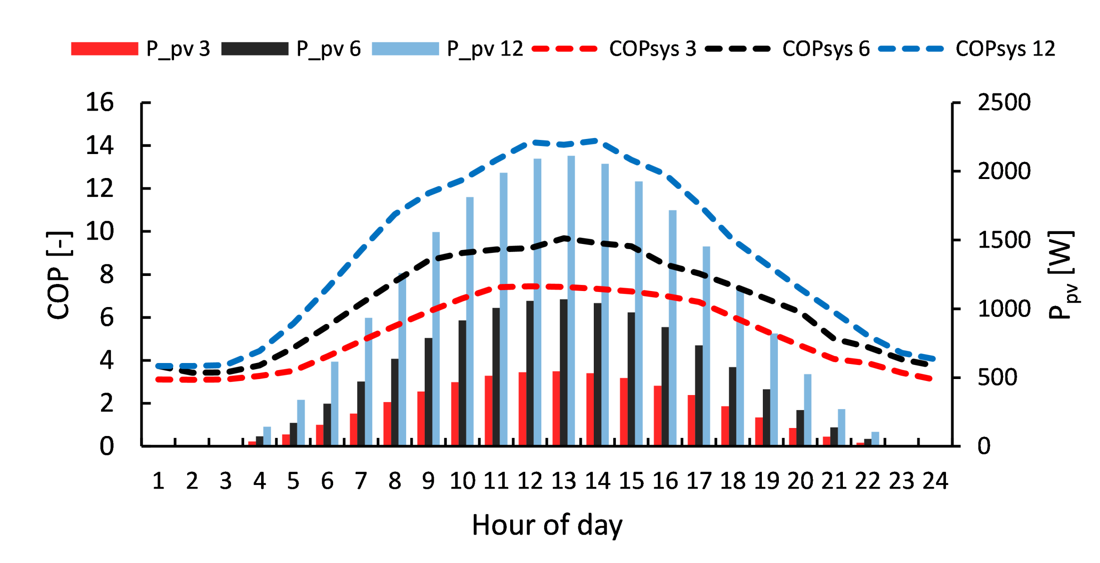

Figure 5.18: *PV power production (P_{pv}) and system COP (COP_{sys}) for June 25th using 3, 6 and 12 PVT modules.*

Comparing the influence the PVT area has on the condenser power for winter and summer conditions, a noticeable difference can be found. Figure 5.19 presents the heat rate in the condenser (condenser power) using 3, 6, and 12 PVT modules for a summer day and a winter day. In the winter, with low ambient temperature and lower solar radiation, the change in condenser power by changing the PVT area is minor. At peak solar radiation (hour 14) there is only a 9 % (96 W) increase from 3 to 12 PVT modules. In the summer, the increase at the same time is 30 % (870 W). The reason is clearly better operating conditions in the summer, with higher solar radiation and ambient temperature, which results in higher PV temperature and therefore COP. This can be seen in Figure 5.16b and Figure 5.17b as the PV temperature difference between 3 and 12 PVT modules is 1.8 °C and 9 °in the winter and summer respectively (hour 14) . Although, it can be noted that the tendency contrast between summer and winter is lower when the solar radiation is low, especially during the night.

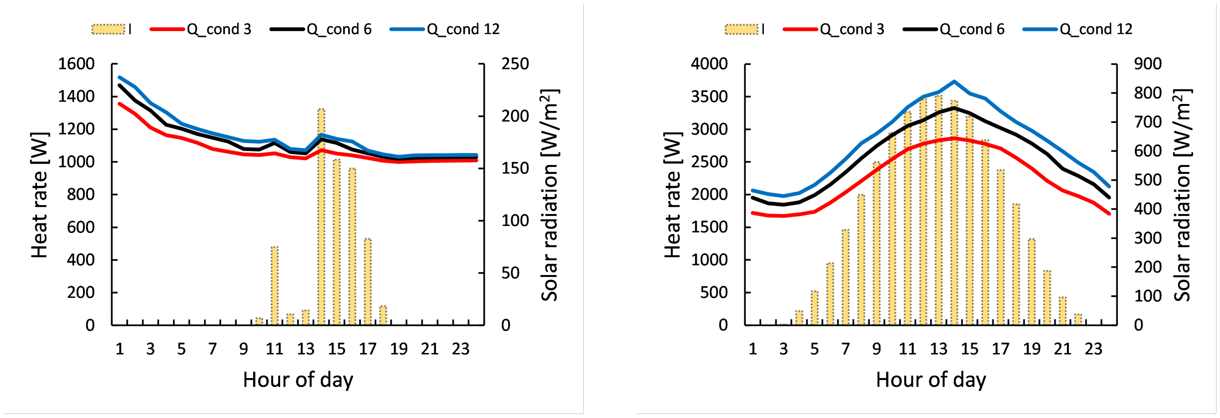

(a) **(b)**

Figure 5.19: *Condenser power (Q_{cond}) and solar radiation (I) using 3, 6 and 12 PVT modules. (a), Winter, February 14th; (b), Summer, June 25th.*

5.4.2 Compressor size

Figure 5.20a shows that to keep the temperature of the PVs close to the ambient temperature, the compressor needs to be of sufficient size. For this particular case, the V_{th} would have to be between $5*10^{-5}m^3$ and $7*10^{-5}m^3$. This results in lower COP than for a smaller compressor if no other system configurations is changed. The reason for drop in COP is larger cooling power leading to lower PV temperature. Using a compressor with displacement volume of $9*10^{-5}m^3$ the maximum PV temperature becomes 14 °C, providing heating power of 13 kW and PVT cooling power of 9 kW. As a comparison, the maximum temperature using a compressor with $2*10^{-5}m^3$ displacement is 25 °C, and the maximum temperature of the PV only is 41 °C (No cooling, only PV panels).

A smaller compressor gives better COP and SSR, but might not provide enough heat energy through the day/week/year to cover the demand as discussed in previous sections. By finding the compressor size (or control) which sufficiently covers the demand, while keeping the COP as high as possible, the system will be most energy- and cost effective.

Figure 5.21a presents the COP and condenser heat rate for different compressor sizes. When the compressor size is increased, the heating rate of the PVT-SAHP increases proportionally, but as a result the COP decreases. An observation is that the slope of change is more significant for summer conditions than for spring conditions. This can be explained due to better operating conditions for the system, i.e. higher ambient temperature and solar radiation.

On the other hand, as seen in Figure 5.21b, increasing the compressor size also results in a larger PV electric power production. The PV panels in the PVT produce 4.3 % more electricity than traditional PV panels using a compressor with $2.2*10^{-5}m^3$ displacement volume, compared to 2.4 % with a $2*10^{-5}m^3$ displacement.

When analysing the performance of the system, it is evaluated using a certain compressor size (V_{th}) and PVT area

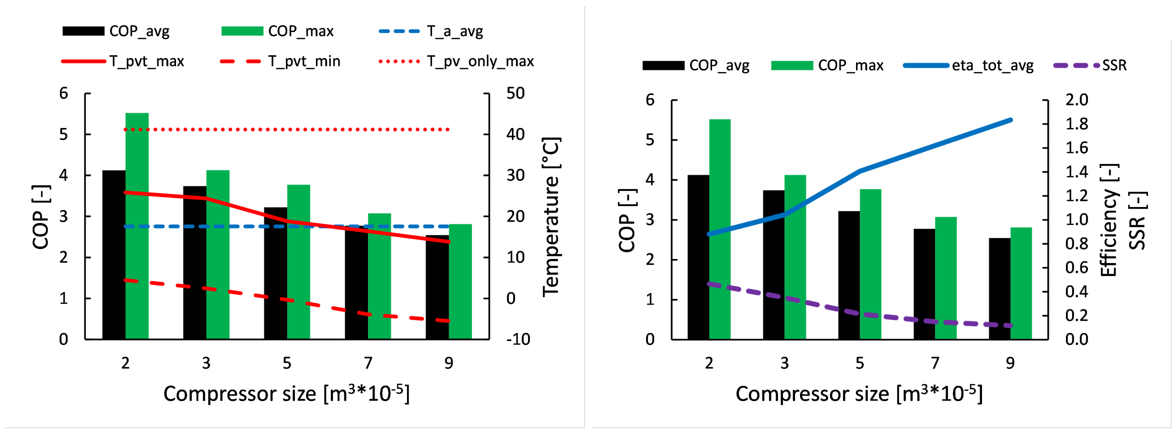

(a) (b)

Figure 5.20: *Effects of changing the compressor size. (a), Average COP (COP_{avg}), maximum COP (COP_{max}), ambient temp. (T_a), maximum and minimum PV temp. (T_{pv}), and maximum PV-only temp. ($T_{pv,only}$) ; (b), Average COP (COP_{avg}), maximum COP (COP_{max}), PVT total efficiency ($\eta_{tot,avg}$), and self-sufficiency rate (SSR).*

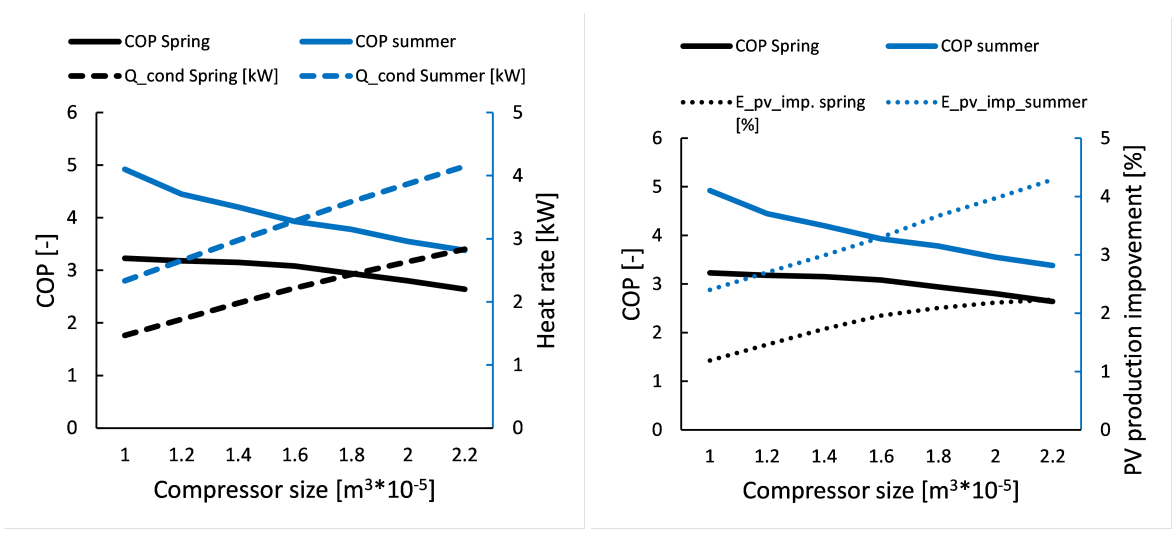

(a) (b)

Figure 5.21: *Performance for different compressor sizes.*

(A_{pvt}). If it is desirable to increase the heating power of the system during the design process, two main considerations should be taken: 1. COP will be reduced with increased compressor size, if PVT area is kept the same; 2. If COP should be kept the same, PVT area therefore must be increased accordingly. To keep the COP approximately the same when modulating/increasing heating power from the design, PVT area to compressor size ratio (Ω_{pvt}) should be kept the same:

$$\Omega_{pvt} = \frac{A_{pvt}}{V_{th,comp}} \qquad \left[\frac{m^2}{m^3}\right]$$

5.4.3 Compressor control

Several ways to control the compressor are proposed:

- On/off
  - Cut off (N=0) when I < Value
  - Cut off (N=0) when $T_{pv} < T_a$-5
  - Cut off (N=0) when $T_{evap} < (T_a$=Value)
- P-control
- PID-control

Controlling the compressor using on/off control with cut off at solar radiation less than 200 W/m^2 during a hot and sunny summer day (June 25th) in Trondheim, gives an average COP of 4.9, COP_{max} of 5.2, and 13 hours operation time (Figure 5.22b). If the cut-off is reduced to 100 W/m^2 (Figure 5.22a) the average COP becomes 4.8, COP_{max} is still 5.2, and operation time is increased to 16 hours.

Changing the compressor size from V_{th}= 1.2 to V_{th}= 3.0, gives average COP of 3.7 and COP_{max} of 4.1 (Figure E.4).

The system on/off control can be utilised to increase the amount of time the system operates under favourable conditions, resulting in better energy performance.

5.4.4 Temperature levels

The range of acceptable outlet water temperature is a system parameter which will influence the energy performance and operation of the PVT+HP system. Figure 5.23 shows that by decreasing it from 55-65 °C to 35-45 °C, the average COP is increased from 3.1 to 5.2. Heating the water to only 30-40 °C gives a COP 5.5. The main reason for the substantial performance improvement is decreased pressure ratio in the compressor and therefore decreased specific compressor work. Compressor efficiencies, both isentropic and volumetric, are also better at lower pressure ratios in the operating range of the compressor (eqs. (4.13) to (4.15)).

In addition to better COP, the total efficiency of the PVT-evaporator and system SSR are also improved by decreasing the temperature lift for the system. The total efficiency of the PVT increases due to larger cooling capacity which reduces the PV temperature and therefore heat loss to the ambient.

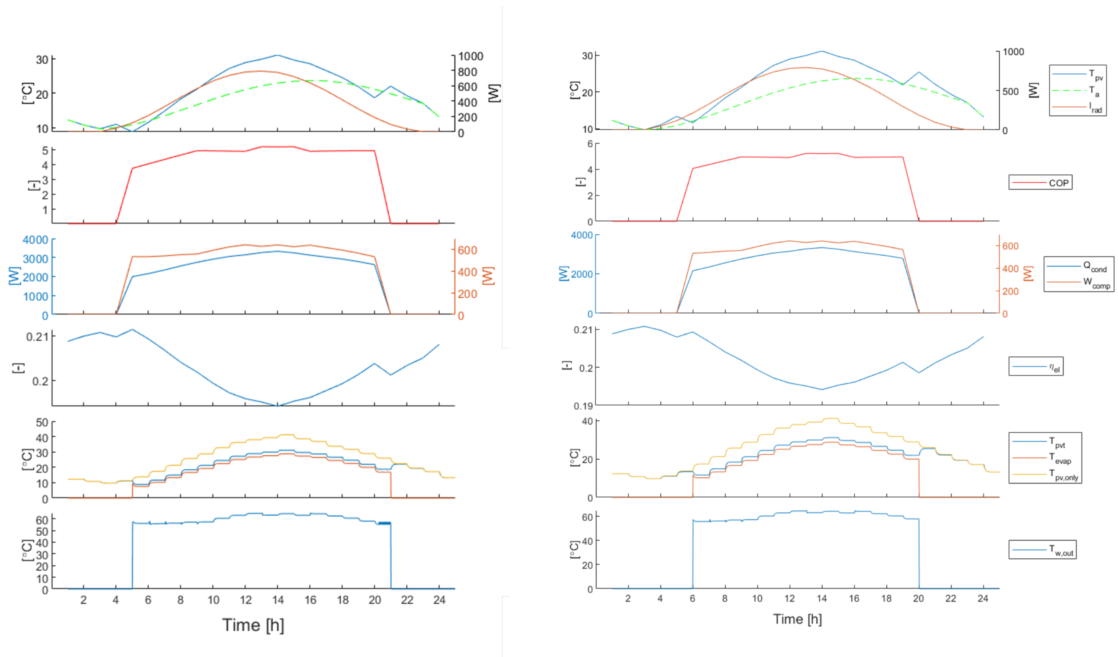

(a) **(b)**

Figure 5.22: *Results for compressor cut-off (N=0) control on June 25th with V_{th}= 1.2 at: (a), I<100 W/m^2; (b), I<200 W/m^2.*

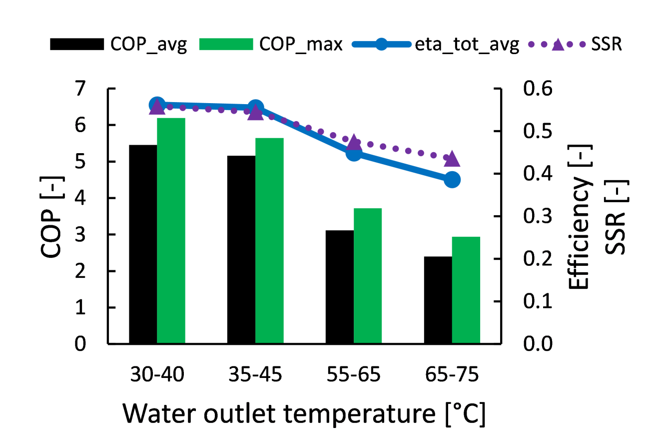

Figure 5.23: *Influence of the outlet water temperature from the condenser on the system COP.*

6 Conclusion

This work investigates the feasibility and energy performance of a single-source R290 direct expansion PVT solar assisted heat pump (DX PVT-SAHP) in the cold climate of Trondheim, Norway, by developing a transient numerical system simulation model and conducting a case study for a small residential house.

The numerical simulation model provides a method to simulate the system performance and system behaviour of the direct expansion solar assisted heat pump system using PVT and R290. It gives the possibility to evaluate system specifications for a chosen climate and building, providing insight into predicted performance and reliability through different seasons.

The simulation model for the PVT+HP system is a transient model taking hourly boundary conditions as solar radiation and ambient temperature, in addition to system configuration parameters such as PVT area and compressor size, into consideration.

The system, providing water heating from 7 °C to 55-65 °C, can reach a COP of 2.6 in the winter with an ambient temperature of -10.9 °C, and a COP of 5.9 in the summer at an ambient temperature of 17.3 °C.

This thesis provides a numerical transient system simulation model which can be used to simulate the performance of the system, and incorporate a control system (compressor controller and water pump controller). Using the model to design a compressor controller for this system ca be useful for increasing the energy performance and stability of the system.

The results show that the PVT-SAHP can achieve a COP of 2.8 in the winter and 5.8 in the summer, heating water from 7 °C to 55-65 °C in Trondheim, Norway. It also achieves better energy performance and results in lower building net electricity demand than a traditional ASHP or electric heating system in Trondheim, Norway. As a consequence, annual energy costs are significantly reduced. Using a PVT-SAHP with 12 PVT modules á 1.68m^2 and a compressor with displacement volume of $6*10^{-5}m^3$, the annual electricity demand for heating is reduced with 67 % compared to an all-electric heating system, and 21 % compared to an ASHP system. The total effect of the PVT-ASHP is even higher as PV electricity production is increased due to keeping the PV temperature lower than for traditional PV-only installations.

Total annual cost for investing in a PVT-SAHP for DHW- and space heating can be significantly lower than for all-electric heating and ASHP, but only slightly lower than using ASHP and PVs with the same area as the PVTs.

System optimisation and parametric investigation results show that increasing the PVT area slightly increases the COP and heating power of the PVT-SAHP. The effect is more noticeable in the summer than in the winter because of higher ambient temperature and solar radiation. Using a larger compressor will increase the heating power of the system, but decrease the COP if PVT area is not changed. The larger compressor will result in a higher cooling power, reducing the temperature of the PV panels, and therefore also the evaporation temperature, leading to less favourable operating conditions for the HP and a lower COP. On the other hand, a larger compressor increases the PV power production.

A draft proposal for a scientific paper based on the main results is included in Appendix A.

7 Further work

Based on the findings in this work, some further topics of research for the DX PVT-SAHP system are proposed:

- Develop detailed system control using VSD compressor (inverted controlled) to control both the PVT-panel temperature and the condenser heating power.
- Investigate other building categories (offices, hotels, hospitals etc.) or other field of application.
- Improve numerical simulation model, especially in regards to computational time.
- In the simulation model, include slope of PVT and improve calculation for solar insolation accordingly, using solar height, zenith etc.
- Further develop the simulation model to be more user friendly, having a front-end user interface which can be utilised for simulation purposes.
- Investigate the PVT-SAHP system experimentally by real-life building implementation in Norway.
- Investigate grid peak load effects, peak shaving potential, and control strategy in regards to time-of-day electricity prices and grid emission factors.
- Further investigate the performance and feasibility of PVT-SAHP system for low temperature space heating.
- Conduct safety/risk analyses with regards to using R290 (propane) as the working fluid, and propose necessary equipment.
- Investigate the benefit of using a micro-channel (roll-bond) evaporator in a R290 heat pump in regards to safety.

References

[1] J. Yao et al. "Performance improvement of vapor-injection heat pump system by employing PVT collector/evaporator for residential heating in cold climate region". In: *Energy* 219 (2021). DOI: *10.1016/j.energy.2020.119636*.

[2] J. Yao et al. "Co-generation ability investigation of the novel structured PVT heat pump system and its effect on the "Carbon neutral" strategy of Shanghai". In: *Energy* 239 (2022). DOI: *10.1016/j.energy.2021.121863*.

[3] Jian Yao et al. "Two-phase flow investigation in channel design of the roll-bond cooling component for solar assisted PVT heat pump application". In: *Energy Conversion and Management* 235 (May 2021), p. 113988. ISSN: 0196-8904. DOI: *10.1016/J.ENCONMAN.2021.113988*.

[4] Jian Yao et al. "Performance analysis of solar assisted heat pump coupled with build-in PCM heat storage based on PV/T panel". In: *Solar Energy* 197 (Feb. 2020), pp. 279–291.

[5] Martin Wolf. "Performance analyses of combined heating and photovoltaic power systems for residences". In: *Energy Conversion* 16.1-2 (1976), pp. 79–90.

[6] Farideh Yazdanifard, Ehsan Ebrahimnia-Bajestan, and Mehran Ameri. "Investigating the performance of a water-based photovoltaic/thermal (PV/T) collector in laminar and turbulent flow regime". In: *Renewable Energy* 99 (Dec. 2016), pp. 295–306.

[7] Giuseppe Emmi, Angelo Zarrella, and Michele De Carli. "A heat pump coupled with photovoltaic thermal hybrid solar collectors: A case study of a multi-source energy system". In: *Energy Conversion and Management* 151 (Nov. 2017), pp. 386–399. ISSN: 0196-8904. DOI: *10.1016/J.ENCONMAN.2017.08.077*.

[8] H. A. Zondag et al. "The yield of different combined PV-thermal collector designs". In: *Solar Energy* 74.3 (2003), pp. 253–269.

[9] M. Chandrasekar and T. Senthilkumar. "Five decades of evolution of solar photovoltaic thermal (PVT) technology – A critical insight on review articles". In: *Journal of Cleaner Production* 322 (Nov. 2021), p. 128997. ISSN: 0959-6526. DOI: *10.1016/J.JCLEPRO.2021.128997*.

[10] M. Mohanraj et al. "Research and developments on solar assisted compression heat pump systems – A comprehensive review (Part A: Modeling and modifications)". In: *Renewable and Sustainable Energy Reviews* 83 (Mar. 2018), pp. 90–123.

[11] M. Mohanraj et al. "Research and developments on solar assisted compression heat pump systems – A comprehensive review (Part-B: Applications)". In: *Renewable and Sustainable Energy Reviews* 83 (2018), pp. 124–155. DOI: *10.1016/j.rser.2017.08.086*.

[12] Clara Good et al. "Hybrid Photovoltaic-thermal Systems in Buildings – A Review". In: *Energy Procedia* 70 (May 2015), pp. 683–690. ISSN: 1876-6102. DOI: *10.1016/J.EGYPRO.2015.02.176*.

[13] A. James et al. "Thermal analysis of heat pump systems using photovoltaic-thermal collectors: a review". In: *Journal of Thermal Analysis and Calorimetry* 144.1 (2021). DOI: *10.1007/s10973-020-09431-2*.

[14] Clara Good, Inger Andresen, and Anne Grete Hestnes. "Solar energy for net zero energy buildings – A comparison between solar thermal, PV and photovoltaic–thermal (PV/T) systems". In: *Solar Energy* 122 (Dec. 2015), pp. 986–996. ISSN: 0038-092X. DOI: *10.1016/J.SOLENER.2015.10.013*.

[15] Jan VIncent Thue. *Bygningsfysikk - Grunnlag*. Trondheim: Fagbokforlaget, 2016, p. 464. ISBN: 9788245019940.

[16] Weiwei Hu et al. "Experimental research on the convective heat transfer coefficient of photovoltaic panel". In: *Renewable Energy* 185 (Feb. 2022), pp. 820–826. ISSN: 0960-1481. DOI: *10.1016/J.RENENE.2021.12.090*.

[17] Jinzhi Zhou et al. "Numerical simulation and experimental validation of a micro-channel PV/T modules based direct-expansion solar heat pump system". In: *Renewable Energy* 145 (Jan. 2020), pp. 1992–2004. ISSN: 0960-1481. DOI: *10.1016/J.RENENE.2019.07.049*.

[18] John K. Kaldellis, Marina Kapsali, and Kosmas A. Kavadias. "Temperature and wind speed impact on the efficiency of PV installations. Experience obtained from outdoor measurements in Greece". In: *Renewable Energy* 66 (June 2014), pp. 612–624. ISSN: 0960-1481. DOI: *10.1016/J.RENENE.2013.12.041*.

[19] Suresh Kumar and S. C. Mullick. "Wind heat transfer coefficient in solar collectors in outdoor conditions". In: *Solar Energy* 84.6 (June 2010), pp. 956–963. ISSN: 0038-092X. DOI: *10.1016/J.SOLENER.2010.03.003*.

[20] Jian Yao et al. "Theoretical analysis on efficiency factor of direct expansion PVT module for heat pump application". In: *Solar Energy* 206 (Aug. 2020), pp. 677–694. ISSN: 0038-092X. DOI: *10.1016/J.SOLENER.2020.04.053*.

[21] S. Armstrong and W. G. Hurley. "A thermal model for photovoltaic panels under varying atmospheric conditions". In: *Applied Thermal Engineering* 30.11-12 (Aug. 2010), pp. 1488–1495. ISSN: 1359-4311. DOI: *10.1016/J.APPLTHERMALENG.2010.03.012*.

[22] Michal Haida et al. "Experimental analysis of the R744 vapour compression rack equipped with the multi-ejector expansion work recovery module". In: *International Journal of Refrigeration* 64 (Apr. 2016), pp. 93–107. ISSN: 01407007. DOI: *10.1016/J.IJREFRIG.2016.01.017*.

[23] Tina Birmpili. "Montreal Protocol at 30: The governance structure, the evolution, and the Kigali Amendment". In: *Comptes Rendus Geoscience* 350.7 (Nov. 2018), pp. 425–431. ISSN: 1631-0713. DOI: *10.1016/J.CRTE.2018.09.002*.

[24] Alibakhsh Kasaeian et al. "Applications of eco-friendly refrigerants and nanorefrigerants: A review". In: *Renewable and Sustainable Energy Reviews* 96 (Nov. 2018), pp. 91–99. ISSN: 1364-0321. DOI: *10.1016/J.RSER.2018.07.033*.

[25] J. F. Chen, Y. J. Dai, and R. Z. Wang. "Experimental and theoretical study on a solar assisted CO2 heat pump for space heating". In: *Renewable Energy* 89 (Apr. 2016), pp. 295–304. ISSN: 0960-1481. DOI: *10.1016/J.RENENE.2015.12.039*.

[26] S. Smitt, I. Tolstorebrov, and A. Hafner. "Integrated CO2 system with HVAC and hot water for hotels: Field measurements and performance evaluation". In: *International Journal of Refrigeration* 116 (Aug. 2020), pp. 59–69. ISSN: 0140-7007. DOI: *10.1016/J.IJREFRIG.2020.03.021*.

[27] Paride Gullo, Armin Hafner, and Krzysztof Banasiak. "Transcritical R744 refrigeration systems for supermarket applications: Current status and future perspectives". In: *International Journal of Refrigeration* 93 (Sept. 2018), pp. 269–310. ISSN: 0140-7007. DOI: *10.1016/J.IJREFRIG.2018.07.001*.

[28] M. Mohanraj, S. Jayaraj, and C. Muraleedharan. "A comparison of the performance of a direct expansion solar assisted heat pump working with R22 and a mixture of R407C-liquefied petroleum gas". In: *Proceedings of the Institution of Mechanical Engineers, Part A: Journal of Power and Energy* 223.7 (2009), pp. 821–833. DOI: *10.1243/09576509JPE764*.

[29] D. Sánchez et al. "Energy impact evaluation of different low-GWP alternatives to replace R134a in a beverage cooler. Experimental analysis and optimization for the pure refrigerants R152a, R1234yf, R290, R1270, R600a and R744". In: *Energy Conversion and Management* 256 (Mar. 2022), p. 115388. ISSN: 0196-8904. DOI: *10.1016/J.ENCONMAN.2022.115388*.

[30] D. Sánchez et al. "Energy performance evaluation of R1234yf, R1234ze(E), R600a, R290 and R152a as low-GWP R134a alternatives". In: *International Journal of Refrigeration* 74 (Feb. 2017), pp. 269–282. ISSN: 0140-7007. DOI: *10.1016/J.IJREFRIG.2016.09.020*.

[31] Giovanni A. Longo et al. "Assessment of the low-GWP refrigerants R600a, R1234ze(Z) and R1233zd(E) for heat pump and organic Rankine cycle applications". In: *Applied Thermal Engineering* 167 (Feb. 2020), p. 114804. ISSN: 1359-4311. DOI: *10.1016/J.APPLTHERMALENG.2019.114804*.

[32] Mustafa Ozsipahi et al. "Experimental study of R290/R600a mixtures in vapor compression refrigeration system". In: *International Journal of Refrigeration* 133 (Jan. 2022), pp. 247–258. ISSN: 0140-7007. DOI: *10.1016/J.IJREFRIG.2021.10.004*.

[33] Xiangqiang Kong et al. "Experimental investigation on a direct-expansion solar-assisted heat pump water heater using R290 with micro-channel heat transfer technology during the winter period". In: *International Journal of Refrigeration* 113 (May 2020), pp. 38–48. ISSN: 0140-7007. DOI: *10.1016/J.IJREFRIG.2020.01.019*.

[34] Miglioli Alessandro et al. "Photovoltaic-thermal solar-assisted heat pump systems for building applications: Integration and design methods". In: *Energy and Built Environment* (July 2021). ISSN: 2666-1233. DOI: *10.1016/J.ENBENV.2021.07.002*.

[35] Reiner Braun et al. "System design and feasibility of trigeneration systems with hybrid photovoltaic-thermal (PVT) collectors for zero energy office buildings in different climates". In: *Solar Energy* 196 (Jan. 2020), pp. 39–48. ISSN: 0038-092X. DOI: *10.1016/J.SOLENER.2019.12.005*.

[36] Chao Zhou et al. "Experimental study on the cogeneration performance of roll-bond-PVT heat pump system with single stage compression during summer". In: *Applied Thermal Engineering* 149 (Feb. 2019), pp. 249–261.

[37] N. Gunasekar and M. Mohanraj. "Performance analysis of solar photovoltaic-thermal hybrid heat pump working with circular and triangular evaporator tube configuration". In: *International Journal of Pharmacy and Technology* 8.4 (2016), pp. 21737–21748.

[38] Hongbing Chen, Saffa B. Riffat, and Yu Fu. "Experimental study on a hybrid photovoltaic/heat pump system". In: *Applied Thermal Engineering* 31.17-18 (Dec. 2011), pp. 4132–4138. ISSN: 1359-4311. DOI: *10.1016/J.APPLTHERMALENG.2011.08.027*.

[39] J. Yao et al. "Performance analysis of a residential heating system using borehole heat exchanger coupled with solar assisted PV/T heat pump". In: *Renewable Energy* 160 (2020), pp. 160–175. DOI: *10.1016/j.renene.2020.06.101*.

[40] Jingyong Cai et al. "A novel PV/T-air dual source heat pump water heater system: Dynamic simulation and performance characterization". In: *Energy Conversion and Management* 148 (Sept. 2017), pp. 635–645. ISSN: 0196-8904. DOI: *10.1016/J.ENCONMAN.2017.06.036*.

[41] Ralney N. Faria et al. "Dynamic modeling study for a solar evaporator with expansion valve assembly of a transcritical CO2 heat pump". In: *International Journal of Refrigeration* 64 (Apr. 2016), pp. 203–213. ISSN: 0140-7007. DOI: *10.1016/J.IJREFRIG.2016.01.004*.

[42] S. K. Chaturvedi, D. T. Chen, and A. Kheireddine. "Thermal performance of a variable capacity direct expansion solar-assisted heat pump". In: *Energy Conversion and Management* 39.3-4 (Feb. 1998), pp. 181–191. ISSN: 0196-8904. DOI: *10.1016/S0196-8904(96)00228-2*.

[43] Yanjun Du, Jianhua Wu, and Che Wang. "Research on control method of a R290 ASHP under low-temperature heating condition". In: *International Journal of Refrigeration* 129 (Sept. 2021), pp. 60–68. ISSN: 0140-7007. DOI: *10.1016/J.IJREFRIG.2021.04.026*.

[44] Rasmus Luthander et al. "Photovoltaic self-consumption in buildings: A review". In: *Applied Energy* 142 (Mar. 2015), pp. 80–94. ISSN: 0306-2619. DOI: *10.1016/J.APENERGY.2014.12.028*.

[45] Muhammad Shahzad Javed et al. "Quantifying techno-economic indicators' impact on isolated renewable energy systems". In: *iScience* 24.7 (July 2021), p. 102730. ISSN: 2589-0042. DOI: *10.1016/J.ISCI.2021.102730*.

[46] Domenico Mazzeo et al. "EnergyPlus, IDA ICE and TRNSYS predictive simulation accuracy for building thermal behaviour evaluation by using an experimental campaign in solar test boxes with and without a PCM module". In: *Energy and Buildings* 212 (Apr. 2020), p. 109812. ISSN: 0378-7788. DOI: *10.1016/J.ENBUILD.2020.109812*.

[47] Danny Jonas et al. "Performance modeling of PVT collectors: Implementation, validation and parameter identification approach using TRNSYS". In: *Solar Energy* 193 (Nov. 2019), pp. 51–64. ISSN: 0038-092X. DOI: *10.1016/J.SOLENER.2019.09.047*.

[48] Angelo Zarrella et al. "The validation of a novel lumped parameter model for photovoltaic thermal hybrid solar collectors: a new TRNSYS type". In: *Energy Conversion and Management* 188 (May 2019), pp. 414–428. ISSN: 0196-8904. DOI: *10.1016/J.ENCONMAN.2019.03.030*.

[49] M. Aldubyan and A. Chiasson. "Thermal Study of Hybrid Photovoltaic-Thermal (PVT) Solar Collectors Combined with Borehole Thermal Energy Storage Systems". In: *Energy Procedia* 141 (Dec. 2017), pp. 102–108. ISSN: 1876-6102. DOI: *10.1016/J.EGYPRO.2017.11.020*.

[50] Y. Yu et al. "Performance comparisons of two flat-plate photovoltaic thermal collectors with different channel configurations". In: *Energy* 175 (May 2019), pp. 300–308. ISSN: 0360-5442. DOI: *10.1016/J.ENERGY.2019.03.054*.

[51] Amirmohammad Behzadi, Ahmad Arabkoohsar, and Yongheng Yang. "Optimization and dynamic techno-economic analysis of a novel PVT-based smart building energy system". In: *Applied Thermal Engineering* 181 (Nov. 2020), p. 115926. ISSN: 1359-4311. DOI: *10.1016/J.APPLTHERMALENG.2020.115926*.

[52] Mohammad Abu-Rumman, Mohammad Hamdan, and Osama Ayadi. "Performance enhancement of a photovoltaic thermal (PVT) and ground-source heat pump system". In: *Geothermics* 85 (May 2020), p. 101809. ISSN: 0375-6505. DOI: *10.1016/J.GEOTHERMICS.2020.101809*.

[53] A. Del Amo et al. "Analysis and optimization of a heat pump system coupled to an installation of PVT panels and a seasonal storage tank on an educational building". In: *Energy and Buildings* 226 (Nov. 2020).

[54] Eric W. Lemmon et al. *NIST Standard Reference Database 23: Reference Fluid Thermodynamic and Transport Properties-REFPROP, Version 10.0, National Institute of Standards and Technology*. Gaithersburg, 2018. DOI: *https://doi.org/10.18434/T4/1502528*. URL: *https://www.nist.gov/srd/refprop*.

[55] Mara Magni et al. "Hourly simulation results of building energy simulation tools using a reference office building as a case study". In: *Data in Brief* 38 (Oct. 2021), p. 107370. ISSN: 2352-3409. DOI: *10.1016/J.DIB.2021.107370*.

[56] Simenergi. *SIMIEN*. URL: *https://simenergi.no/simien/*.

[57] Standard Norge. *SN-NSPEK 3031:2020 -Bygningers energiytelse Beregning av energibehov og energiforsyning*. 2020.

[58] *Forskrift om tekniske krav til byggverk (Byggteknisk forskrift)*. 2018. URL: *https://lovdata.no/dokument/SF/forskrift/2017-06-19-840*.

[59] Signe Ryssdal. "High Temperature Heat Pumps in Integrated Energy Systems". MA thesis. NTNU, 2020.

[60] S. K. Chaturvedi et al. "Two-stage direct expansion solar-assisted heat pump for high temperature applications". In: *Applied Thermal Engineering* 29.10 (July 2009), pp. 2093–2099. ISSN: 13594311. DOI: *10.1016/j.applthermaleng.2008.10.010*.

[61] Levon Ghabuzyan et al. "Thermal Effects on Photovoltaic Array Performance: Experimentation, Modeling, and Simulation". In: *Applied Sciences* 11.4 (2021). DOI: *10.3390/app11041460*. URL: *https://doi.org/10.3390/app11041460*.

[62] Aoife Houlihan Wiberg et al. "A net zero emission concept analysis of a single-family house". In: *Energy and Buildings* 74 (May 2014), pp. 101–110. ISSN: 0378-7788. DOI: *10.1016/J.ENBUILD.2014.01.037*.

A Scientific draft paper proposal

Article

Model development and performance analysis of an R290 direct expansion solar assisted heat pump system using PVT.

Kristoffer Wigdahl Lie [1]*, Vojislav Novakovic [1] and Yanjun Dai [2,3]

1 Department of Energy and Process Engineering, Norwegian University of Science and Technology, Trondheim, NO-7491, Norway
2 Institute of Refrigeration and Cryogenics, Shanghai Jiao Tong University, Shanghai, 200240, China
3 Engineering Research Center of Solar Energy and Refrigeration, MOE, China
* Correspondence: kristowl@ntnu.no; Tel.:47894980

Abstract: A novel Photovoltaic-thermal (PVT) module which may generate more electricity than a normal PV module, and can also output thermal energy from the received solar radiation, is under development. The power from PVT module can be used for driving heat pump to further lift the temperature of heat from PVT module and thus meet the regiments for comfortable heating. This study investigates the modelling and simulation of a single-source Direct Expansion Photovoltaic Solar Assisted Heat Pump (DX PVT-SAHP) system using R290 for hot water heating. A numerical transient simulation model of the PVT-SAHP were developed in MATLAB. A case study was then done for the system operating in Trondheim, Norway. Feasibility with regards to both energy performance and economy were investigated, and influence of system configurations such as PVT area and compressor size on the performance were evaluated.The results show that the PVT-SAHP can achieve a COP of 2.8 in the winter and 5.8 in the summer, heating water from 7 °C to 55-65 °C in Trondheim, Norway. It also achieves better annual energy performance and leads to lower building net annual electricity demand than a traditional air-source heat pump (ASHP) (21 %) or electric heating (67 %) system in Trondheim. The economic analysis shows that although with higher investment costs, the PVT-SAHP has a lifetime annual cost which is lower than for an ASHP and electric boiler.

Keywords: PVT; Heat pump; PVT-SAHP; R290; DHW heating; Space Heating

Citation: Lie, K.W.; Novakovic, V.; Dai, Y. Title. *Energies* **2022**, *1*, 0. https://doi.org/

Received:
Accepted:
Published:

1. Introduction

One of the most influential sectors to the rising global emissions is the building sector, contributing with large amounts of energy consumption, in addition to embedded emissions from both construction and demolition. The high-tempo development of urban areas results in even larger activity, and special focus in the planning of future energy systems must be given to achieve low-emission and low energy solutions. The photovoltaic thermal (PVT) panel was first introduced by Wolf et al.[1] in 1976. Since then, large amounts of research have been done to develop the system[2–6]. A novel Photovoltaic-thermal (PVT) module which may generate more than 10 % electricity than that of the normal PV module and can also output thermal energy with about 40 % of the received solar radiation is under development [7–9]. The power from PVT module can be used for driving heat pump to further lift the temperature of heat from PVT module and thus meet the regiments for comfortable heating [10–15]. The aim of this work is to contribute to development of the mathematical model of a novel PVT module in combination with a heat pump system, and investigate the performance of the system in cold Nordic climate.

2. Methods

2.1. Model overview

The system modelled in this work is a single-source DX PVT-SAHP system using R290 (Propane) as the refrigerant. It is modelled and simulated in MATLAB. The thermophysical properties of the refrigerant and water are extracted from the REFPROP[16] database using a plug-in dll. A simplified schematic of the investigated PVT-SAHP can be seen in Figure 1.

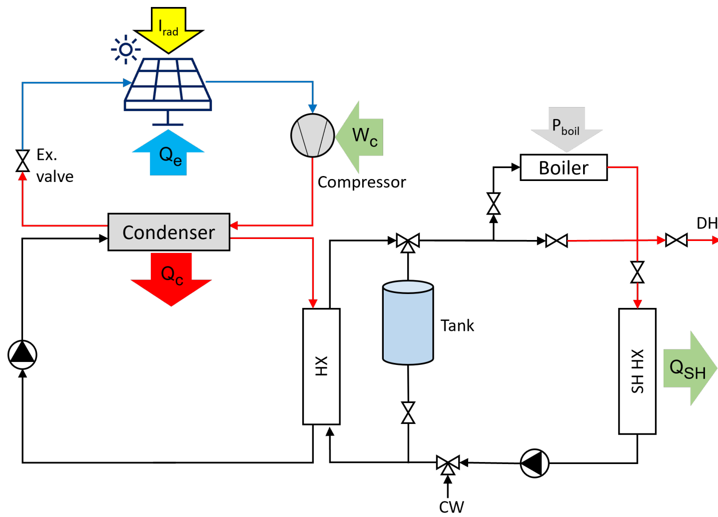

Figure 1. Schematic diagram for the whole energy system. Including both energy production (PVT+HP and boiler), energy storage (tank), and load side model. Ex.valve = expansion valve; HX = Heat exchanger; CW = Cold city water; DHW=Domestic hot water; I_{rad}=Solar radiation; Q_e=Evaporation heat transfer; Q_c=Condenser heat transfer; W_c=Compressor work; P_{boil}=Boiler power; Q_{SH}=Heat transfer to space heating.

2.2. Mathematical model

2.2.1. PVT evaporator

The transient balance equation (energy conservation) can be described as:

$$C_{pv}\frac{\delta T_{pv}}{\delta t} = G_{eff} - P_{el,pv} - Q_{loss} - Q_{evap} \quad (1)$$

m_{pv} is the mass [kg] of the PV module, c_{pv} is specific heat of PV [J/(kgK)], δT_{pv} and δt is change in PV temperature and time respectively, G_{eff} is effective solar irradiation 2,

$$G_{eff} = \alpha_p * I * A_{pv} \quad (2)$$

$P_{el,pv}$ is the electrical power production (Equation 3),

$$P_{pv} = A_{pv} I \tau_{g,pv} \alpha_p \beta_p \eta_{pv}, \quad (3)$$

Q_{loss} is heat loss from the PV, and Q_{evap} is heat transfer to the refrigerant in the evaporator.

Heat transfer rate (Q_{th}) from the PV cells to the refrigerant (Equation 4):

$$Q_{th} = Q_u = Q_{abs} - Q_{loss} \quad (4)$$

,where Q_u is the total useful solar heat received by the PVT and Q_{loss} is the overall heat loss in the PVT.

The heat loss (Q_{loss}) is calculated using overall heat loss coefficient (U_{loss}), PVT collector area (A_{pvt}) and temperature of PV cells (T_p) and ambient air (T_a)[17]:

$$Q_{loss} = U_{loss} \cdot A_{pv} \cdot (T_{pv} - T_a) \tag{5}$$

$$U_{loss} = \left[\frac{1}{h_{cd,p-c} + h_{rd,p-c}} + \frac{1}{h_{cv,c-a} + h_{rd,c-a}} \right]^{-1} \tag{6}$$

,where cd is conduction, rd is radiation, cv is convection, "p" is pv panel, "c" is glazing cover, and "a" is ambient. The radiative, conductive, and convective heat transfer coefficients is calculated as[18,19] :

$$h_{rd,p-c} = \epsilon_p * \sigma * (T_p + T_c) * (T_p^2 + T_c^2) \tag{7}$$

$$h_{rd,c-a} = \epsilon_p * \sigma * (T_c + T_a) * (T_c^2 + T_a^2) \tag{8}$$

$$h_{cv,c-a} = (13.07 + 2.18 * 0) + (3.65 - 0.26 * 0) * v_{air} \tag{9}$$

$$h_{cd,p-c} = \frac{1}{\delta_c / \kappa_C} \tag{10}$$

The useful energy gain which can be transferred to the refrigerant can be described as [17]:

$$Q'_u = 12 * \frac{1}{2} * \frac{W}{\sqrt{3}} * \frac{T_{pv} - T_R}{\frac{1}{D} * (\frac{\delta_{eva}}{\kappa_{eva}} + \frac{\delta_{ei}}{\kappa_{ei}} + \frac{\delta_{rb}}{\kappa_{rb}}) + \frac{1}{h_{eq} * \pi * D}} \tag{11}$$

W is the roll-bond fluid-channel pattern width, D is roll-bond fluid channel width, δ is the layer thickness of eva grease (eva), electric insulation (ei) and roll-bond panel (rb), while h_{eq} is equivalent heat transfer coefficient between roll-bond panel and refrigerant. For further description it is referred to the literature[17]. By implementing the heat removal factor, the heat gain of the fluid in the PVT (Q_u') can be also described using the heat loss coefficient (U_{loss}), inlet fluid temperature (T_f) and ambient temperature (T_a) [17]:

$$Q_u{}' = A_{pv} * F_R * \Big[(\tau_{g,pv} \alpha_p) * I * (1 - \eta_{pv}) - U_{loss} * (T_f - T_a) \Big] \tag{12}$$

Because the evaporating process is isothermal in a DX evaporator, the refrigerant temperature (T_R) is the same as the evaporation temperature (T_{evap}) through the whole component, and the heat removal factor (F_R) is then equal to the efficiency factor (F') [17], and:

$$F_R = F' \tag{13}$$

Using Equation 12, Equation 11, Equation 13, the efficiency factor is calculated as:

$$F' = 12 * \frac{1}{2} * \frac{W}{\sqrt{3}} * \frac{T_{pv} - T_{evap}}{\frac{1}{D} * (\frac{\delta_{eva}}{\kappa eva} + \frac{\delta_{ei}}{\kappa_{ei}} + \frac{\delta_{rb}}{\kappa_{rb}}) + \frac{1}{h_{eq} * \pi * D}} * \frac{1}{A_{pv}} * \frac{1}{(\tau_{g,pv} \alpha_p) * I * (1 - \eta_{pv}) - U_{loss} * (T_{evap} - T_a)} \tag{14}$$

The calculated efficiency factor (F')(Equation 14) is then used to obtain the useful heat gain (Q_u') through Equation 12:

$$Q_u{}' = A_{pv} * F' * \left[(\tau_{g,pv} \alpha_p) * I * (1 - \eta_{pv}) - U_{loss} * (T_{evap} - T_a) \right]$$

The heat transfer from the PV to the roll-bond evaporator is assumed to be ideal, with no pressure losses. The evaporation heat transfer is then described as:

$$Q_{evap} = Q'_u \tag{15}$$

The heat rate (Q_{evap}) transferred from the heat source to the refrigerant in the evaporator can be expressed as

$$Q_e = \dot{m}_R * (h_1 - h_4) \tag{16}$$

,where $\dot{m}_R$ is the refrigerant mass flow rate [kg/s], h_1 and h_4 is specific enthalpy (kJ/kg) at evaporator outlet and inlet respectively.

Equation 15,Equation 12 and Equation 16 is used to check if the energy balance in the PVT evaporator is reached for a given time step, I.e check if the HP thermodynamic cycle and PVT component has the same Q_{evap}. If the difference between the two sides of the equation is larger than a set tolerance criteria, the evaporation temperature is adjusted. The new evaporation temperature is calculated using Equation 12:

$$T_{evap} = \frac{(\tau_{g,pv}\alpha_p) * I * (1 - \eta_{pv}) - \frac{Q_{evap}}{A_{pv}*F'} + U_{loss} * T_a}{U_{loss}}$$

2.2.2. Compressor

The compressor model calculates the refrigerant temperature out of the compressor/into the condenser (T_2), enthalpy at compressor outlet (h_2), mass flow rate of the refrigerant ($\dot{m}_R$), and compressor work (W_c). Equations used are Equation 17,

$$w_{comp} = \frac{h_{2,is} - h_1}{\eta_{is}} = \frac{w_{comp,is}}{\eta_{is}} \tag{17}$$

The inputs to the compressor model is refrigerant pressure (P_{evap}), density (ρ_1), enthalpy (h_1) and entropy (s_1) at the evaporator outlet; pressure (P_{cond}) in the condenser; and compressor speed (N). The isentropic and volumetric efficiencies are calculated using the compressor pressure ratio (Π). Since it is assumed no pressure losses in the heat exchangers or pipes, they become [10]:

$$\Pi = \frac{P_{cond}}{P_{evap}} \tag{18}$$

$$\eta_{is} = -0.17938 + 0.87501 * \Pi - 0.30014 * \Pi^2 + 0.04135 * \Pi^3 - 0.00206 * \Pi^4 \tag{19}$$

$$\lambda_c = 0.0011 * \Pi^2 - 0.0487 * \Pi + 0.9979 \tag{20}$$

2.2.3. Condenser and valve

Delivered heat rate in the condenser is described by:

$$Q_c = \dot{m}_R * (h_2 - h_3) \tag{21}$$

Heat transferred through the condenser is calculated using the condenser overall U-value (U_c), heat exchanging area (A_c), and the logarithmic mean temperature difference (LMTD).

$$Q_{cond} = U_c * A_c * LMTD_c \tag{22}$$

$$LMTD = \frac{\Delta T_1 - \Delta T_2}{ln\frac{\Delta T_1}{\Delta T_2}} \tag{23}$$

Since the condensing temperature is "guessed" before the compressor model is solved, a loop is made to determine the actual temperature. The outlet water temperature is calculated using as:

$$T_{w,out} = T_{w,in} + Q_{cond}/(C_{p,w} * m_w); \tag{24}$$

To calculate the new condensing temperature, Equation 23 and Equation 24 are combined [20]:

$$T_{cond} = \frac{T_{w,in} - T_{w,out} * e^{\left(\frac{T_{w,out} - T_{w,in}}{LMTD}\right)}}{1 - e^{\left(\frac{T_{w,out} - T_{w,in}}{LMTD}\right)}}$$

The expansion valve is modelled as isenthalpic:

$$h_4 = h_1 \tag{25}$$

2.2.4. Algorithm

The algorithm for solving the system are presented in Figure 2

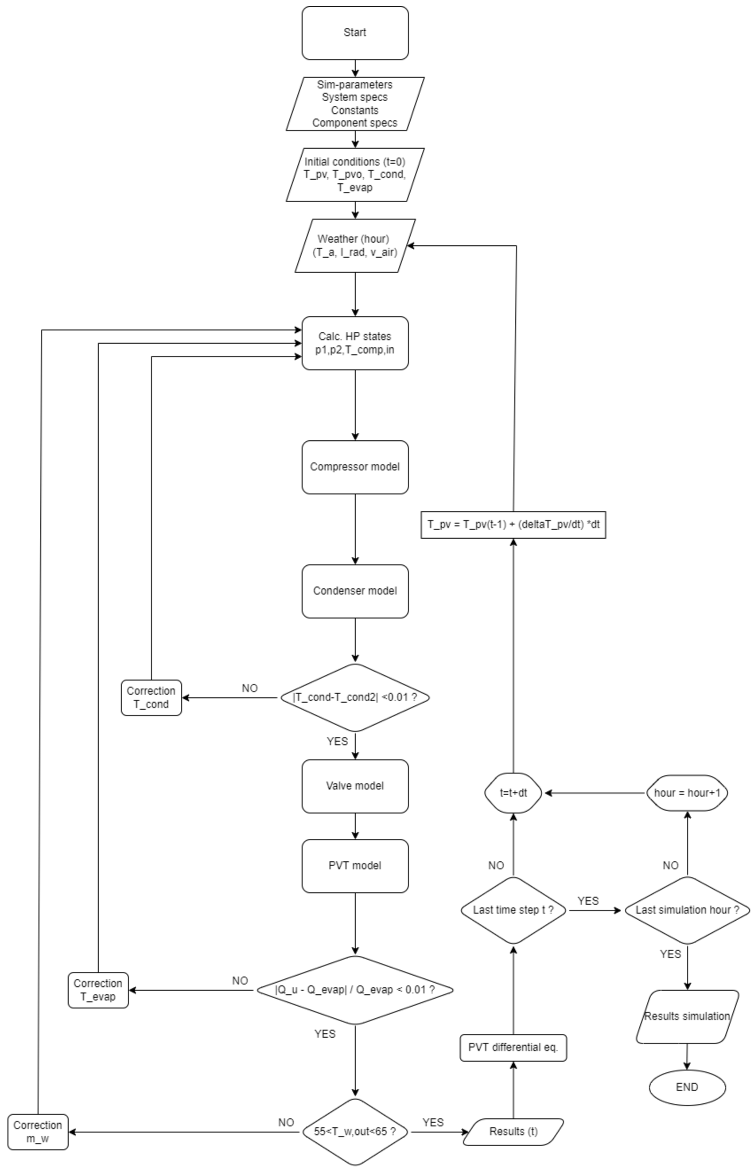

Figure 2. Algorithm for numerical simulation model of the PVT-ASHP.

2.3. Case study

The case building studied are a 150m^2 single-family residential house in Trondheim, Norway. The building is modelled using the simulation software SIMIEN [21], internal loads from the Norwegian standard SN-NSPEK 3031[22], and energy- and ventilation requirements from the Norwegian building regulations [23]. Room temperature set point is The PVT-SAHP system is evaluated against several other energy systems consisting of electric boiler, air-source heat pump (ASHP), and PV panels. system configurations are presented in Table 1.

Table 1. Evaluated case study system configurations.

Label	Config	PVTs	PVs
El.only	Electric boiler	0	0
ASHP	Base + ASHP	0	0
ASHP+3PVs	Base + ASHP and PV	0	3
ASHP+6PVs	Base + ASHP and PV	0	6
ASHP+12PVs	Base + ASHP and PV	0	12
3PVT-SAHP	Base + PVT-SAHP	3	0
6PVT-SAHP	Base + PVT-SAHP	6	0
12PVT-SAHP	Base + PVT-SAHP	12	0

3. Results and discussion

The results for the system simulation and case study are presented and discussed in this chapter.

3.1. PVT area

In the summer (Figure 3), the cooling effect the PVT-ASHP is noticeable due to high solar radiation. The average and max. COP is increased from 4.5 to 4.8 and 5.1 to 5.8 respectively. The reason is higher PV temperature, which is increased from 31 to 34 °C because of a higher heat exchanging area of the PVT modules. The thermal efficiency drops from 52 to 19 %. Reducing the number of PVT modules to 3, the average COP decrease to 4.1 and max. COP to 4.9. The PV temperature becomes lower with a max. of 26 °C. PV efficiency improvement is increased to 5.2 %, and thermal efficiency to 78 %. SSR is 0.44.

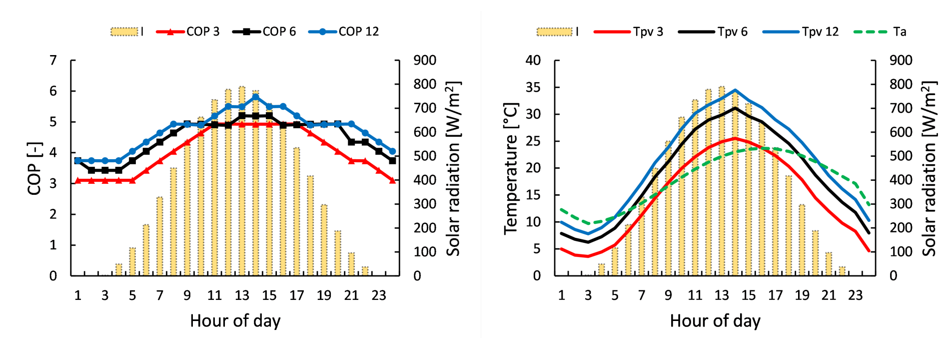

(a) **(b)**

Figure 3. **(a)** PV temperature (T_{pv}), ambient temperature (T_a), solar radiation(I), and COP for June 25th using 3, 6 and 12 PVT modules.; **(b)**, condensation power for different compressor sizes.

Comparing the influence the PVT area has on the condenser power for winter and summer conditions, a noticeable difference can be found. Figure 4 presents the heat rate in the condenser (condenser power) using 3, 6, and 12 PVT modules for a summer day and a winter day. In the winter, with low ambient temperature and lower solar radiation, the change in condenser power by changing the PVT area is minor. At peak solar radiation (hour 14) there is only a 9 % (96 W) increase from 3 to 12 PVT modules. In the summer, the increase at the same time is 30 % (870 W). The reason is clearly better operating conditions in the summer, with higher solar radiation and ambient temperature, which results in higher PV temperature and therefore COP. This can be seen in Figure 3b as the PV temperature difference between 3 and 12 PVT modules is 1.8 °C and 9 °in the winter and summer respectively (hour 14) . Although, it can be noted that the tendency contrast between summer and winter is lower when the solar radiation is low, especially during the night.

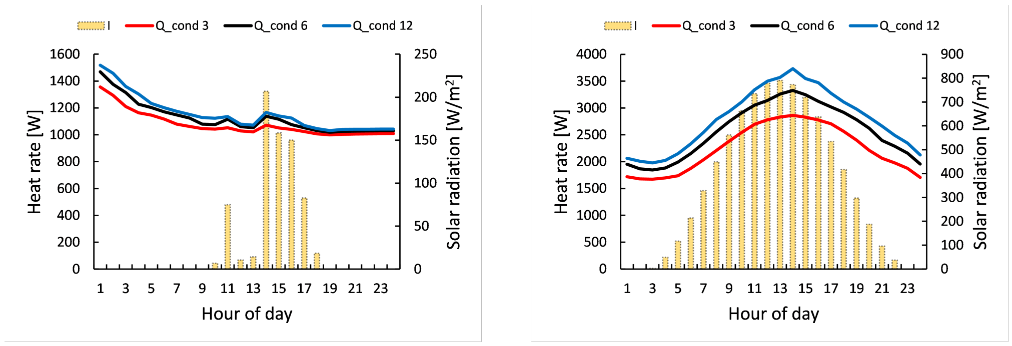

(a) **(b)**

Figure 4. Condenser power (Q_{cond}) and solar radiation (I) using 3, 6 and 12 PVT modules. **(a)**, Winter, February 14th; **(b)**, Summer, June 25th.

3.2. Compressor size

Figure 5a shows that to keep the temperature of the PVs close to the ambient temperature, the compressor needs to be of sufficient size. For this particular case, the V_{th} would have to be between 5*10^{-5}m^3 and 7*10^{-5}m^3. This results in lower COP than for a smaller compressor if no other system configurations is changed. The reason for drop in COP is larger cooling power leading to lower PV temperature. Using a compressor with displacement volume of 9*10^{-5}m^3 the maximum PV temperature becomes 14 °C, providing heating power of 13 kW and PVT cooling power of 9 kW. As a comparison, the maximum temperature using a compressor with 2*10^{-5}m^3 displacement is 25 °C, and the maximum temperature of the PV only is 41 °C (No cooling, only PV panels). Figure 5a presents the COP and condenser heat rate for different compressor sizes. When the compressor size is increased, the heating rate of the PVT-SAHP increases proportionally, but as a result the COP decreases. An observation is that the slope of change is more significant for summer conditions than for spring conditions. This can be explained due to better operating conditions for the system, i.e. higher ambient temperature and solar radiation.

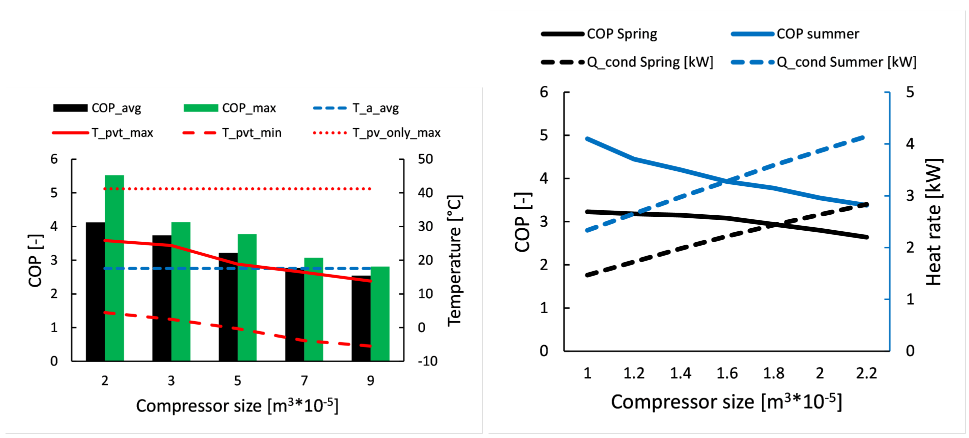

(a) **(b)**

Figure 5. Effects of changing the compressor size. (a), Average COP (COP_{avg}), maximum COP (COP_{max}), ambient temp. (T_a), maximum and minimum PV temp. (T_{pv}), and maximum PV-only temp. ($T_{pv,only}$) ; (b), Average COP (COP_{avg}), maximum COP (COP_{max}), PVT total efficiency ($\eta_{tot,avg}$), and self-sufficiency rate (SSR).

3.3. Annual performance

The annual delivered energy, electricity usage, PV electricity production, and net electricity for the building model with the different system configurations are presented in Figure 6. The delivered heating power from the electric boiler (Q_{el}) is 100 % for the baseline configuration since it is the only heating component. If an ASHP with an SCOP of 3.0 is utilised for space heating, the electricity usage for the building is significantly reduced. Comparing the PVT-SAHP system against the electric boiler, the net electricity demand for heating purpose is reduced with 52 %, 75 %, and 93 % using the 3, 6, and 12 PVT systems respectively. The PV production through the year for these PVT-SAHP configurations are 1294 kWh, 2589 kWh and 5178 kWh respectively.

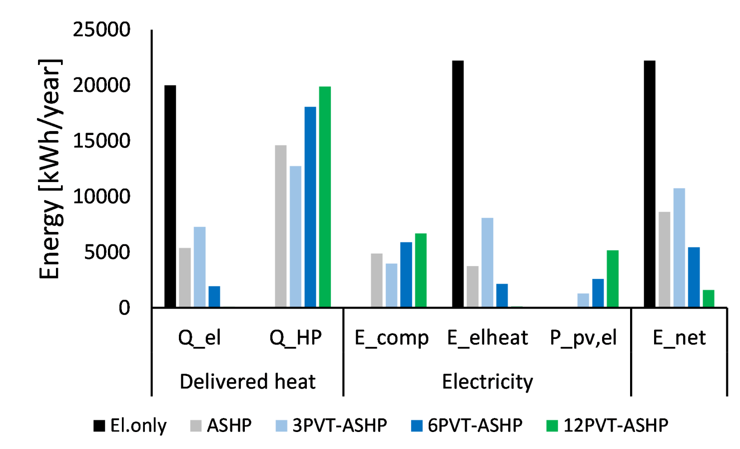

Figure 6. Delivered heat energy, electricity usage and production, and net electricity for a year. Q_{el} and Q_{HP} is delivered heat from el.boiler and heat pump; E_{comp}=compressor electricity usage; E_{elheat}= Boiler electricity usage; $P_{pv,el}$=PV electricity production; and E_{net}=Net electricity usage.

4. Conclusions

This work investigates the feasibility and energy performance of a single-source R290 direct expansion PVT solar assisted heat pump (DX PVT-SAHP) in the cold climate of Trondheim, Norway, by developing a transient numerical system simulation model and conducting a case study for a small residential house.

The results show that the PVT-SAHP can achieve a COP of 2.8 in the winter and 5.8 in the summer, heating water from 7 °C to 55-65 °C in Trondheim, Norway. It also achieves better energy performance and results in lower building net electricity demand than a traditional ASHP or electric heating system in Trondheim, Norway. As a consequence, annual energy costs are significantly reduced. Using a PVT-SAHP with 12 PVT modules á 1.68m^2 and a compressor with displacement volume of $6*10^{-5}m^3$, the annual electricity demand for heating is reduced with 67 % compared to an all-electric heating system, and 21 % compared to an ASHP system. The total effect of the PVT-ASHP is even higher as PV electricity production is increased due to keeping the PV temperature lower than for traditional PV-only installations.

System optimisation and parametric investigation results show that increasing the PVT area slightly increases the COP and heating power of the PVT-SAHP. The effect is more noticeable in the summer than in the winter because of higher ambient temperature and solar radiation. Using a larger compressor will increase the heating power of the system, but decrease the COP if PVT area is not changed. The larger compressor will result in a higher cooling power, reducing the temperature of the PV panels, and therefore also the evaporation temperature, leading to less favourable operating conditions for the HP and a lower COP. On the other hand, a larger compressor increases the PV power production.

Author Contributions: Conceptualization, Yanjun Dai and Kristoffer W. Lie.; methodology, Kristoffer W. Lie.; software, Kristoffer W. Lie.; validation, Kristoffer W. Lie.; formal analysis, Kristoffer W. Lie.; investigation, Kristoffer W. Lie.; resources, Kristoffer W. Lie.; data curation, Kristoffer W. Lie.; writing—original draft preparation, Kristoffer W. Lie.; writing—review and editing, Vojislav Novakovic and Yanjun Dai; visualization, Kristoffer W. Lie.; supervision, Vojislav Novakovic and Yanjun Dai.; project administration, Vojislav Novakovic and Yanjun Dai; funding acquisition, Vojislav Novakovic and Yanjun Dai. All authors have read and agreed to the published version of the manuscript.

Funding: This project is part of the research project between Norway and China: "Key technologies and demonstration of combined cooling, heating and power generation for low-carbon neighborhoods/ buildings with clean energy e ChiNoZEN". The research was funded by the Ministry of Science and Technology of China (MOST project number 2019YFE0104900), and from the Research Council of Norway (NRC project number 304191 - ENERGIX).

Institutional Review Board Statement: Not applicable.

Informed Consent Statement: Not applicable.

Data Availability Statement: Not applicable.

Conflicts of Interest: The authors declare no conflict of interest.

Sample Availability: Samples of the compounds ... are available from the authors.

Abbreviations

The following abbreviations are used in this manuscript:

ASHP	Air-Source Heat Pump
COP	Coefficient of Performance
PVT	Photovoltaic thermal panel
PVT-SAHP	Photovoltaic Thermal Solar Assisted Heat Pump

Appendix A

Appendix A.1

The appendix provides a description of the building model used in the case study. Specifications used into SIMIEN are presented in Table A1.

Table A1. Specifications for the building model used in the case study.

Parameter	Input	Note
Heated floor area	150 m^2	
Floors	2	
Area per floor	75 m^2	
Floor height	3 m	
Facade lengths	$\sqrt{75}$ m	
Window area	15 % of BRA	
Windows	8	One at each facade at each floor
Window area	2.8 m^2	Included frame area
Heat from equipment	60 %	Fraction of equipment load
Heat from lights	100 %	Fraction of lights load
Heat from occupants	1.5 W/m^2	
Heating set point	22 °C	Room temperature set point

Appendix B

All appendix sections must be cited in the main text. In the appendices, Figures, Tables, etc. should be labeled, starting with "A"—e.g., Figure A1, Figure A2, etc.

References

1. Wolf, M. Performance analyses of combined heating and photovoltaic power systems for residences. *Energy Conversion* **1976**, *16*, 79–90.
2. Chandrasekar, M.; Senthilkumar, T. Five decades of evolution of solar photovoltaic thermal (PVT) technology – A critical insight on review articles. *Journal of Cleaner Production* **2021**, *322*, 128997. https://doi.org/10.1016/J.JCLEPRO.2021.128997.
3. Mohanraj, M.; Belyayev, Y.; Jayaraj, S.; Kaltayev, A. Research and developments on solar assisted compression heat pump systems – A comprehensive review (Part A: Modeling and modifications). *Renewable and Sustainable Energy Reviews* **2018**, *83*, 90–123.
4. Emmi, G.; Zarrella, A.; De Carli, M. A heat pump coupled with photovoltaic thermal hybrid solar collectors: A case study of a multi-source energy system. *Energy Conversion and Management* **2017**, *151*, 386–399. https://doi.org/10.1016/J.ENCONMAN.2017.08.077.
5. Zondag, H.A.; de Vries, D.W.; van Helden, W.G.; van Zolingen, R.J.; van Steenhoven, A.A. The yield of different combined PV-thermal collector designs. *Solar Energy* **2003**, *74*, 253–269.
6. Yazdanifard, F.; Ebrahimnia-Bajestan, E.; Ameri, M. Investigating the performance of a water-based photovoltaic/thermal (PV/T) collector in laminar and turbulent flow regime. *Renewable Energy* **2016**, *99*, 295–306.
7. Yao, J.; Zheng, S.; Chen, D.; Dai, Y.; Huang, M. Performance improvement of vapor-injection heat pump system by employing PVT collector/evaporator for residential heating in cold climate region. *Energy* **2021**, *219*. https://doi.org/10.1016/j.energy.2020.119636.
8. Yao, J.; Dou, P.; Zheng, S.; Zhao, Y.; Dai, Y.; Zhu, J.; Novakovic, V. Co-generation ability investigation of the novel structured PVT heat pump system and its effect on the "Carbon neutral" strategy of Shanghai. *Energy* **2022**, *239*. https://doi.org/10.1016/j.energy.2021.121863.
9. Yao, J.; Liu, W.; Zhao, Y.; Dai, Y.; Zhu, J.; Novakovic, V. Two-phase flow investigation in channel design of the roll-bond cooling component for solar assisted PVT heat pump application. *Energy Conversion and Management* **2021**, *235*, 113988. https://doi.org/10.1016/J.ENCONMAN.2021.113988.
10. Yao, J.; Xu, H.; Dai, Y.; Huang, M. Performance analysis of solar assisted heat pump coupled with build-in PCM heat storage based on PV/T panel. *Solar Energy* **2020**, *197*, 279–291.
11. Alessandro, M.; Aste, N.; Claudio, D.P.; Fabrizio, L. Photovoltaic-thermal solar-assisted heat pump systems for building applications: Integration and design methods. *Energy and Built Environment* **2021**. https://doi.org/10.1016/J.ENBENV.2021.07.002.
12. Mohanraj, M.; Belyayev, Y.; Jayaraj, S.; Kaltayev, A. Research and developments on solar assisted compression heat pump systems – A comprehensive review (Part-B: Applications). *Renewable and Sustainable Energy Reviews* **2018**, *83*, 124–155. https://doi.org/10.1016/j.rser.2017.08.086.
13. Zhou, C.; Liang, R.; Zhang, J.; Riaz, A. Experimental study on the cogeneration performance of roll-bond-PVT heat pump system with single stage compression during summer. *Applied Thermal Engineering* **2019**, *149*, 249–261.
14. Gunasekar, N.; Mohanraj, M. Performance analysis of solar photovoltaic-thermal hybrid heat pump working with circular and triangular evaporator tube configuration. *International Journal of Pharmacy and Technology* **2016**, *8*, 21737–21748.
15. Zhou, J.; Ma, X.; Zhao, X.; Yuan, Y.; Yu, M.; Li, J. Numerical simulation and experimental validation of a micro-channel PV/T modules based direct-expansion solar heat pump system. *Renewable Energy* **2020**, *145*, 1992–2004. https://doi.org/10.1016/J.RENENE.2019.07.049.
16. Lemmon, E.W.; Bell, I.H.; Huber, M.L.; McLinden, M.O. NIST Standard Reference Database 23: Reference Fluid Thermodynamic and Transport Properties-REFPROP, Version 10.0, National Institute of Standards and Technology, 2018. https://doi.org/https://doi.org/10.18434/T4/1502528.
17. Yao, J.; Chen, E.; Dai, Y.; Huang, M. Theoretical analysis on efficiency factor of direct expansion PVT module for heat pump application. *Solar Energy* **2020**, *206*, 677–694. https://doi.org/10.1016/J.SOLENER.2020.04.053.
18. Thue, J.V. *Bygningsfysikk - Grunnlag*; Fagbokforlaget: Trondheim, 2016; p. 464.
19. Hu, W.; Li, X.; Wang, J.; Tian, Z.; Zhou, B.; Wu, J.; Li, R.; Li, W.; Ma, N.; Kang, J.; et al. Experimental research on the convective heat transfer coefficient of photovoltaic panel. *Renewable Energy* **2022**, *185*, 820–826. https://doi.org/10.1016/J.RENENE.2021.12.090.
20. Ryssdal, S. High Temperature Heat Pumps in Integrated Energy Systems. PhD thesis, NTNU, 2020.
21. Simenergi. SIMIEN.
22. Standard Norge. SN-NSPEK 3031:2020 -Bygningers energiytelse Beregning av energibehov og energiforsyning, 2020.
23. Forskrift om tekniske krav til byggverk (Byggteknisk forskrift), 2018.

B Simulation model MATLAB code

```
% Program to simulate the performance of PVT+HP for a given time (hours)

    Weather = readtable ('Trondheim-v rmappe\Trondheim_NO-hour.dat'); % Read weather data
    %Weather = readtable('PVT_HP_R134a_Shanghai.xlsx');
    %Data_shanghai = readtable('PVT_MiddleScale_inputData.xlsx');
    %Data_radiation = readtable('PVT_MiddleScale_inputData.xlsx','Sheet',2);
%% 1: Simulation key parameters:
Refrigerant = 'Propane' ;
hours_simulated = 720*3 ; % Simulation time. 24 = one day ; 168 = one week ; 720 ~ one month (30 days)
start_hour = 2 ; % Which hour of weather file to start sim. Must be >2.
    % 17.june=4008 ; 14.feb.=1056; 7.mars=1560, 19.apr=2593 25.juni=4201
run_time_tot = 3600; % Run time for program [seconds] per time-step (hour)
dt = 60 ; % Internal time-step for system program [seconds]
step_length= run_time_tot/dt;
single_plots = 0 ; % Single plots? Yes=1 , No=0
plot_scatter = 0 ; % Scatter plots? Yes=1 , No=0
comp_control = 0 ; % Include compressor control? On/off=1 , P=2 , No=0


% PVT+HP system components specs.:
PVT_modules = 6 ; % Number of PVT modules, 1.68 m2 per module
V_th = 1.2 *10^-5; % [m3], R134a, https://www.directindustry.com/prod/tecumseh/product-8541-2047551.html
%V_th = 12.55 *10^-6; % Model: SECOP NLE12.6CNL
A_cond = 1 ; % Condenser HX area
U_cond = 2200; % W/m2K , assumed average for condenser
UA_cond = A_cond * U_cond ;
A_rbhx = 1.4 ; % [m^2], roll-bond HX surface area against refrigerant. Assumed.
A_rbhx_tot = A_rbhx * PVT_modules ;
V_tank = 300 ; % Storage tank volume, [L]
T_storage = 60 ; % Storage temperature level


%V_displacement = 49 ; % [m3/h], displacement volume compressor
%V_th = 0.00228 / 50 ; % [m3] For propane, 11 PVTs
%V_displacement = 49 ; % For R134a, 24 PVTs Shanghai middle-scale rig
%V_displacement = 14.35 ; % [m3/h] For R134a, 24 PVTs Shanghai middle-scale
```

```
rig. From datasheet
%V_th = (V_displacement/3600) / 50 ; % [m3/round]

% Storage control:
Storage_cutoff = 1 ; % when to stop taking energy from the storage, [kWh]
Storage_cutoff_J = Storage_cutoff *1000*3600;
%% Building Load Model

BRA_building = 150; % m2, heated floor area for building.
DHW_usage_m2 = [0.62, 0.34 , 0.21 , 0.11 , 0.14 , 0.69 , 4.26 , 8.48 , 5.77 , 2.44 , 2.58 , 2.58 , 2.64 , 2.68 , 2.23 , 1.99 , 1.96 , 8.48 , 8.83 , 2.92 , 2.95 , 2.68 , 2.03 , 1.01];
equipment_m2 = [1 1 1 1 1 1 1 1.9 1.9 1 1 1 1 1 1 2.9 4.8 4.8 4.8 4.3 4.3 2.4 2.4 1];
lights_m2 = [0.3 0.3 0.3 0.3 0.3 0.3 1.7 1.7 1.7 1.7 1.7 1.7 1.7 1.7 1.7 1.7 1.7 1.7 1.7 1.7 1.7 1.7 1.7 0.3];

load_electric = (equipment_m2 + lights_m2) * BRA_building; % W
DHW_usage = DHW_usage_m2 *BRA_building;
Load_DHW = repmat(DHW_usage,1,round(8760/24)); % DHW load for the whole year (hourly)

Load_model_results = readtable ('Load_model\Master_timeverdier_final.txt'); % Read load model data
Load_spaceheat = (Load_model_results.Romoppv__W_).';
%% Constants
sigma = 5.6703 * 10^(-8); % W/(m^2*K^4), Stefan boltzmann constant
C_p_water = 4184 ; % Specific heat water, [J/kgK]. For T=20degC. Assumed constant (Eng.Toolbox)
rho_water = 983 ; % kg/m3

comp_heat_loss = 0.10 ; % Heat loss in compressor.
T_sh = 5 ; % Superheat out of evaporator, deg C
T_w_in = 7 ;

N_nom = 50; % nominal rotational speed, rad/s (Hz)
E_storage_max = V_tank/1000 * rho_water * C_p_water * 10^(-3) * (1/3600) *(T_storage-T_w_in)*3600*1000; % [J]
%% REFPROP start-up
    %[v,e] = pyversion; system(['"', e, '" -m pip install --user -U ctREFPROP ']);
```

```
    RP = py.ctREFPROP.ctREFPROP.REFPROPFunctionLibrary('C:\Program Files (x86)\REFPROP');

    MASS_SI = RP.GETENUMdll(int8(0),'MASS BASE SI').iEnum;
    iMass = int8(1); % 0: molar fractions; 1: mass fractions
    iFlag = int8(0); % 0: don't call SATSPLN; 1: call SATSPLN
    z = {1.0}; % mole fractions, here a pure fluid, so mole fraction of 1.0

%% 2: PVT model specs.

T_rc = 298; % [K] Reference condition PV temp.
eta_rc = 0.199; % [-] PV efficiency at ref. condition temp.
beta_pv = 0.0039; % [1/K] Temperature coefficient PV eff.

% Design parameters
    A_pvt = 1.68*PVT_modules; % PVT area, m2, 1.68 m2 per module

    delta_c = 3.5 *10^(-3); % [m]
    epsilon_c = 0.84; % [-]
    kappa_c = 1.05; % Found from https://www.engineeringtoolbox.com/thermal-conductivity-d_429.html
    tau_g_pv = 0.9; % [-]
    delta_pv = 0.3 *10^(-3); % [m]
    epsilon_p = 0.96; % [-]
    alpha_p = 0.85; % [-], absorption ratio PV
    kappa_p = 203; % [W/(m*degC)]
    alpha_b = 0.8; % [-], absorption ratio baseboard
    delta_EVA = 0.5 *10^(-3); % [m]
    kappa_EVA = 0.311; % [W/(m*degC)]
    delta_ei = 0.5 *10^(-3); % [m]
    kappa_ei = 0.15; % [W/(m*degC]
    %Insulation material = ....(Tedlar)
    beta_p = 0.9; % [-]
    L_pvt = 2.0; % [m]
    W_pvt = 1.0; % [m]
    %A_pvt = L_pvt * W_pvt; % [m2]
    kappa_rb = 151; % [W/(m*K]
    delta_rb = 0.9 *10^(-3); % [m]
    rb_fc_width = 10 *10^(-3); % [m], roll-bond fluid channel width
    rb_fc_height = 2.8 *10^(-3); % [m], roll-bond fluid channel height
    %rb_fc_length = HAR IKKE; % [m], total lenght of roll-bond fluid channel
```

```

    % Material densities:
    rho_g = 3000 ; % kg/m^3
    rho_pv = 2330 ;
    rho_EVA = 960 ;
    rho_ei = 1200 ;
    rho_rb = 2712 ; % Aluminum. From Engineering Toolbox

    % Material specific heat capacities:
    Cp_g = 500 ; % J/kgK
    Cp_pv = 677;
    Cp_EVA = 2090 ;
    Cp_ei = 1250 ;
    Cp_rb = 910 ; % Aluminum

    % Material thermal capacitance calculations:
    C_g = A_pvt * rho_g * Cp_g * delta_c;
    C_pv = A_pvt * rho_pv * Cp_pv * delta_pv;
    C_eva = A_pvt * rho_EVA * Cp_EVA * delta_EVA;
    C_ei = A_pvt * rho_ei * Cp_ei * delta_ei;
    C_rb = A_pvt * rho_rb * Cp_rb * delta_rb;

    % PVT module thermal capacity:
    C_tot = C_g + C_pv + C_eva + C_ei + C_rb; % J/K


    % Roll-bond design
        % Approximately area fractions of the whole rb-evaporator:
        fraction_hexagon = 0.83 ;
        fraction_grid = 0.11 ;
        fraction_rectangle = 0 ;
        fraction_linear = 0.06 ;

        D = rb_fc_width ; % fluid channel width
        W = 35*10^(-3) ; % pattern width hexagon [mm]
        L = 60*10^(-3) ; % pattern length hexagon [mm]
        h_eq = 3000 ; % HT-coeff between collector pipe and fluid. Assumed [W
            /m2K]

%% PV-model specs.
epsilon_bs = 0.9 ; % Emissivity backsheet-material (polyvinylidene fluoride)
```

```
    (Swann and Stoliarov 2021).

%% Initial conditions first iteration
     T_pv = Weather.Ta(start_hour); % degree C
     %T_pv = Data_shanghai.Var5(1);
     %T_pv = 10 ;
     T_pv_only_store(start_hour*step_length -1) = T_pv+273.15;
     %T_cover = 21; % degree C
     T_cond_initial = 30 ;
     T_evap_initial = T_pv - 5 ;
     N = N_nom;
     E_storage_initial = 0.5*E_storage_max; % Inital stored heat energy is
         half of maximum storage capacity.
%% Variable creation
hours_tot = hours_simulated ;
end_hour = start_hour + hours_simulated -1 ;
% Variables wanted stored:
T_p_plot = zeros(1,end_hour);
T_pv_only_plot = zeros(1,end_hour);
dt_plot = zeros(1,end_hour);
W_comp_plot = zeros(1,end_hour);
Q_evap_plot = zeros(1,end_hour);
COP_plot = zeros(1,end_hour);
eta_el_plot = zeros(1,end_hour);

P_pv_el_accum = zeros(1,end_hour);
Q_cond_accum = zeros(1,end_hour);
W_comp_accum = zeros(1,end_hour);

T_comp_in_store = zeros(1,end_hour);
T_comp_out_store = zeros(1,end_hour);
T_cond_out_store = zeros(1,end_hour);
P_comp_in_store = zeros(1,end_hour);
P_comp_out_store = zeros(1,end_hour);
P_ratio_store = zeros(1,end_hour);

P_pv_toComp = zeros(1,end_hour);
E_storage = zeros(1,end_hour*step_length);
Q_boiler = zeros(1,end_hour*step_length);

%For PV-only:
```

```
P_pv_only_accum = zeros(1,end_hour);
P_pv_el_improved = zeros(1,end_hour);
eta_el_improved = zeros(1,end_hour);

%Needed for first iteration:
k=1;
T_p_plot(start_hour -1) = T_pv;
it_CondLoop = 0 ;
T_cond_store = zeros(1,hours_tot*step_length);
T_cond_store(start_hour*step_length) = T_cond_initial + 273.15;
it_EvapLoop = 0 ;
T_evap_store = zeros(1,hours_tot*step_length);
T_evap_store(start_hour*step_length) = T_evap_initial + 273.15;
iteration_WaterTemp = 0;
dhw_time = 1 ;
U_loss_store = [];
Comp_operationHours = 0;
E_storage(start_hour*step_length) = E_storage_initial;
I = Weather.Bh(start_hour) + Weather.Dh(start_hour);
if comp_control == 1
        if I <50
            N = 0;
        else
            N = N_nom;
        end
    end
%% 3: MAIN SIMULATION %%%%%%%%%%%%%%%%%%%%%%%%%%%%%%%%%%%%%
%%%%%%%%%%%%%%%%%%%%%%%%%%%%%%%%%%%%%%%%%%%%%%%%%%%%%%%%
% Create window showing simulation progress:
    progress = waitbar(0,'Please wait...');
    set(progress,'Position', [200 250 600 50]);
    tic
    elapsed_time = 0;

% Start simulation loop:
for hour = start_hour:end_hour

    % Import boundary conditions:

        % For real hourly weather data (.dat):
        T_a_cels = Weather.Ta(hour); % Outdoor air temp., degree C
```

```
        I = Weather.Bh(hour) + Weather.Dh(hour); % Solar radiation, W/m2
        v_air = Weather.FF(hour); % Wind speed, m/s
        %

        % From measured data at Shanghai rig (Excel):
        %T_a_cels = 28; % Outdoor air temp., degree C
        %I = Weather.SolarRadiationIntensity(hour); % Solar radiation, W/m2
        %v_air = 1.5; % Wind speed, m/s

        % From measured data at Shanghai middle scale rig (Excel):
        %I = Data_radiation.I(hour-1); % Solar radiation, W/m2
        %v_air = 1.5; % Wind speed, m/s

        T_a = T_a_cels + 273.15;

    % Initial conditions/first guess for each time-step (hour)

        T_pv = T_p_plot(hour-1); % Set start temp. for new hour to previous hour end value
        T_p = T_pv + 273.15;
        T_pv_only = T_pv_only_store(hour*step_length-1); % Set start temp. for new hour to previous hour end value


%% 3A: Loop for program per hour
k = 0;

while k< (step_length)
    k=k+1;
    progress = waitbar((hour-start_hour)/hours_simulated,progress,['Computing.... |  ',num2str(hour-start_hour),' h and ',num2str(k*60/step_length),' min',' of ', num2str(hours_simulated),' hours done. Elapsed time is: ',num2str(round(elapsed_time/60,1)),' min.']);
%% Input values each system time-step (min)
%Compressor controller:
    if comp_control == 0
        N = N_nom;
    end

    if comp_control == 2
                if T_pv < (T_a_cels-15)
```

```
                    N = 0 ;
                elseif T_pv < (T_a_cels -5)
                     N = N_nom * ( (T_a - T_p) / 10);
                else
                    N = N_nom ; % actual rotational speed, rad/s (Hz)
                end
            %{
                if T_pv < (T_a_cels -5)
                    N = 0 ;
                elseif T_pv < (T_a_cels+5)
                     N = N_nom * ( (T_p - T_a) / 5);
                else
                    N = 50 ; % actual rotational speed, rad/s (Hz)
                end
            %}

        part_load = N/N_nom ; % Part load, [-]
    end


m_w_vol = 0.05 ; %water flow rate condenser, [m3/h], 6.6 for test-rig
    Shanghai
T_w_out = 0 ; % Needed to start while loop for each iteration k
if N >0  % If compressor is on, enter HP loop, else parameters set to zero (
    W_comp = 0...)
    while T_w_out < 55 || T_w_out > 65 % Keep outlet water temp. between 55
        and 70 degrees C
        iteration_WaterTemp = iteration_WaterTemp +1 ;
        if T_w_out > 100
            m_w_vol = m_w_vol+0.05 ;
        elseif T_w_out > 65
            m_w_vol = m_w_vol+0.003 ;
        elseif T_w_out < 65 && T_w_out>55
            m_w_vol = m_w_vol;
        else m_w_vol = m_w_vol-0.003 ;
        end
        m_w = m_w_vol /3600 * 1000 ; % water flow rate condenser, [kg/s]
        %T_w_in = Data_shanghai.Var2((k+(hour-2)*60)) ;
        %T_a_cels = Data_shanghai.Var5((k+(hour-2)*60)); % Outdoor air temp.,
             degree C
        %T_a = T_a_cels + 273.15;
```

```
%% HP
Refr = Refrigerant; % Refrigerant
%% 3A.1: Initial guesses each time-step (dt)
    %Temperatures
    T_evap = T_evap_store(hour*step_length + k - 1); % K
    T_cond = T_cond_store(hour*step_length + k - 1); % K, set first guess to
        previus minute cond.temp.


%% 3A.2: Compressor calc.

    %W_comp_nom = ; % kW, Rated power
    %lambda_c = ; % Volumetric  compressor efficiency, see calc. in state
        point 2
    %eta_is = ; % Isentropic compressor efficiency, see calc. in state point
        2

%V_th = 1.22 * 10^(-5) * part_load; % m^3/rev Displacement volume (
    theoretical suction volume)
%V_th = 0.000182 / 50 ; % For propane, 2 PVTs
%V_th = 0.000363 / 50 ; % For propane, 4 PVTs
%V_th = 0.000467 / 50 ; % For isobutane
    T_comp_in = T_evap + T_sh; % Inlet temp. at compressor

T_cond2 = T_cond + 1; % Reset T_cond2 value to start loop
T_evap2 = T_evap + 1; %
Q_u = 1000 ; % Needed to start loop
Q_evap = 0 ; % Needed to start loop

%while abs(T_evap-T_evap2) > 0.01
while (abs(Q_u-Q_evap) / Q_evap) > 0.05
    it_EvapLoop = it_EvapLoop + 1 ;
    T_comp_in = T_evap + T_sh;
    T_cond2 = T_cond + 1 ;

while abs(T_cond - T_cond2 ) > 0.01
    it_CondLoop = it_CondLoop + 1 ;
    % State point 1: Out of evaporator / Into compressor

        p_1_get = RP.REFPROPdll(Refr,'TQ','P',MASS_SI,iMass,iFlag,T_evap,1,z)
            ;
```

```
        o1_p = double(p_1_get.Output);
        p_1_SI = o1_p(1); % Pa
        p_1 = p_1_SI/(10^5); % Bar

        h_1_get = RP.REFPROPdll(Refr,'PT','h',MASS_SI,iMass,iFlag,p_1_SI,
            T_comp_in,z);
        o1_h = double(h_1_get.Output);
        h_1 = o1_h(1); % J/kg

        s_1_get = RP.REFPROPdll(Refr,'PT','S',MASS_SI,iMass,iFlag,p_1_SI,
            T_comp_in,z);
        o1_s = double(s_1_get.Output);
        s_1 = o1_s(1); % J/(kgK)

        v_1_get = RP.REFPROPdll(Refr,'PT','D',MASS_SI,iMass,iFlag,p_1_SI,
            T_comp_in,z);
        o1_v = double(v_1_get.Output);
        v_1 = o1_v(1); % kg/m^3, density at state 1

            %T_1_get = RP.REFPROPdll(Refr,'PQ','T',MASS_SI,iMass,iFlag,p_1_SI
                ,1,z);
            %o1_T = double(T_1_get.Output);
            %T_1 = o1_T(1); % kelvin, temp. at state 1

    % State point 2
        p_2_get = RP.REFPROPdll(Refr,'TQ','P',MASS_SI,iMass,iFlag,T_cond,1,z)
            ;
        o2_p = double(p_2_get.Output);
        p_2_SI = o2_p(1); % Pa
        p_2 = p_2_SI/(10^5); % Bar

        p_ratio = p_2/p_1 ;
        %eta_is = -0.00000461*p_ratio^6 + 0.00027131*p_ratio^5 - 0.00628605*
            p_ratio^4 + 0.07370258*p_ratio^3 - 0.46054399*p_ratio^2 +
            1.40653347*p_ratio - 0.87811477 ;
        %eta_is = 0.7;
        eta_is = -0.17938 + 0.87501*(p_ratio) -0.30014*(p_ratio^2) +
            0.04135*(p_ratio^3) - 0.00206*(p_ratio^4);
        lambda_c = 0.0011*p_ratio^2 - 0.0487*p_ratio + 0.9979 ;

        h_2_is_get = RP.REFPROPdll(Refr,'PS','h',MASS_SI,iMass,iFlag,p_2_SI,
```

```
            s_1,z);
        o2_h_is = double(h_2_is_get.Output);
        h_2_is = o2_h_is(1); % J/kg, enthalpy with isentropic compression

        h_2_ad = h_1 + (h_2_is-h_1)/eta_is ; % Outlet enthalpy without heat
            loss (adiabatic compression)

        h_comp_out = h_1 + ( (h_2_is-h_1)/eta_is * (1-comp_heat_loss) ); %
            Real outlet enthalpy
        h_2 = h_comp_out ;

        T_2_get = RP.REFPROPdll(Refr,'PH','T',MASS_SI,iMass,iFlag,p_2_SI,h_2,
            z);
        o2_T = double(T_2_get.Output);
        T_2 = o2_T(1); % kelvin, temp. at state 1

    % Operation:
        v_suc = v_1;
        m_comp = N * v_suc * V_th * lambda_c;

        m_R = m_comp;
        w_comp = (h_2_ad-h_1); % J/kg
        W_comp = w_comp * m_R; % Compressor work, W

    T_comp_out = T_2;
    %T_cond_out = T_4;
    P_comp_in = p_1;
    P_comp_out = p_2;
    P_ratio = P_comp_out / P_comp_in ;

%% 3A.3: Condenser calc.

    % State point 3
        h_3_get = RP.REFPROPdll(Refr,'TQ','h',MASS_SI,iMass,iFlag,T_cond,0,z)
            ;
        o3_h = double(h_3_get.Output);
        h_3 = o3_h(1); % J/kg

    q_cond = (h_2-h_3); % Heat transfer condenser/gas cooler, J/kg
    Q_cond = q_cond *m_R; % W

```

```
    % Calculating water temperatures:
        T_w_out = T_w_in + Q_cond / (C_p_water*m_w) ;
        T_w_avg = (T_w_out + T_w_in)/2 ;

    % Calc. new condensing temp.:
        LMTD_cond = Q_cond/UA_cond;
        B = exp((T_w_out-T_w_in)/LMTD_cond);

        T_cond2 = 273.15 + (T_w_in-T_w_out*B)/(1-B);
        dT_cond = (T_cond2 - T_cond) / 2 ;
        T_cond = T_cond + dT_cond ;
end
%% 3A.4: Valve
    % State point 4
        h_4 = h_3;

        p_4_get = RP.REFPROPdll(Refr,'TQ','P',MASS_SI,iMass,iFlag,T_cond,0,z)
            ;
        o4_p = double(p_4_get.Output);
        p_4 = o4_p(1)/(10^5); % Bar
        p_4_pa = p_4*10^5;

%% 3A.5: PVT-calculations
%%%%%%%%%% PVT electrical
    eta_el_pv_ideal = eta_rc * (1 - beta_pv * (T_p-T_rc));
    eta_el = eta_el_pv_ideal;
%%%%%%%%%%

%%%%%%%%%% PVT heat balance
    Q_abs =  A_pvt * I * tau_g_pv * (alpha_p*beta_p*(1-eta_el) + alpha_b*(1-
        beta_p));
    q_evap = (h_1-h_4); % J/kg
    Q_evap = q_evap*m_R;
%%%%%%%%%%

%%%%%%%%%%%%%%%%%%%%%%%%%% Calculation of heat transfer loss glass cover and PV

        % Subscripts:
            % T_p = PV temp.,   T_a = ambient temp.
            % cd = conduction , cv = convection , rd = radiation
            % pc = panel to glass cover , ca = glass cover to ambient
```

```
        % pv = PV panels , EVA = eva grease
        % ei = electrical insulation , rb = roll-bond panel
        % ref = refrigerant , g = ground

        T_c = T_p; % Assuming same temp. in glass cover as in PV. Only in
            use for radiation
        T_ground = T_a ; % Ground temp. assumed to be ambient temp.

        % From PV panels and up:
            h_cd_pc = 1/ (delta_c/kappa_c);
            %h_rd_pc = epsilon_p * sigma * (T_p + T_c) * (T_p^2 + T_c^2);
            %h_cv_ca = 2.8 + 3*v_air;
            %h_cv_ca = 18*sqrt(v_air/L_pvt); %byggfys.bok s.205
            %h_cv_ca = 5 + 4.5*v_air-0.14*(v_air^2); %Loside,(v_air <10 m
                /s), byggfys.bok s.61
            %h_cv_ca = 5 + 4.5*v_air; % Leside,(v_air<8 m/s), byggfys.bok
                s.61
            %h_cv_ca = 25 + 1.2*v_air;
            %h_cv_ca = 6.9 + 3.87*v_air ; % Kumar 2010
            %h_cv_ca = (13.07+2.18*0) + (3.65-0.26*0)*v_air; % Hu et al.,
                tilt = 0 deg
            h_cv_ca = (13.07+2.18*pi/6) + (3.65-0.26*pi/6)*v_air; % Hu et
                al., tilt = 30 deg
            h_rd_ca = epsilon_c * sigma * (T_c + T_a)*(T_c^2 + T_a^2);

        % From PV panels and down:
            h_cd_pv_eva = 1/ (delta_EVA/kappa_EVA);
            h_cd_eva_ei = 1/ (delta_ei/kappa_ei);
            h_cd_ei_eva = 1/ (delta_ei/kappa_ei); % Samme som h_cd_eva_ei
                , men nytt lag p  undersiden av elektrisk isolasjon
            h_cd_eva_rb = 1/ (delta_rb/kappa_rb);
            h_cv_rb_ref = 3000 ;
            h_cv_ref_a = 2.8 + 3*v_air;
            %h_cv_ref_a = (13.07+2.18*pi/6) + (3.65-0.26*pi/6)*v_air;
            h_rd_ref_g = epsilon_c * sigma * (T_evap + T_ground)*(T_evap
                ^2 + T_ground^2);


        %Total:
            h_r_lw = epsilon_c * sigma * (T_c + T_a)*(T_c^2 + T_a^2);
            %h_cv_free = 1.31*(T_c_pv_only - T_a)^(1/3); Fra Jones and
```

```
                %Underwood 2001("A thermal model for photovoltaic systems")
                h_cv_forced = h_cv_ca ;

                q_r_lw = -h_r_lw *(T_c - T_a);
                q_r_lw_bok = alpha_p*(sigma*(T_a)^4) - epsilon_c*sigma*((T_c)^4);
                %q_conv = -(h_cv_forced + h_cv_free) *(T_c_pv_only - T_a);Fra Jones and
                %Underwood 2001
                q_conv = -(h_cv_forced) *(T_c- T_a); % Without h_cv_free
                q_r_sw = alpha_p * I  ;

        %U_loss = (1/(h_cd_pc+h_rd_pc) + 1/(h_cv_ca+h_rd_ca))^(-1); % heat
                %loss coefficient over the PV panels
        %U_loss_top = (1/(h_cd_pc) + 1/(h_cv_ca+h_rd_ca))^(-1); % heat loss coefficient without h_rd_pc [Yao 2021 Two-phase flow...]
        %U_loss_down = (1/h_cd_pv_eva + 1/h_cd_eva_ei + 1/h_cd_ei_eva + 1/h_cd_eva_rb + 1/h_cv_rb_ref + 1/(h_cv_ref_a + h_rd_ref_g))^(-1); % Heat loss coefficient under the PV panels
        %U_loss_down = (1/h_cd_pv_eva + 1/h_cd_eva_ei + 1/h_cd_ei_eva + 1/h_cd_eva_rb)^(-1); % Uten manglende uttrykk

        U_loss_up = (1/(h_cd_pc) + 1/(h_cv_ca+h_rd_ca))^(-1); % heat loss coefficient  [Yao 2021 Two-phase flow...]
        U_loss_low = (1/h_cd_pv_eva + 1/h_cd_eva_ei + 1/h_cd_ei_eva + 1/h_cd_eva_rb + 1/h_cv_rb_ref + 1/(h_cv_ref_a + h_rd_ref_g))^(-1); % Heat loss coefficient under the PV panels
        %U_loss_low = (1/h_cd_pv_eva + 1/h_cd_eva_ei + 1/h_cd_ei_eva + 1/h_cd_eva_rb)^(-1); % Uten manglende uttrykk
        %U_loss = U_loss_top + U; % Overall heat loss coefficient, W/(m2*K)
        U_loss = U_loss_up + U_loss_low;
        Q_loss = U_loss * A_pvt * (T_p-T_a);
        U_loss_store = [U_loss_store, U_loss];

%%%%%%%%%%%%%%%%%%%%%%%%%%%%%%%%%%%%%%

%%%%%%%%%%%%%%%%%%%%%%%%%%%%%%%%%%%%%%%%%%%%%% U-value calc. PV to refrigerant
        U_pv_rb = ( 1/h_cd_pv_eva + 1/h_cd_eva_ei + 1/h_cd_eva_ei + 1/h_cd_eva_rb)^(-1);
        %U_pv_R = ( 1/h_cd_pv_eva + 1/h_cd_eva_ei + 1/h_cd_eva_ei + 1/h_cd_eva_rb +1/h_cv_rb_ref)^(-1);
```

```
        U_pv_R = 2200  ; % Assumed  [W/m2K]
        q_cd_pv_R = U_pv_R  *(T_p-T_evap);
%%%%%%%%%%%%%%%%%%%%%%%%%%%%%%%%

P_pv_el = A_pvt * I * tau_g_pv * alpha_p * beta_p * eta_el; % PV electrical
    power output, W
Q_th = Q_abs - Q_loss  ;
Q_evap_hx = U_pv_R * A_rbhx_tot * (T_p-T_evap);



        X1 = (tau_g_pv*(alpha_p*beta_p + alpha_b*(1-beta_p)) * I *(1-eta_el)
            - U_loss*(T_evap-T_a));
        X2 = (T_p-T_evap) / (1/D*(delta_EVA/kappa_EVA + delta_ei/kappa_ei +
            delta_rb/kappa_rb) + 1/(h_eq*pi*D));
        F_prime_NY = 12*0.5*W/sqrt(3) * X2 * 1/(W*L) * 1/X1  ;
        Q_u = A_pvt * F_prime_NY * (tau_g_pv*(alpha_p*beta_p + alpha_b*(1-
            beta_p)) * I *(1-eta_el) - U_loss*(T_evap-T_a))  ;

        residual(it_EvapLoop) = abs(Q_u-Q_evap) / Q_evap;
        discrepancy(it_EvapLoop) = Q_u-Q_evap;

% Energy balance to find new evaporation temp.:
    %T_evap2 = T_p - Q_evap/(U_pv_R*A_rbhx_tot);
    %dT_evap = (T_evap2-T_evap) / 2 ;
    %T_evap = T_evap + dT_evap  ;
    %{
    T_evap2 = ( (tau_g_pv*(alpha_p*beta_p + alpha_b*(1-beta_p)) * I *(1-
        eta_el)) - (Q_evap/(A_pvt*F_prime_NY)) + U_loss*(T_evap-T_a) ) /
        U_loss;
    dT_evap = (T_evap2-T_evap)/2;
    T_evap = T_evap + dT_evap;
    %}

% Check residual and adjust evaporation temp.:
    if (Q_u - Q_evap) > 10
                T_evap = T_evap + 0.02;
            elseif (Q_u - Q_evap) < (-10)
                %{
                if discrepancy(it_EvapLoop) > discrepancy(it_EvapLoop-1)
                    T_evap = T_evap + 0.02;
```

```
                        else
                        T_evap = T_evap - 0.02;
                        end
                        %}
                        T_evap = T_evap -0.02;
                  else
                        T_evap = T_evap;
      end

end % End evaporator loop
end % End T_w_out >55 loop
%% Performance evaluation

COP = q_cond / w_comp; % HP COP
SSR_comp = P_pv_el / W_comp ; % self-sufficiency compressor

else % PVT-calc. if N = 0. No heat through evaporation.

      W_comp = 0;
      Q_cond = 0;
      Q_evap = 0;
      COP = 0;
      T_w_out = 0;
      T_cond = 273.15;
      T_evap = 273.15;
      m_w = 0;
      SSR_comp = 0;
      %%%%%%%%%% PVT electrical
            eta_el_pv_ideal = eta_rc * (1 - beta_pv * (T_p-T_rc));
            eta_el = eta_el_pv_ideal;
      %%%%%%%%%%

      %%%%%%%%%% PVT heat absorbed
            Q_abs =  A_pvt * I * tau_g_pv * (alpha_p*beta_p*(1-eta_el) + alpha_b
                 *(1-beta_p));
      %%%%%%%%%%

      %%%%%%%%%%%%%%%%%%%%%%%%%% Calculation of heat transfer loss glass cover and
            PV

                  % Subscripts:
```

```
            % T_p = PV temp.,  T_a = ambient temp.
            % cd = conduction , cv = convection , rd = radiation
            % pc = panel to glass cover , ca = glass cover to ambient
            % pv = PV panels , EVA = eva grease
            % ei = electrical insulation , rb = roll-bond panel
            % ref = refrigerant , g = ground

            T_c = T_p; % Assuming same temp. in glass cover as in PV. Only in use for radiation
            T_ground = T_a ; % Ground temp. assumed to be ambient temp.

            % From PV panels and up:
                h_cd_pc = 1/ (delta_c/kappa_c);
                h_cv_ca = (13.07+2.18*pi/6) + (3.65-0.26*pi/6)*v_air; % Hu et al., tilt = 30 deg
                h_rd_ca = epsilon_c * sigma * (T_c + T_a)*(T_c^2 + T_a^2);

            % From PV panels and down:
                h_cd_pv_eva = 1/ (delta_EVA/kappa_EVA);
                h_cd_eva_ei = 1/ (delta_ei/kappa_ei);
                h_cd_ei_eva = 1/ (delta_ei/kappa_ei); % Samme som h_cd_eva_ei, men nytt lag p  undersiden av elektrisk isolasjon
                h_cd_eva_rb = 1/ (delta_rb/kappa_rb);
                h_cv_rb_ref = 3000 ;
                h_cv_ref_a = 2.8 + 3*v_air;
                h_rd_ref_g = epsilon_c * sigma * (T_p + T_ground)*(T_p^2 + T_ground^2);


        U_loss_up = (1/(h_cd_pc) + 1/(h_cv_ca+h_rd_ca))^(-1); % heat loss coefficient [Yao 2021 Two-phase flow...]
        U_loss_low = (1/h_cd_pv_eva + 1/h_cd_eva_ei + 1/h_cd_ei_eva + 1/h_cd_eva_rb + 1/h_cv_rb_ref + 1/(h_cv_ref_a + h_rd_ref_g))^(-1); % Heat loss coefficient under the PV panels
        U_loss = U_loss_up + U_loss_low;
        Q_loss = U_loss * A_pvt * (T_p-T_a);
        U_loss_store = [U_loss_store, U_loss];

    %%%%%%%%%%%%%%%%%%%%%%%%%%%%%%%%
```

```
    P_pv_el = A_pvt * I * tau_g_pv * alpha_p * beta_p * eta_el; % PV
        electrical power output, W
    Q_th = Q_abs - Q_loss ; % (Steady state considereation)

end

if I > 0
    eta_th = Q_th / (A_pvt*I); % PVT thermal efficiency
    eta_th2 = Q_evap / (A_pvt*I);
    eta_el_2 = P_pv_el / (A_pvt*I); % PVT electrical efficiency
    eta_tot = (Q_cond + P_pv_el) / (A_pvt*I); % Overall efficiency
else
    eta_th = 0; % PVT thermal efficiency
    eta_th2 = 0;
    eta_el_2 = 0; % PVT electrical efficiency
    eta_tot = 0; % Overall efficiency
end


G_eff = alpha_p * I * A_pvt; % Effective solar radiation, [W]
dTp_dt = ((G_eff -P_pv_el - Q_loss - Q_evap) / (C_tot)) ; % [K/s], Change in
    PV temp. per time step
%dTp_dt = (A_pvt*(q_r_sw + q_conv + q_r_lw)-P_pv_el-Q_evap) / (C_tot);
dT = dTp_dt * dt;

T_p_store(step_length*hour+k) = T_p;
T_p_store_cels(step_length*hour+k) = T_p-273.15;
%T_pv_check(60*hour+k) = T_pv;
W_comp_check (step_length*hour+k) = W_comp;
T_p = T_p + dT;
k_plot (step_length*hour+k) = step_length*hour+k;

T_cond_store(step_length*hour+k) = T_cond;
T_evap_store(step_length*hour+k) = T_evap;
T_w_out_store(step_length*hour+k) = T_w_out;
COP_store(step_length*hour+k) = COP;

%% PV-only calc.

%%%%%%%%%% PV electrical
```

```
    eta_el_pv_only = eta_rc * (1 - beta_pv * (T_pv_only-T_rc));
%%%%%%%%%%

%%%%%%%%%%%%%%%%%%%%%%% Calculation of heat transfer loss glass cover and PV

        % Subscripts:
            % T_p = PV temp.,  T_a = ambient temp.
            % cd = conduction , cv = convection , rd = radiation
            % pc = panel to glass cover , ca = glass cover to ambient
            % pv = PV panels , EVA = eva grease
            % ei = electrical insulation, rb = roll-bond panel , bs = backsheet
            % ref = refrigerant , g = ground

            T_c_pv_only = T_pv_only; % Assuming same temp. in glass cover as in PV. Only in use for radiation
            T_sky = T_a;
            % From PV panels and up:
                %h_cd_pc = 1/ (delta_c/kappa_c);
                %h_rd_pc = epsilon_p * sigma * (T_p + T_c) * (T_p^2 + T_c^2);
                %h_cv_ca = 2.8 + 3*v_air;
                %h_cv_ca = 18*sqrt(v_air/L_pvt); %byggfys.bok s.205
                %h_cv_ca = 5 + 4.5*v_air-0.14*(v_air^2); %Loside,(v_air <10 m/s), byggfys.bok s.61
                %h_cv_ca = 5 + 4.5*v_air; % Leside,(v_air<8 m/s), byggfys.bok s.61
                %h_cv_ca = (13.07+2.18*0) + (3.65-0.26*0)*v_air;
                %From Thue 2016:
                h_rd_ca_pv_only = epsilon_c * sigma * (T_c_pv_only + T_a)*(T_c_pv_only^2 + T_a^2);

                h_rd_bs_a_pv_only = epsilon_bs * sigma * (T_pv_only + T_ground)*(T_pv_only^2 + T_ground^2);
            %Total:
                h_r_lw_pv_only = epsilon_c * sigma * (T_c_pv_only + T_a)*(T_c_pv_only^2 + T_a^2);
                %h_cv_free = 1.31*(T_c_pv_only - T_a)^(1/3); Fra Jones and
                %Underwood 2001("A thermal model for photovoltaic systems")
                h_cv_forced = h_cv_ca ;

                q_r_lw_pv_only = -h_r_lw_pv_only *(T_c_pv_only - T_a);
```

```
                    q_r_lw_bok = alpha_p*(sigma*(T_a)^4) - epsilon_c*sigma*((
                        T_c_pv_only)^4);
                    %q_conv = -(h_cv_forced + h_cv_free) *(T_c_pv_only - T_a);Fra
                        Jones and
                    %Underwood 2001
                    q_conv_pv_only = -(h_cv_forced) *(T_c_pv_only - T_a); %
                        Without h_cv_free
                    q_r_sw = alpha_p * I   ;

          % U-values:
          U_loss_top_pv_only = (1/(h_cd_pc) + 1/(h_cv_ca) + 1/(h_rd_ca_pv_only)
              )^(-1); % heat loss coefficient without h_rd_pc [Yao 2021 Two-
              phase flow...]
          U_loss_down_pv_only = (1/h_cd_pv_eva + 1/h_cd_eva_ei + 1/h_cd_eva_rb
              + 1/h_cv_ca +1/h_rd_bs_a_pv_only )^(-1);
          Q_loss_pv_only = A_pvt *( U_loss_top_pv_only * (T_pv_only-T_a) +
              U_loss_down_pv_only * (T_pv_only-T_ground) );

%%%%%%%%%%%%%%%%%%%%%%%%%%%%%%%%%%%%%%%%

P_pv_only = A_pvt * I * tau_g_pv * alpha_p * beta_p * eta_el_pv_only; % PV
    electrical power output, W

%dTpv_only_dt = ((G_eff -P_pv_only - Q_loss_pv_only) / (C_tot)) ; % [K/s],
    Change in PV temp. per time step
dTpv_only_dt = (A_pvt*(q_r_sw + q_conv_pv_only + 2*q_r_lw_pv_only)-P_pv_only)
    / (C_tot);
dT_pv_only = dTpv_only_dt * dt;

T_pv_only = T_pv_only + dT_pv_only ;
T_pv_only_store(step_length*hour+k) = T_pv_only;
T_pv_only_store_cels(step_length*hour+k) = T_pv_only-273.15;
%T_pv_check(60*hour+k) = T_pv;
k_plot (step_length*hour+k) = step_length*hour+k;
dTpv_only_dt_store(step_length*hour+k) = dTpv_only_dt;
N_comp_store(step_length*hour+k) = N;
m_w_store(step_length*hour+k) = m_w;
delta_pv_amb(step_length*hour+k) = T_p - T_a;

% Load side:
Q_demand_total(hour) = Load_spaceheat(hour) + Load_DHW(hour);
```

```

if comp_control == 1
        if I <50
            N = 0;
        else
            N = N_nom;
        end
    end

if Q_cond >= Q_demand_total(hour) % If condensation power is greater than heating load, store the surplus heat production
        if E_storage(step_length*hour+k -1) >= E_storage_max % If the storage capacity is reached
            Q_storage(step_length*hour+k) = 0 ;
            % N = reduced % Reduce compressor speed to meet demand, or turn off
        else
            Q_storage(step_length*hour+k) = Q_cond - Q_demand_total(hour);
        end
        Q_boiler(step_length*hour+k) = 0 ;
    elseif E_storage(step_length*hour+k -1) > Storage_cutoff_J % If there is heat stored => Use stored heat
        Q_storage(step_length*hour+k) = Q_cond - Q_demand_total(hour) ;
        Q_boiler(step_length*hour+k) = 0;
    else
        Q_storage(step_length*hour+k) = 0 ;
        Q_boiler(step_length*hour+k) = Q_demand_total(hour) - Q_cond ; % Peak elheater provides deficit heat
end

E_storage(step_length*hour+k) =  E_storage(step_length*hour+k -1) + Q_storage(step_length*hour+k)*dt  ; % Energy stored [J]
elapsed_time = toc;

% Compressor control
if comp_control == 3
        if Q_demand_total(hour)>500
            if  Q_cond > Q_demand_total(hour)
                if E_storage(step_length*hour+k -1) > (E_storage_max -(0.5*3600*1000))
                    W_load_match = Q_demand_total(hour)/COP; % Approximate
```

```
                            comp.work to meet demand
                            m_comp_match = W_load_match/w_comp ;
                            N = (v_suc * V_th * lambda_c) / m_comp_match;
                            if N<10
                                N = 0 ;
                            end
                        else
                            N = N_nom ;
                        end
                    else
                        N = N_nom;
                    end
            elseif Q_demand_total(hour)<500 || E_storage(step_length*hour+k -1) <
                (E_storage_max -(0.5*3600*1000))
                N = N_nom;
            else
                N = 0 ;
            end
end

end % Move to next min (k)

% Store values:

T_p_plot(hour) = T_p-273.15;
T_pv_only_plot(hour) = T_pv_only;
dt_plot(hour) = hour;
W_comp_plot(hour) = W_comp ;
Q_evap_plot(hour) = Q_evap;
Q_cond_plot(hour) = Q_cond;
COP_plot(hour) = COP;
eta_el_plot(hour) = eta_el;
P_pv_el_store(hour) = P_pv_el ;



if N>0
    Comp_operationHours = Comp_operationHours + 1;
    I_operation(hour) = I;
    if P_pv_el > W_comp
        P_pv_toComp(hour) = W_comp; % PV production when compressor is on
```

```
    else P_pv_toComp(hour) = P_pv_el;
    end
    SSR_comp_store(hour) = SSR_comp;
    if I>0
        Q_th_store(hour) = Q_th;
        eta_th_store(hour) = eta_th;
        eta_th2_store(hour) = eta_th2;
    else
        Q_th_store(hour) = 0;
        eta_th_store(hour) = 0;
        eta_th2_store(hour) = 0;
    end
    T_comp_in_store(hour) = T_comp_in;
    T_comp_out_store(hour) = T_comp_out;
    %T_cond_out_store(hour) = T_cond_out;
    P_comp_in_store(hour) = P_comp_in;
    P_comp_out_store(hour) = P_comp_out;
    P_ratio_store(hour) = P_ratio;
end

Q_cond_accum (hour) = Q_cond_accum (hour-1) + Q_cond_plot (hour);
W_comp_accum (hour) = W_comp_accum (hour-1) + W_comp_plot (hour);
P_pv_el_accum (hour) = P_pv_el_accum (hour-1) + P_pv_el;
P_pv_only_accum(hour) = P_pv_only_accum (hour-1) + P_pv_only;
P_pv_el_improved(hour) = P_pv_el_accum (hour) - P_pv_only_accum (hour);
eta_el_improved(hour) = eta_el - eta_el_pv_only;


%% Load side model [Domestic hot water (DHW) and space heating (SH)]
if Q_cond > DHW_usage(dhw_time)
    Q_DHW(hour) = DHW_usage(dhw_time);
    Q_SpaceHeat(hour) = Q_cond - DHW_usage(dhw_time);
else
    Q_DHW(hour) = Q_cond;
    Q_SpaceHeat(hour) = 0 ;
end

DHW_coverage_hour(hour) = Q_DHW(hour) / DHW_usage(dhw_time);
Heat_fraction_DHW(hour) = Q_DHW(hour) / Q_cond ;
Heat_fraction_SH(hour) = 1 - Heat_fraction_DHW(hour) ;
```

```
dhw_time = dhw_time + 1 ;
if dhw_time == 25
    dhw_time = 1;
end

end % End given hour, and move to next hour

close(progress)

%% Print performance indices:
    T_a_sim = Weather.Ta(start_hour:end_hour,:).' ;
    I_rad_sim = ( Weather.Bh(start_hour:end_hour,:) + Weather.Dh(start_hour:end_hour,:) ).' ;
    E_demand_tot = sum(Q_demand_total);

    COP_sim_max = max(COP_plot)
    Q_cond_sim_tot = Q_cond_accum(hour) /1000 % Total delivered heat [kWh]
    P_comp_sim_tot = W_comp_accum(hour) / 1000 % Total power consumption [kWh]
    COP_sim_avg = Q_cond_sim_tot / P_comp_sim_tot % Average COP of simulation
    P_pv_el_tot = P_pv_el_accum(hour) / 1000 % Total electrical power production [kWh]
    E_pv_improved = P_pv_el_improved(hour)*10^(-3) ;
    E_pv_improved_perc = E_pv_improved / (P_pv_only_accum(hour)/1000) *100
    SSR_tot = sum(P_pv_toComp) / W_comp_accum(hour) % Self-sufficiency rate
    SSR_th_tot = (E_demand_tot - sum(Q_boiler/step_length)) / E_demand_tot ;
    SCR_tot = (sum(P_pv_toComp)) / (P_pv_el_tot*1000) % Self-consumption rate
    DHW_coverage_tot = Q_cond_sim_tot / ((sum(DHW_usage)/24)*10^(-3)*hours_simulated)
    T_amb_avg = mean(T_a_sim)
    I_rad_avg = mean(I_rad_sim)
    I_rad_max = max(I_rad_sim)
    T_pv_max = max(T_p_store_cels(start_hour*step_length+1:length(T_p_store_cels)));
    T_pv_only_max = max(T_pv_only_store_cels(start_hour*step_length+1:length(T_p_store_cels)));
    T_pv_min = min(T_p_store_cels(start_hour*step_length+1:length(T_p_store_cels)));
    eta_th_sim_avg = sum(Q_th_store) / (sum(I_operation)*A_pvt) *100
    eta_el_sim_avg = P_pv_el_tot*1000 / (sum(I_rad_sim)*A_pvt) *100
    %eta_tot_sim_avg =
```

```
    Q_cond_max = max(Q_cond_plot);
    W_comp_max = max(W_comp_plot);

    E_storage_kWh = E_storage/1000/3600;
    Q_storage_sign = -Q_storage;

    Results = table(T_amb_avg,I_rad_avg,I_rad_max,COP_sim_max,COP_sim_avg,
        T_pv_only_max,T_pv_max,T_pv_min,E_pv_improved_perc,eta_th_sim_avg,
        SSR_tot,SCR_tot,'VariableNames',{'Avg. amb. temp.', 'Irad_avg.','
        Irad_max','COP max','COP avg','Tpv only max','Tpv_max','Tpv_min','PV
        prod. improved [%]','\eta_{th}_avg','SSR','SCR'});
%% Make table and export to excel
    %dt_transp = dt_plot.' ;
    %Results_tab = table(dt_plot.', Ambient_temp.', Solar_rad.' , T_p_plot.',
         COP_plot.', eta_el_plot.', P_pv_el_accum.' , Q_cond_plot.',
        Q_evap_plot.', W_comp_plot.', 'VariableNames',{'dt_plot', '
        Ambient_temp', 'Solar_rad' , 'T_p_plot', 'COP_plot', 'eta_el_plot', '
        PV power' , 'Q_cond_plot', 'Q_evap_plot', 'W_comp_plot'});
    %writetable(Results_tab,'PVT_HP_results_v2.xlsx','Sheet',1);
%% Import data and transpose from Middle scale rig Shanghai
%{
T_w_out_MSRig = ( Data_shanghai.Var3(1:1739,:) ).' ;
%W_comp_MSRig = ( Data_shanghai.Var9((start_hour-1):end_hour,:) ).' ;


count=0;
for second = 1:60:1680
    count=count+1;
    COP_rig(count) = Data_shanghai.Var15(second);
    W_comp_MSRig(count) = Data_shanghai.Var9(second);
    Q_cond_MSRig(count) = Data_shanghai.Var11(second);
end
%}
for j = 1:length(T_cond_store)
    T_cond_store_cels(j) = T_cond_store(j)-273.15;
    T_evap_store_cels(j) = T_evap_store(j) - 273.15;
end

delta_pv_evap = T_p_store - T_evap_store;

```

```
%% Plotting

Ambient_temp = Weather.Ta(1:end_hour,:).' ;
Solar_rad = ( Weather.Bh(1:end_hour,:) + Weather.Dh(1:end_hour,:) ).' ;
%Solar_rad = ( Data_radiation.I((start_hour-1):end_hour,:) ).' ;

figure('Name', 'PV temp')
hold on
yyaxis left
plot(dt_plot(start_hour:(length(dt_plot))) , T_p_plot(start_hour:(length(
    dt_plot)))) % PV temp.
plot(dt_plot(start_hour:(length(dt_plot))) , Ambient_temp(start_hour:(length(
    dt_plot))),'Color','g','LineStyle','--');
xlabel('Time [h]')
ylabel('Temperature [\circC]')
yyaxis right
%Solar_rad = Weather.SolarRadiationIntensity(2:87,:).' ;
plot(dt_plot(start_hour:(length(dt_plot))) , Solar_rad(start_hour:(length(
    dt_plot)))) % Solar radiation
%plot(dt_plot((start_hour-1):length(dt_plot)),Solar_rad);
ylabel('Radiation [W]')
legend('T_{pv}','T_{amb}','I_{rad}','Location','northoutside','Orientation','
    horizontal')
xticks([((start_hour-1):12:(length(dt_plot)))])
xticklabels([(0:12:hours_simulated)])
hold off

if single_plots == 1
%COP_rig = Data_shanghai.Var15';
figure('Name', 'COP')
    hold on
    yyaxis left
    plot(dt_plot(start_hour:(length(dt_plot))), COP_plot(start_hour:(length(
        dt_plot))),'Color','r','LineStyle','-')
    %plot(dt_plot,COP_rig)
    set(gca,'ycolor','r')
    xlabel('Time [h]')
    ylabel ('COP [-]')
    yyaxis right
    plot(dt_plot(start_hour:(length(dt_plot))) , Ambient_temp(start_hour:(
        length(dt_plot))),'Color','b','LineStyle','-');
```

```
    set(gca,'ycolor','b')
    ylabel (' T_a [\circC]')
    legend('COP','Ambient temp.') %,'Experimental')
    hold off

figure('Name', 'COP min')
    hold on
    plot(k_plot(start_hour*step_length+1:length(COP_store)), COP_store(start_hour*step_length+1:length(COP_store)))
    %plot(dt_plot, T_evap_store)
    xlabel('Time [min]')
    ylabel ('COP [-]')
    hold off

figure('Name', 'Compressor power')
    hold on
    plot( dt_plot(start_hour:(length(dt_plot))) , W_comp_plot(start_hour:(length(W_comp_plot))))
    %plot(dt_plot(2:(length(dt_plot))),W_comp_MSRig(2:(length(W_comp_plot))))
    xlabel('Time [h]')
    ylabel( 'W_{comp} [W]')
    %legend('Simulated') %,'Experimental'
    hold off

figure('Name', 'Heat transfer')
    hold on
    plot( dt_plot(start_hour:(length(dt_plot))), Q_cond_plot(start_hour:(length(dt_plot))) )
    xlabel('Time [h]')
    ylabel ('Q [W]')
    plot( dt_plot(start_hour:(length(dt_plot))), Q_evap_plot(start_hour:(length(dt_plot))) )
    %plot(dt_plot(2:(length(dt_plot))) , Q_cond_MSRig(2:(length(Q_evap_plot))))
    legend('Q_{cond}','Q_{evap}') %,'Q_{cond,exp.}'
    hold off

figure('Name', 'PV electrical efficiency')
plot(dt_plot(start_hour:(length(dt_plot))), eta_el_plot(start_hour:(length(dt_plot))))
xlabel('Time [h]')
```

```
ylabel ('\eta_{el} [-]')

figure('Name', 'Outlet water temperatures')
    hold on
    plot(k_plot(start_hour*step_length+1:length(T_w_out_store)),
        T_w_out_store(start_hour*step_length+1:length(T_w_out_store)))
    %plot(k_plot(121:length(T_w_out_store)), T_w_out_MSRig(1:length(
        T_w_out_store)-120))
    plot(k_plot(start_hour*step_length+1:length(T_w_out_store)),
        T_cond_store_cels(start_hour*step_length+1:length(T_w_out_store)))
    %plot(k_plot(121:length(T_evap_store_cels)), T_evap_store_cels(121:length
        (T_evap_store_cels)))
    %plot(dt_plot, T_evap_store)
    xlabel('Time [min]')
    ylabel ('Temperature [\circC]')
    %legend('T_{w,out,sim}','T_{w,out,exp}','T_{cond}')
    legend('T_{w,out,sim}','T_{cond}')
    hold off

figure('Name', 'PVT-evap. temperatures')
    hold on
    plot(k_plot(start_hour*step_length+1:length(T_p_store_cels)),
        T_p_store_cels(start_hour*step_length+1:length(T_p_store_cels)))
    plot(k_plot(start_hour*step_length+1:length(T_p_store_cels)),
        T_evap_store_cels(start_hour*step_length+1:length(T_p_store_cels)))
    %plot(dt_plot, T_evap_store)
    xlabel('Time [h]')
    ylabel ('Temperature [\circC]')
    legend('T_{pv}','T_{evap}')
    hold off

figure('Name', 'PV-only temperature')
    plot(k_plot(start_hour*step_length+1:length(T_pv_only_store_cels)),
        T_pv_only_store_cels(start_hour*step_length+1:length(
        T_pv_only_store_cels)))
    xlabel('Time [h]')
    ylabel('Temperature [\circC]')
   %%
figure('Name', 'PV-PVT temp. diff.')
    plot(k_plot(start_hour*step_length+1:length(T_pv_only_store_cels)),
        T_pvt_pv_diff(start_hour*step_length+1:length(T_pv_only_store_cels)))
```

```
    xlabel('Time [h]')
    ylabel('Temperature [\circC]')
    %%

figure('Name', 'Heat usage load side')
    hold on
    yyaxis left
    plot(dt_plot(start_hour:(length(dt_plot))), Q_DHW(start_hour:(length(
        dt_plot))))
    plot(dt_plot(start_hour:(length(dt_plot))), Q_SpaceHeat(start_hour:(
        length(dt_plot))))
    xlabel('Time [h]')
    ylabel ('Heat rate [W]')
    yyaxis right
    plot(dt_plot(start_hour:(length(dt_plot))), Heat_fraction_DHW(start_hour
        :(length(dt_plot))))
    ylabel ('Fraction [-]')
    legend('Q_{DHW}','Q_{SH}','DHW frac.')
    hold off

figure('Name', 'Compressor speed')
    plot(k_plot(start_hour*step_length+1:length(T_pv_only_store_cels)),
        N_comp_store(start_hour*step_length+1:length(T_pv_only_store_cels)))
    xlabel('Time [h]')
    ylabel('Compressor speed [rpm]')
%%
figure('Name', 'PV-ambient temp.diff')
    hold on
    plot(k_plot(start_hour*step_length+1:length(T_pv_only_store_cels)),
        delta_pv_amb(start_hour*step_length+1:length(T_pv_only_store_cels)))
    plot(k_plot(start_hour*step_length+1:length(T_pv_only_store_cels)),
        delta_pv_evap(start_hour*step_length+1:length(T_pv_only_store_cels)))
    xlabel('Time [h]')
    ylabel('\DeltaT [\circC]')
    legend('T_{pv}-T_{a}','T_{pv}-T_{evap}')
    hold off
%%
%% Plot DHW load
figure('Name', 'DHW coverage')
    hold on
    yyaxis left
```

```
    plot(dt_plot(start_hour:(length(dt_plot))), Q_DHW(start_hour:(length(
        dt_plot))),'Color','r','LineStyle','-');
    plot(dt_plot(start_hour:(length(dt_plot))), DHW_usage,'Color','b','
        LineStyle','--')
    xlabel('Time [h]')
    ylabel ('Heat rate [W]')
    yyaxis right
    plot(dt_plot(start_hour:(length(dt_plot))), DHW_coverage_hour(start_hour
        :(length(dt_plot))))
    ylabel ('Coverage [-]')
    legend('Q_{DHW}','Q_{DHW, load}','DHW coverage')
hold off

end

%% Scatter plots
%COP_rig = Data_shanghai.Var15';
if plot_scatter == 1

    figure('Name', 'COP scatter')
        hold on
        yyaxis left
        scatter(COP_plot(start_hour:(length(dt_plot))),Ambient_temp(
            start_hour:(length(dt_plot))))
        %plot(dt_plot,COP_rig)
        xlabel('COP [-]')
        ylabel ('Ambient temp [\circC]')
        yyaxis right
        scatter(COP_plot(start_hour:(length(dt_plot))),Solar_rad(start_hour:(
            length(dt_plot))))
        ylabel ('Solar radiation [W/m^2]')
        legend('Simulated') %,'Experimental')
        hold off

    figure('Name', 'COP-T_a scatter')
        hold on
        scatter(Ambient_temp(start_hour:(length(dt_plot))),COP_plot(
            start_hour:(length(dt_plot))))
        %plot(dt_plot,COP_rig)
        ylabel('COP [-]')
        xlabel ('Ambient temp [\circC]')
```

```
        hold off

    figure('Name', 'COP-T_p scatter hourly')
        hold on
        scatter(T_p_plot(start_hour:(length(dt_plot))),COP_plot(start_hour:(length(dt_plot))))
        %plot(dt_plot,COP_rig)
        ylabel('COP [-]')
        xlabel ('T_{pv} [\circC]')
        hold off

    figure('Name', 'COP-T_p scatter min.')
        hold on
        %scatter(T_p_store(start_hour:(length(dt_plot))),COP_plot(start_hour:(length(dt_plot))))
        scatter(T_p_store_cels(start_hour*step_length+1:length(T_p_store_cels)),COP_store(start_hour*step_length+1:length(T_p_store_cels)))
        %plot(dt_plot,COP_rig)
        ylabel('COP [-]')
        xlabel ('T_{pv} [\circC]')
        hold off

    figure('Name', 'Comp.work scatter')
        hold on
        scatter( Ambient_temp(start_hour:(length(dt_plot))) , W_comp_plot(start_hour:(length(W_comp_plot))))
        %plot(dt_plot,COP_rig)
        ylabel('W_{comp} [W]')
        xlabel ('Ambient temp [\circC]')
        hold off

    figure('Name', 'Comp.work-T_pv scatter')
        hold on
        scatter( T_p_plot(start_hour:(length(dt_plot))) , W_comp_plot(start_hour:(length(W_comp_plot))))
        %plot(dt_plot,COP_rig)
        ylabel('W_{comp} [W]')
        xlabel ('T_{pv} [\circC]')
        hold off

    figure('Name', 'PV-temp-T_a scatter')
```

```
        hold on
        scatter( Ambient_temp(start_hour:(length(dt_plot))) , T_p_plot(
            start_hour:(length(dt_plot))))
        %plot(dt_plot,COP_rig)
        ylabel('T_{pv} [\circC]')
        xlabel ('Ambient temp [\circC]')
        hold off

    figure('Name', 'PV-temp-I_rad scatter')
        hold on
        scatter( Solar_rad(start_hour:(length(dt_plot))) , T_p_plot(
            start_hour:(length(dt_plot))))
        %plot(dt_plot,COP_rig)
        ylabel('T_{pv} [\circC]')
        xlabel ('Solar radiation [W/m^2]')
        hold off

    figure('Name', 'Q_cond-T_pv scatter')
        hold on
        scatter(T_p_plot(start_hour:(length(dt_plot))),Q_cond_plot(start_hour
            :(length(dt_plot))))
        %plot(dt_plot,COP_rig)
        xlabel('T_{pv} [\circC]')
        ylabel ('Heat transfer [W] [W/m^2]')
        hold off

%% Duration curves
    PV_temp_sorted = sort(T_p_plot(start_hour:(length(dt_plot))));
    COP_sorted = sort(COP_plot(start_hour:(length(dt_plot))));
    %Q_cond_sorted = sort(Q_cond_plot) ;
    %W_comp_sorted = sort(W_comp_plot) ;

    figure('Name','T_p duration')
        plot( dt_plot(start_hour:(length(dt_plot))) , PV_temp_sorted)
        %plot(dt_plot,COP_rig)
        ylabel('T_{pv} [\circC]')
        xlabel ('Hours [h]')

    figure('Name','COP duration')
        plot( dt_plot(start_hour:(length(dt_plot))) , COP_sorted)
        %plot(dt_plot,COP_rig)
```

```
        ylabel('COP [-]')
        xlabel ('Hours [h]')

    %{
    figure('Name', 'Q_{cond} duration')
    plot(dt_plot, Q_cond_sorted)
    xlabel('Hours [h]')
    ylabel ('Q_{cond} [W]')

    figure('Name', 'W_{comp} duration')
    plot(dt_plot, W_comp_sorted)
    xlabel('Hours [h]')
    ylabel ('W_{comp} [W]')
    %}
end
%% Plot several figures in one
figure('Name','Several plots')
    set(gcf,'position',[200,100,600,600])
    t = tiledlayout(6,1);

    ax1 = nexttile;
        hold on
        yyaxis left
        plot(ax1 , dt_plot(start_hour:(length(dt_plot))) , T_p_plot(start_hour:(length(dt_plot)))) % PV temp.
        plot(ax1 , dt_plot(start_hour:(length(dt_plot))) , Ambient_temp(start_hour:(length(dt_plot))),'Color','g','LineStyle','--');
        ylabel('[\circC]')
        ax1.YColor = 'k';
        yyaxis right
        plot(dt_plot(start_hour:(length(dt_plot))) , Solar_rad(start_hour:(length(dt_plot)))) % Solar radiation
        ylabel('[W]')
        yticks([0 200 400 600 800 1000])
        ax1.YColor = 'k';
        legend('T_{pv}','T_a','I_{rad}','Location','eastoutside','Orientation','vertical')
        hold off

    ax2 = nexttile;
        plot(dt_plot(start_hour:(length(dt_plot))), COP_plot(start_hour:(
```

```
            length(dt_plot))),'Color','r','LineStyle','-')
        %yticklabels([ax1,ax2],['T','COP '])
        ylabel('[-]')
        ylim([0 6])
        legend('COP','Location','eastoutside','Orientation','vertical')


    ax3 = nexttile;
        hold on
        yyaxis left
        plot( dt_plot(start_hour:(length(dt_plot))), Q_cond_plot(start_hour:(
            length(dt_plot))) )
        ylabel ('[W]')
        ylim([0 5000])
        yticks([0 1000 2000 3000 4000])
        yyaxis right
        ylabel ('[W]')
        ylim([200 800])
        plot( dt_plot(start_hour:(length(dt_plot))) , W_comp_plot(start_hour
            :(length(W_comp_plot))))
        legend('Q_{cond}','W_{comp}','Location','eastoutside','Orientation','
            vertical')
        yticks([0 200 400 600 800])
        hold off

    ax4 = nexttile;
        plot(dt_plot(start_hour:(length(dt_plot))), eta_el_plot(start_hour:(
            length(dt_plot))))
        ylabel ('[-]')
        legend('\eta_{el}','Location','eastoutside','Orientation','vertical')


    ax5 = nexttile;
        hold on
        plot(k_plot(start_hour*step_length+1:length(T_p_store_cels)),
            T_p_store_cels(start_hour*step_length+1:length(T_p_store_cels)))
        plot(k_plot(start_hour*step_length+1:length(T_p_store_cels)),
            T_evap_store_cels(start_hour*step_length+1:length(T_p_store_cels))
            )
        plot(k_plot(start_hour*step_length+1:length(T_pv_only_store_cels)),
            T_pv_only_store_cels(start_hour*step_length+1:length(
```

```
            T_pv_only_store_cels)))
        ylabel('[\circC]')
        yticks([-20 -15 -10 -5 0 5 10 15 20 25 30 40 50])
        legend('T_{pvt}','T_{evap}','T_{pv,only}','Location','eastoutside','
            Orientation','vertical')
        hold off

    ax6 = nexttile;
        plot(k_plot(start_hour*step_length+1:length(T_w_out_store)),
            T_w_out_store(start_hour*step_length+1:length(T_w_out_store)))
        ylabel('[\circC]')
        %yticks([0 10 20 30 40 50 60])
        yticks([55 60 65])
        legend('T_{w,out}','Location','eastoutside','Orientation','vertical')

    linkaxes([ax1,ax2,ax3,ax4],'x');
    linkaxes([ax5,ax6],'x');
    xlabel(t,'Time [h]')
    %xticks(ax4,[0 1 2 3 4 5 6 7 8 9 10 11 12 13 14 15 16 17 18 19 20 21 22
        23 24 25])
    xticks([ax1,ax2,ax3,ax4],((start_hour+1):2:(length(dt_plot))))
    xticks([ax5,ax6],((start_hour*step_length+dt):dt*2:length(T_p_store_cels)
        ))
    yticks(ax2,[1 2 3 4 5 6])
    %yticks(ax)

    xticklabels([ax1,ax2,ax3,ax4,ax5],{})
    xticklabels(ax6,(2:2:hours_simulated))
    %xticklabels(ax3,{0:5:hours_simulated})
    box([ax1,ax2,ax3,ax4,ax5,ax6],'off')
    t.TileSpacing = 'tight';

%% Plot load side
figure('Name', 'Load side plots')
    hold on
    yyaxis left
    plot(k_plot(start_hour*step_length+1:length(T_w_out_store)),
        E_storage_kWh(start_hour*step_length+1:length(T_w_out_store)))
    xlabel('Time [min]')
    ylabel ('Energy stored [kWh]')
    yyaxis right
```

```
    plot(k_plot(start_hour*step_length+1:length(T_w_out_store)), Q_boiler(
        start_hour*step_length+1:length(T_w_out_store)))
    plot(k_plot(start_hour*step_length+1:length(T_w_out_store)),
        Q_storage_sign(start_hour*step_length+1:length(T_w_out_store)))

    ylabel ('Power [W]')
    legend('Energy stored','El. boiler power','Storage heat rate')
    hold off

figure('Name','Several plots load side')
    set(gcf,'position',[200,100,600,600])
    t = tiledlayout(6,1);

    ax1 = nexttile;
        hold on
        yyaxis left
        plot(ax1 , dt_plot(start_hour:(length(dt_plot))) , T_p_plot(
            start_hour:(length(dt_plot)))) % PV temp.
        plot(ax1 , dt_plot(start_hour:(length(dt_plot))) , Ambient_temp(
            start_hour:(length(dt_plot))),'Color','g','LineStyle','--');
        ylabel('[\circC]')
        ax1.YColor = 'k';
        yyaxis right
        plot(dt_plot(start_hour:(length(dt_plot))) , Solar_rad(start_hour:(
            length(dt_plot)))) % Solar radiation
        ylabel('[W]')
        yticks([0 200 400 600 800 1000])
        ax1.YColor = 'k';
        legend('T_{pv}','T_a','I_{rad}','Location','eastoutside','Orientation
            ','vertical')
        hold off

    ax2 = nexttile;
        plot(dt_plot(start_hour:(length(dt_plot))), COP_plot(start_hour:(
            length(dt_plot))),'Color','r','LineStyle','-')
        %yticklabels([ax1,ax2],['T','COP '])
        ylabel('[-]')
        ylim([0 6])
        legend('COP','Location','eastoutside','Orientation','vertical')
```

```
    ax3 = nexttile;
        hold on
        yyaxis left
        plot( dt_plot(start_hour:(length(dt_plot))), Q_cond_plot(start_hour:(
            length(dt_plot))) )
        ylabel ('[W]')
        ylim([0 5000])
        yticks([0 1000 2000 3000 4000])
        yyaxis right
        ylabel ('[W]')
        ylim([200 800])
        plot( dt_plot(start_hour:(length(dt_plot))) , W_comp_plot(start_hour
            :(length(W_comp_plot))))
        legend('Q_{cond}','W_{comp}','Location','eastoutside','Orientation','
            vertical')
        yticks([0 200 400 600 800])
        hold off

    ax4 = nexttile;
        hold on
        plot(dt_plot(start_hour:(length(dt_plot))), Load_spaceheat(start_hour
            :(length(dt_plot))))
        plot(dt_plot(start_hour:(length(dt_plot))), Load_DHW(start_hour:(
            length(dt_plot))),'Color','r','LineStyle','--')
        ylabel ('[W]')
        legend('Q_{spaceheat}','Q_{DHW}','Location','eastoutside','
            Orientation','vertical')
        hold off
    %{
    ax6 = nexttile;
        plot(k_plot(start_hour*step_length+1:length(T_w_out_store)),
            T_w_out_store(start_hour*step_length+1:length(T_w_out_store)))
        ylabel('[\circC]')
        %yticks([0 10 20 30 40 50 60])
        yticks([55 60 65])
        legend('T_{w,out}','Location','eastoutside','Orientation','vertical')
    %}

    ax7 = nexttile;
        hold on
        plot(k_plot(start_hour*step_length+1:length(T_w_out_store)),
```

```
        Q_storage_sign(start_hour*step_length+1:length(T_w_out_store)))
        plot(k_plot(start_hour*step_length+1:length(T_w_out_store)), Q_boiler
            (start_hour*step_length+1:length(T_w_out_store)))
        ylabel('[W]')
        %yticks([0 10 20 30 40 50 60])
        %yticks([55 60 65])
        legend('Q_{storage}','Q_{boiler}','Location','eastoutside','
            Orientation','vertical')

    linkaxes([ax1,ax2,ax3,ax4],'x');
    linkaxes([ax7],'x');
    xlabel(t,'Time [h]')
    %xticks(ax4,[0 1 2 3 4 5 6 7 8 9 10 11 12 13 14 15 16 17 18 19 20 21 22
        23 24 25])
    xticks([ax1,ax2,ax3,ax4],((start_hour-1):12:(length(dt_plot))))
    xticks([ax7],((start_hour*step_length-dt):dt*12:length(T_p_store_cels)))
    yticks(ax2,[1 2 3 4 5 6])
    yticks([ax4,ax7],[0 1000 2000 3000 4000 5000 6000 7000])
    %yticks(ax)

    xticklabels([ax1,ax2,ax3,ax4,ax7],{})
    xticklabels(ax7,(0:12:hours_simulated))
    %xticklabels(ax3,{0:5:hours_simulated})
    box([ax1,ax2,ax3,ax4,ax7],'off')
    t.TileSpacing = 'tight';

%% Plot PV-temp, ambient temp, solar rad., and COP

figure('Name','Temp, rad, and COP')
    set(gcf,'position',[200,100,500,300])
    t = tiledlayout(2,1);

    ax1 = nexttile;
        hold on
        yyaxis left
        plot(ax1 , dt_plot(start_hour:(length(dt_plot))) , T_p_plot(
            start_hour:(length(dt_plot)))) % PV temp.
        plot(ax1 , dt_plot(start_hour:(length(dt_plot))) , Ambient_temp(
            start_hour:(length(dt_plot))),'Color','g','LineStyle','--');
        ylabel('[\circC]')
        ax1.YColor = 'k';
```

```matlab
        yyaxis right
        plot(dt_plot(start_hour:(length(dt_plot))) , Solar_rad(start_hour:(length(dt_plot)))) % Solar radiation
        ylabel('[W]')
        yticks([0 200 400 600 800 1000])
        ax1.YColor = 'k';
        legend('T_{pv}','T_a','I_{rad}','Location','north','Orientation','horizontal')
        hold off

    ax2 = nexttile;
        plot(dt_plot(start_hour:(length(dt_plot))), COP_plot(start_hour:(length(dt_plot))),'Color','r','LineStyle','-')
        %yticklabels([ax1,ax2],['T','COP '])
        ylabel('[-]')
        ylim([0 6])
        legend('COP','Location','north','Orientation','horizontal')


    linkaxes([ax1,ax2],'x');
    xlabel(t,'Date')
    xticks([ax1,ax2],[(start_hour-1):168:(length(dt_plot)),2160])
    yticks(ax1,[0 100 200 300 400 500 600 700 800 900 1000])
    yticks(ax2,[1 2 3 4 5 6])
    %yticks(ax)

    xticklabels([ax1],{})
    %xticklabels(ax2,(1:168:hours_simulated))
    xticklabels(ax2,([01.01 07.01, 14.01, 21.01, 28.01, 04.02, 11.02, 18.02, 25.02, 04.03, 11.03, 18.03, 25.03, 31.03]))
    box([ax1,ax2],'off')
    t.TileSpacing = 'tight';


%% Plot Cond. power, comp.power, and load demands (Q_sh + Q_DHW)

figure('Name','Heating power and loads')
        set(gcf,'position',[200,100,500,300])
        hold on
        plot( dt_plot(start_hour:(length(dt_plot))), Q_cond_plot(start_hour:(length(dt_plot))),'linewidth',1.5)
```

```
        plot(dt_plot(start_hour:(length(dt_plot))), Load_spaceheat(start_hour:(length(dt_plot))),'Color','b','LineStyle','--')
        stairs(dt_plot(start_hour:(length(dt_plot))), Load_DHW(start_hour:(length(dt_plot))),'Color','r','LineStyle','--')
        ylabel ('Heating power [W]')
        ylim([0 5000])
        yticks([0 1000 2000 3000 4000 5000 6000 7000])
       %{
        yyaxis right
        ylabel ('[W]')
        ylim([200 800])
        plot( dt_plot(start_hour:(length(dt_plot))) , W_comp_plot(start_hour:(length(W_comp_plot))),'LineStyle','-.')
        yticks([0 200 400 600 800])
       %}
        legend('Q_{cond}','Q_{SH}','Q_{DHW}','Location','northoutside','Orientation','horizontal')
        hold off


    xlabel('Time [h]')
    xticks(((start_hour-1):12:(length(dt_plot))))
    xticklabels((0:12:hours_simulated))
    box('off')


figure('Name','Heating power and storage')
        set(gcf,'position',[750,100,500,300])
        hold on
        yyaxis left
        plot(k_plot(start_hour*step_length+1:length(T_w_out_store)), E_storage_kWh(start_hour*step_length+1:length(T_w_out_store)),'Color','b','LineStyle','--')
        xlabel('Time [h]')
        ylabel ('Energy stored [kWh]')
        yyaxis right
        plot(k_plot(start_hour*step_length+1:length(T_w_out_store)), Q_storage_sign(start_hour*step_length+1:length(T_w_out_store)),'Color','black','LineStyle','-')
        plot(k_plot(start_hour*step_length+1:length(T_w_out_store)), Q_boiler(start_hour*step_length+1:length(T_w_out_store)),'Color','r','
```

```
    LineStyle','-')

    ylabel ('Power [W]')
    legend('E_{stored}','Q_{storage}','Q_{boiler}','Location','
        northoutside','Orientation','horizontal')
    xlabel('Time [h]')
    xticks(((start_hour*step_length-dt):dt*3:length(T_p_store_cels)))
    xticklabels((0:12:hours_simulated))
    box('off')
    hold off
```

C PVT module specifications

This appendix shortly describes the specifications of the utilised PVT module. Relevant material properties of the layers in the module component can be seen in Table C.1.

Table C.1: *PVT model layer properties [2][21].*

Layer	**Label**	**Thickness (δ)**	**Conductivity ($\varkappa$)**	**Density (ρ)**	**Specific heat capacity (c_p)**
Unit	-	mm	W/mK	kg/m^3	J/kgK
Glass cover	g	3.5	NA	3000	500
PV cells	pv	0.3	203	2330	677
EVA-grease	EVA	0.5	0.311	960	2090
E-insulation (TPT)	ei	0.5	0.15	1200	1250
Roll-bond	rb	0.9	151	2712	910

D Building model specifications

This appendix shortly describes the specifications of the building model used for the case study in Trondheim, Norway. Relevant TEK87 and TEK 17 building energy requirements, as well as a comparison to an nZEB proposal, is provided in Table D.1

Table D.1: *Input values used in SIMIEN compared to the energy saving measures in TEK17 [58] and a proposed net ZEB solution for residential houses [62].*

Parameter	**TEK17**	**nZEB proposal**	**TEK87**
U-value external wall	$\leq$ 0.18 W/m^{2}K	0.12 W/m^{2}K	0.30 W/m^{2}K
U-value roof	$\leq$ 0.13 W/m^{2}K	0.10 W/m^{2}K	0.20 W/m^{2}K
U-value floor	$\leq$ 0.10 W/m^{2}K	0.07 W/m^{2}K	0.30 W/m^{2}K
U-value window and doors	$\leq$ 0.80 W/m^{2}K	0.65 W/m^{2}K	2.4 W/m^{2}K
Normalised thermal bridge value	$\leq$ 0.05 W/m^{2}K	0.03 W/m^{2}K	0.05 W/m^{2}K
Air change per hour at 50 Pa pressure difference	$\leq$ 0.6 h^{-1}	0.3 h^{-1}	4.0 h^{-1}
Window area compared to heated gross area	$\leq$ 25%	–	17.8%

E Simulation results

E.1 June 25th

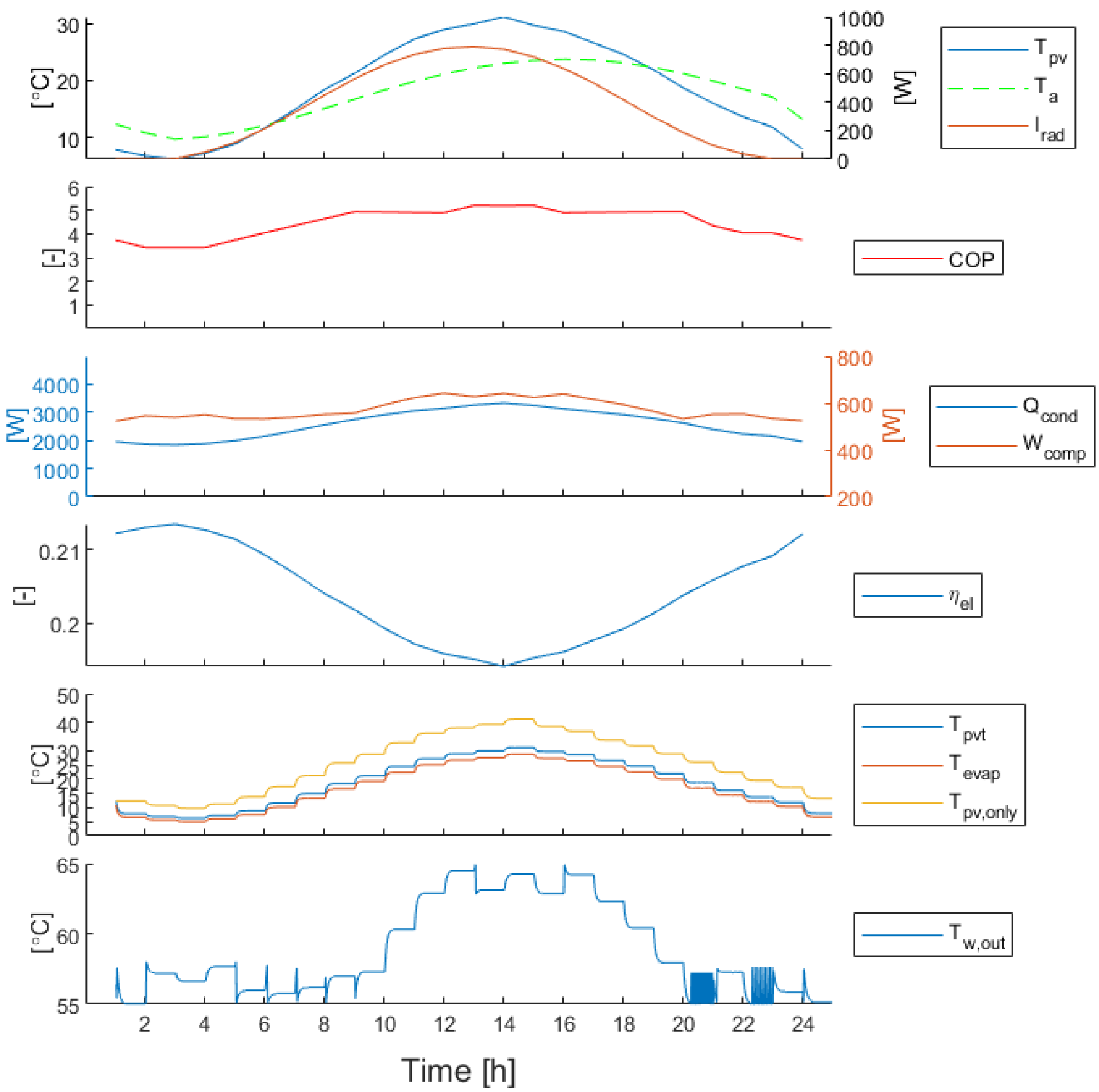

Figure E.1: *Simulation for June 25th with 6 PVT modules and 1.2 compressor size.*

E.2 February 14th

E.3 First week of March

E.4 Compressor control

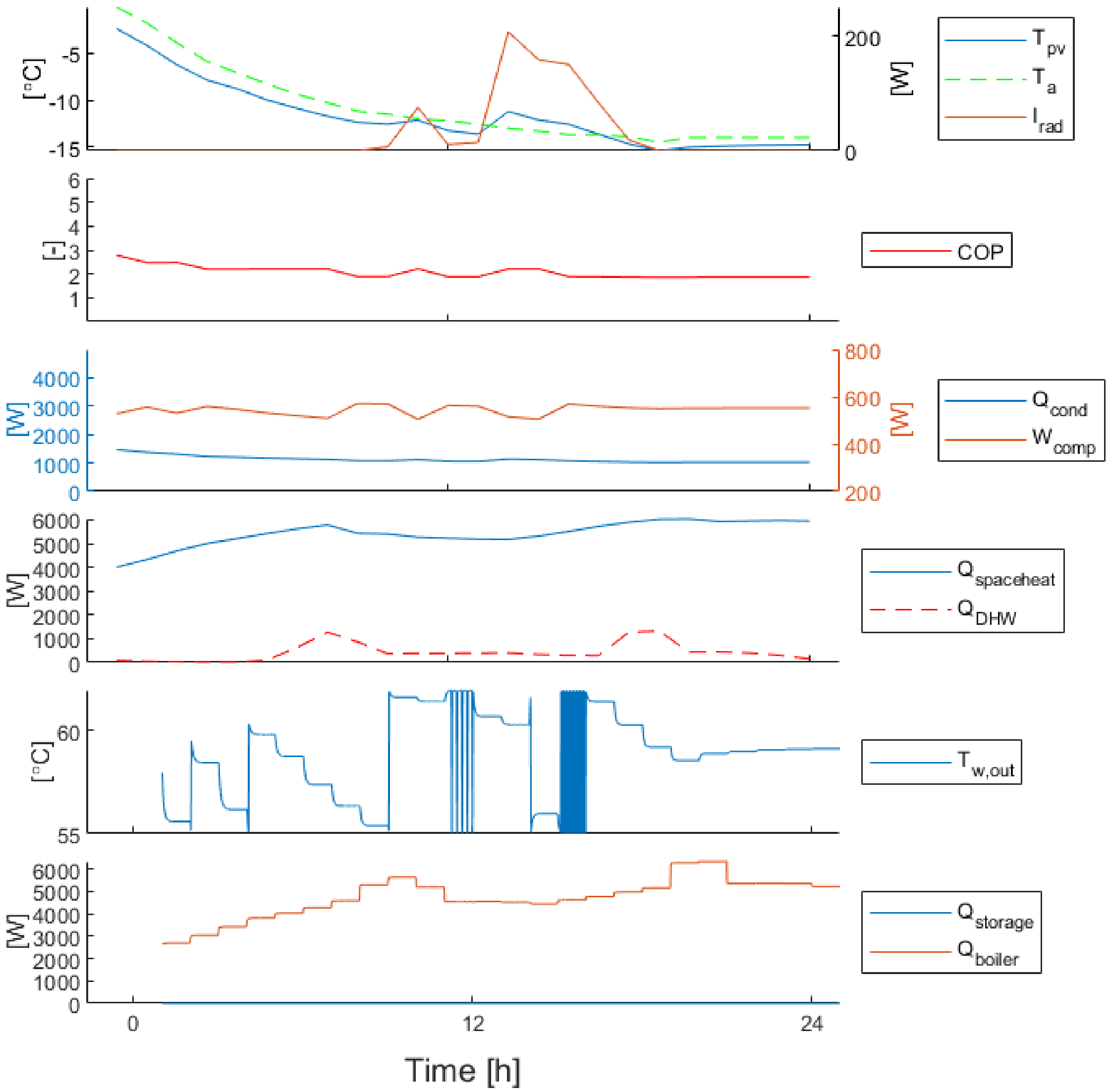

Figure E.2: *Simulation for February 14th with 6 PVT modules and 1.2 compressor size.*

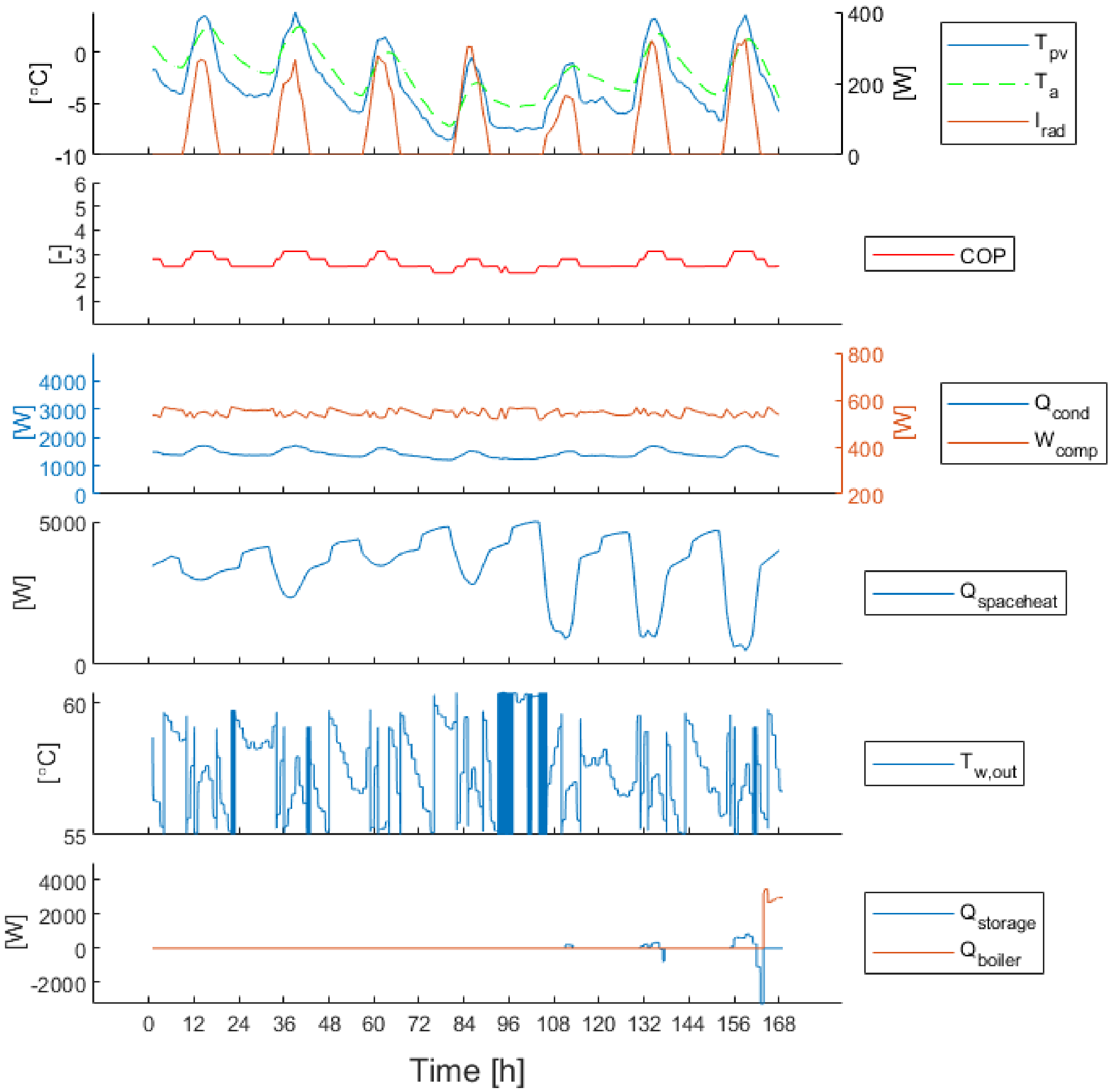

Figure E.3: *Simulation results for the first week of March.*

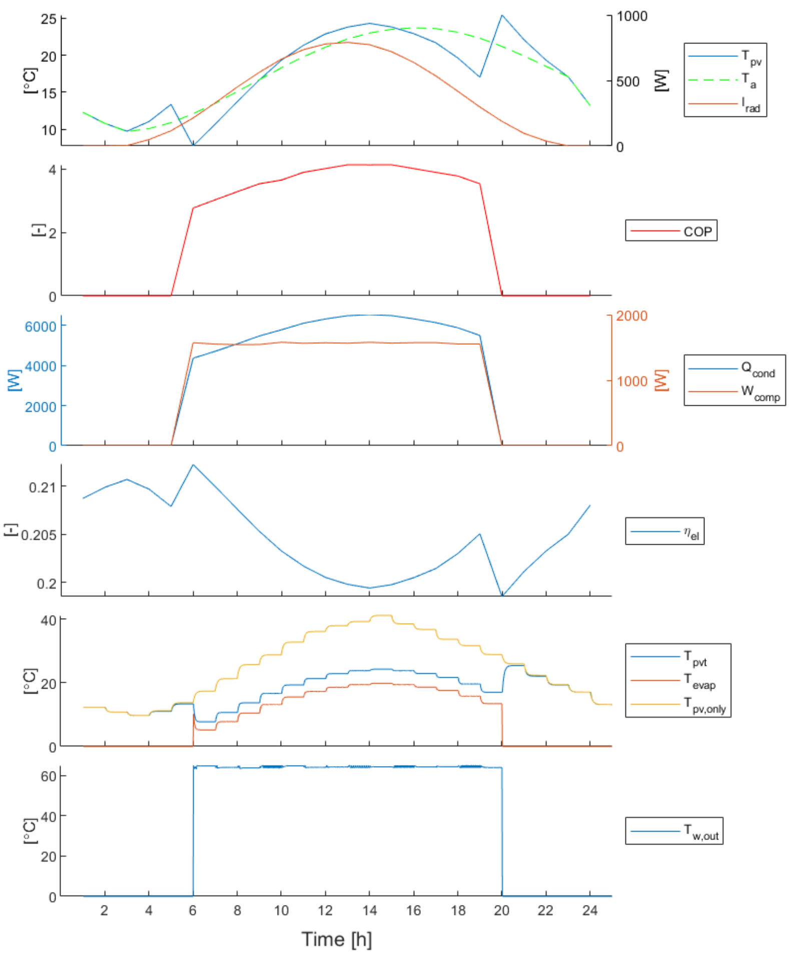

Figure E.4: *Results for compressor cut-off (N=0) at I<200 W/m^2 for June 25th with V_{th}= 3.0.*

Kristoffer Wigdahl Lie

Model Development and Performance Analysis of an R290 DX Solar Assisted Heat Pump System using PVT.

NTNU
Norwegian University of
Science and Technology